
# Synthesis, analysis and reactions of novel silaorganics

Ísak Sigurjón Bragason

**Faculty of Physical Sciences**
**University of Iceland**
**2013**

# Synthesis, analysis and reactions of novel silaorganics

Ísak Sigurjón Bragason

90 ECTS thesis submitted in partial fulfillment of a
*Magister Scientiarum* degree in Chemistry

Advisors
Prof. Ingvar Árnason
Prof. Ágúst Kvaran

External examiner
Pálmar Ingi Guðnason

Faculty of Physical Sciences
School of Engineering and Natural Sciences
University of Iceland
Reykjavik, February 2013

Synthesis, analysis and reactions of novel silaorganics
Novel silaorganics: Synthesis, analysis & reactions
90 ECTS thesis submitted in partial fulfillment of a *Magister Scientiarum* degree in Chemistry



Faculty of Physical Sciences
School of Engineering and Natural Sciences
University of Iceland
Hjarðarhaga 2-4
101, Reykjavik
Iceland

Telephone: 525 4000

Bibliographic information:
Ísak Sigurjón Bragason, 2013, Synthesis, analysis and reactions of novel silaorganics, M.Sc. thesis, Faculty of Physical Sciences, University of Iceland.

Printing: Samskipti ehf, Síðumúla 4, 108 Reykjavík

Reykjavik, Iceland, February 2013

# Abstract

We wanted to investigate further the alcoholysis of $Cp^*Ti(\mu\text{-}O_3)[(^tBu)Si{-}CH_2]_3$ (**1**), an adamantane complex, previously shown to form a dimeric structure, **2**, upon reaction with MeOH (Scheme 1). Samples were prepared to compare the rate of reaction at different temperatures and with or without exposure to light. Although the results were only partly conclusive, temperature appears to have a mild effect on the reaction rate. Light exposure turned out to be a deciding factor in the outcome of these reactions.

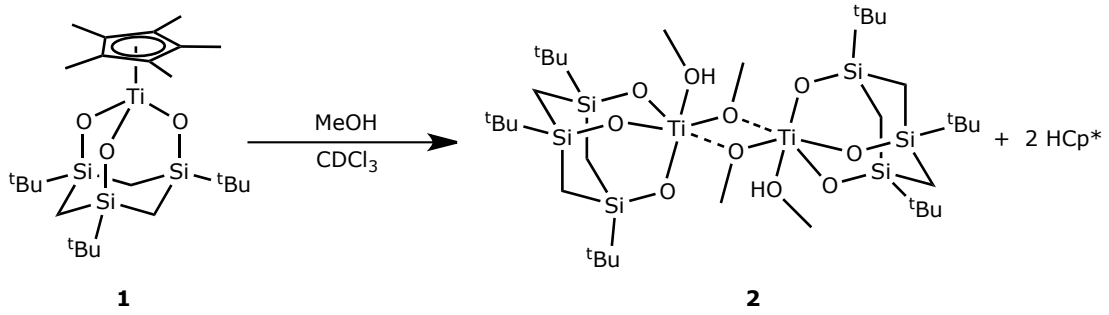


**1** **2**

*Scheme 1: Formation of a dimer, **2**, upon the reaction of **1** with MeOH.*

Analogous samples containing **1** and one of three phenols (PhOH, *p*-$^t$BuPhOH and *p*-$NO_2$PhOH) were prepared. These indicate that unsubstituted phenol gives the fastest reaction rate. The products from those reactions, however, are unlikely to be dimeric as evidence of $Cp^*$ coordinated to the metal centre can still be found.

A synthetic route was sought from 1,3,5-trisilacyclohexane (**4**) to a suitable precursor for the synthesis of a kinetically stabilized 1,3,5-trisilabenzene. Several novel substituted 1,3,5-trisilacyclohexanes were synthesized and characterized by NMR and X-ray crystallographic techniques. This research culminated in the successful synthesis of 1,3,5-trichloro-1,3,5-tris(Dipp)-1,3,5-trisilacyclohexane (**8**) (Dipp = 2,6-di(isopropyl)phenyl), which we believe is a promising precursor to 1,3,5-trisilabenzene (Scheme 2).

Alkali metal salts of transition metal complex anions were synthesized and reacted with 1-halo-1-silacyclohexane (halo = chloro, bromo) in the hope of obtaining a series of transition metal complexes bearing Cp and CO ligands as well as a silacyclohexane moiety. Despite the fact that a reaction occurs between these alkali metal salts and the carbosilane, isolation and unequivocal characterization of the products has not been achieved.

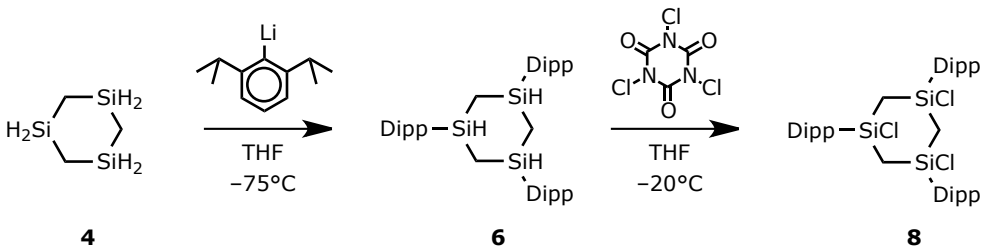


**4** **6** **8**

*Scheme 2: Synthetic route from **4** to **8**, a promising precursor to 1,3,5-trisilabenzene.*

We planned to synthesize the adamantane complex $Cp^*Ti(\mu\text{-}O_3)[DisSi{-}O]_3$ by the reaction of $[DisSi(OH){-}O]_3$ (**9**) (Dis = $-CH(SiMe_3)_2$) with $Cp^*TiCl_3$. However, the reaction did not yield the expected product but rather a large tricyclic compound, **11** (Scheme 3). After repeated trials at the synthesis we reached a yield of 46% of the pure product.

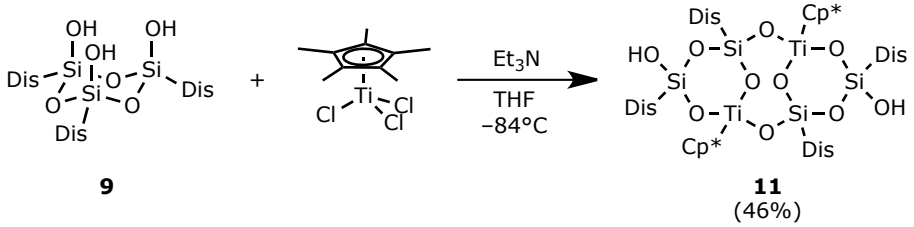


**9** **11** (46%)

*Scheme 3: Formation of the tricyclic **11** upon the reaction of **9** with $Cp^*TiCl_3$.*

Finally we describe the temperature calibration of a Bruker NMR probe head specially adapted to DNMR experiments at very low temperature in connection with conformational studies of sila- and germaorganics.

# Útdráttur

Við lögðum upp með að rannsaka frekar alkóhólrof $Cp^*Ti(\mu\text{-}O_3)[(^tBu)Si{-}CH_2]_3$ (**1**), sem er adamantanlaga komplex, en fyrri rannsóknir höfðu sýnt að hann myndar tvíliðu, **2**, með hvarfi við metanól (Skema 1). Útbúin voru sýni í þeim tilgangi að bera saman hraða hvarfsins við mismunandi hitastig og með eða án aðkomu ljóss. Þrátt fyrir að niðurstöður okkar hafi ekki verið óyggjandi í alla staði virðist hitastig hafa dálítil áhrif á hvarfhraðann. Aðgengi ljóss reyndist hafa úrslitaáhrif um útkomu þessara hvarfa.

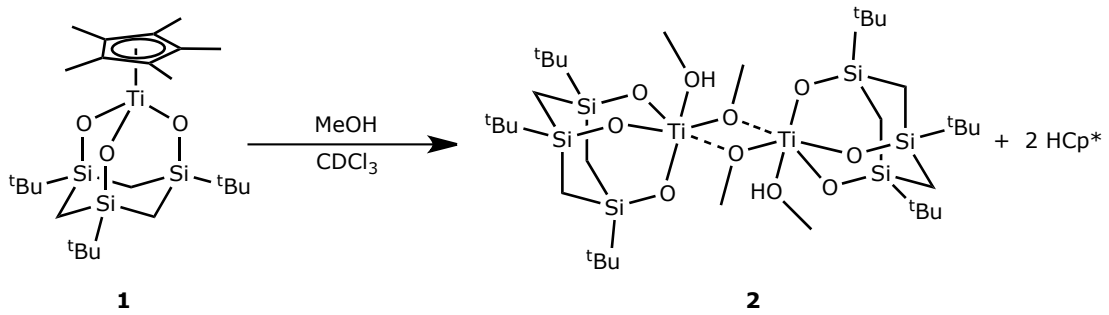


**1** **2**

*Skema 1: Myndun tvíliðu, **2**, með hvarfi **1** við metanól.*

Sambærileg sýni sem innihalda **1** ásamt einu þriggja fenóla (PhOH, *p*-$^t$BuPhOH og *p*-$NO_2$PhOH) benda til að ósetið fenól gefi mestan hvarfhraða. Það kom hins vegar í ljós að myndefni þessara hvarfa eru sennilega ekki tvíliður þar sem merki fundust um $Cp^*$ sem enn er tengt málminum.

Leitað var leiða við nýsmíði hentugs forefnis fyrir hraðafræðilega stöðgað 1,3,5-trísílabensen úr 1,3,5-trísílasýklóhexani. Ný 1,3,5-trísílasýklóhexön með ýmsum sethópum voru smíðuð og greind með NMR og einkristallagreiningum. Þessar rannsóknir náðu hámarki þegar það heppnaðist að smíða 1,3,5-tríklóró-1,3,5-tris(Dipp)-1,3,5-trísílasýklóhexan (**8**), sem við teljum vera álitlegan forvera 1,3,5-trísílabensens (Skema 2).

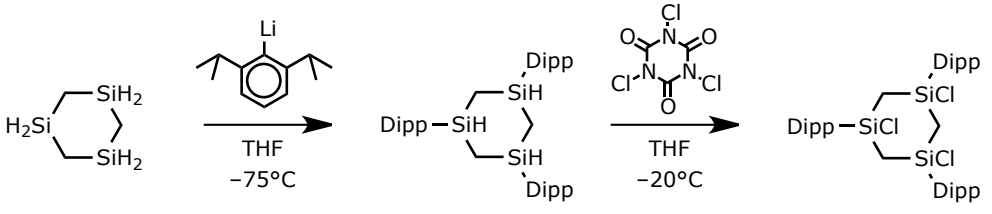


**4** **6** **8**

*Skema 2: Leið að smíði 1,3,5-trísílabensen forverans **8**, með **4** sem upphafsefni.*

Alkalísölt komplexra hliðarmálmajóna voru smíðuð og þau hvörfuð við 1-haló-1-sílasýklóhexan (haló = klóró, brómó) í von um að smíða mætti röð komplexa þar sem hliðarmálmurinn ber tenglana Cp og CO auk sílasýklóhexan tengils. Þrátt fyrir að hvörf hafi átt sér stað milli alkalísaltanna og sílasýklóhexansins heppnaðist ekki að einangra myndefnin eða greina þau með óyggjandi hætti.

Við ætluðum okkur að smíða adamantanlaga komplexið $Cp^*Ti(\mu\text{-}O_3)[DisSi{-}O]_3$ með hvarfi $[DisSi(OH){-}O]_3$ (**9**) (Dis = $-CH(SiMe_3)_2$) við $Cp^*TiCl_3$. Myndefni hvarfsins reyndist hins vegar ekki vera það sem við ætluðum, heldur stór þriggja hringja sameind, **11** (Skema 3). Eftir ítrekaðar tilraunir við smíðina náðum við 46% heimtum af hreinu efni.

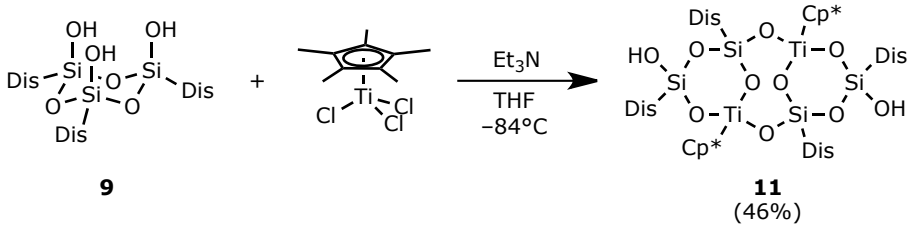


**9** **11** (46%)

*Skema 3: Myndun þriggja hringja sameindarinnar **11** við hvarf **9** og $Cp^*TiCl_3$.*

Að lokum gerum við grein fyrir hitastigskvörðun á Bruker NMR mælihaus sem notaður er við lághita DNMR mælingar tilheyrandi stellingarhverfurannsóknum á lífrænum efnum sem innihalda kísil eða germaníum.

# Table of contents

# List of Schemes

# List of Figures

# List of Tables

# Abbreviations

| | |
|---|---|
| Bbt | 2,6-bis[bis(trimethylsilyl)methyl]-4-[tris(trimethylsilyl)methyl]phenyl |
| Cp | cyclopentadienyl |
| $Cp^*$ | pentamethylcyclopentadienyl |
| $Cp^{xpm}$ | 1-(*para*-methyl)phenyl-2,3,4,5-tetramethyl-cyclopentadienyl |
| DCPD | dicyclopentadiene |
| DEPT | distortionless enhancement by polarization transfer |
| Dipb | 1,3-diisopropylbenzene |
| Dipp | 2,6-di(isopropyl)phenyl |
| DippBr | 2,6-di(isopropyl)phenylbromide |
| DippCl | 2,6-di(isopropyl)phenylchloride |
| Dis | bis(tri(methyl)silyl)methyl |
| DMSO | dimethylsulfoxide |
| DNMR | dynamic nuclear magnetic resonance |
| duryl | 2,3,5,6-tetra(methyl)phenyl |
| ESI-MS | electrospray ionization mass spectrometry |
| $Et_2O$ | diethylether |
| $Et_3N$ | triethylamine |
| EtOH | ethanol |
| $Fp^-$ | $\eta^5$-cyclopentadienyliron dicarbonyl anion |
| HPLC | high performance liquid chromatography |
| HSE | homodesmotic stabilization energy |
| ICR | Institute for Chemical Research |
| INEPT | insensitive nuclei enhanced by polarization transfer |
| $^i$PrOH | isopropanol |
| ISE | isodesmic stabilization energy |
| MeLi | methyllithium |
| MeOH | methanol |
| Mes | mesityl [2,3,5-tri(methyl)phenyl] |
| MesBr | mesitylbromide |

| | |
|---|---|
| MS | mass spectrometry |
| NaCp | sodium cyclopentadienide |
| NBS | N-bromosuccinimide |
| NMR | nuclear magnetic resonance |
| p.a. | pro analysi |
| pet. ether | petrol ether |
| PhOH | phenol |
| RT | room temperature |
| SCC | short column chromatography |
| Tbt | 2,4,6-tris[bis(trimethylsilyl)methyl]phenyl |
| $^{t}$BuLi | *tert*-butyllithium |
| $^{t}$BuOH | *tert*-butanol |
| TCCA | trichloroisocyanuric acid |
| THF | tetrahydrofuran |
| TLC | thin layer chromatography |
| TMS | tetramethylsilane |
| TSCH | 1,3,5-trisilacyclohexane |

# Numbered compounds

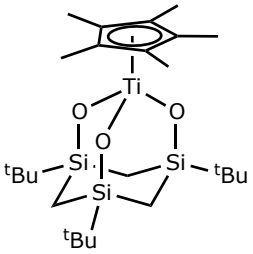

**1**

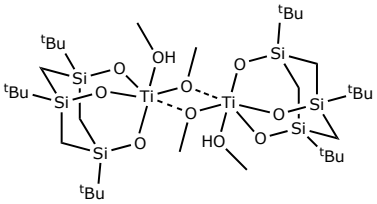

**2**

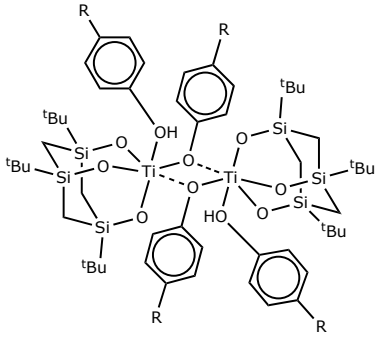

**3a** (R=H)
**3b** (R=$^t$Bu)
**3c** (R=$NO_2$)

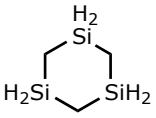

**4**

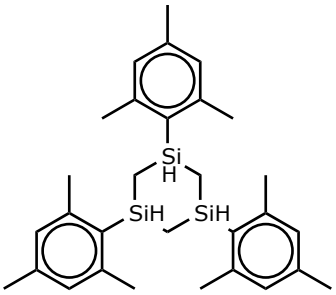

**5**

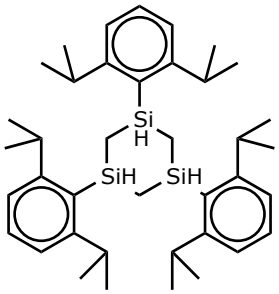

**6**

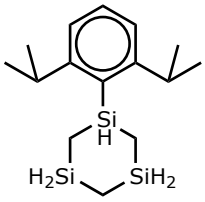

**7**

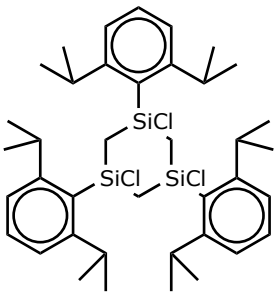

**8**

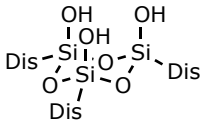

**9**

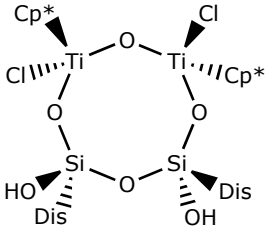

**10**

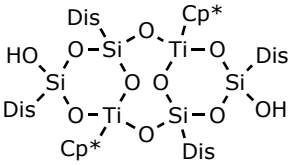

**11**

# Acknowledgements

Firstly I would like to thank my advisor, Prof. Ingvar H. Árnason, for his guidance and advice throughout my studies. It has been a pleasant and informative experience working with him.

**At the University of Iceland I would like to thank:**

Dr. Sigríður Jónsdóttir for NMR and MS measurements.

Svana H. Stefánsdóttir for providing chemicals and generally being very helpful.

Sverrir Guðmundsson for making what I needed out of glass and fixing what I broke.

The other members of the Árnason group, Nanna Rut Jónsdóttir and Katrín Lilja Sigurðardóttir for the useful discussions and the good times.

Þorvaldur Snæbjörnsson, for providing me with 1-bromo-1-silacyclohexane.

My coworkers at the Science Institute for their company and help on various small matters.

**At Kyoto University I would like to thank:**

Prof. Norihiro Tokitoh for allowing me to be a member of his excellent group for three months.

Assistant Prof. Yoshiyuki Mizuhata for his extensive guidance during my research at the Tokitoh laboratory.

Other members of the Tokitoh lab for various advice and help getting to know a new lab quickly.

**I would also like to thank:**

The Icelandic Centre for Research (RANNÍS) for financial support.

The Scandinavia-Japan Sasakawa Foundation for financially supporting my stay in Japan.

Heinrich Uffelmann for custom-made glassware.

My family and friends for their support throughout my studies.

Last but not least my wife, Hildigunnur Þórsdóttir, for all her love, support and understanding.

# 1 Introduction

Silicon is the second most abundant element in the Earth's crust after oxygen, accounting for 27.2% of the crusts weight.[1] It is also the closest homologue of the elemental backbone of life as we know it — carbon. Each of these two elements has a vast chemistry which does not, or to a very insignificant extent, exist for the other. Silicon has the extensive chemistry of silicates and the plethora of organic substances, grounded in the covalent chemistry of carbon is well known to all students of chemistry. The subjects of research discussed in this thesis, however, belong to the much smaller, and more specific, but significant area of chemistry where these two elements meet — the chemistry of organosilicon compounds.

The research described in this thesis, although with the common theme of silicon chemistry, is somewhat segmented. Firstly it deals with research to further understand the nature of alcoholysis reactions of $Cp^*Ti(\mu\text{-}O_3)[(^t Bu)Si{-}CH_2]_3$ ($Cp^* = C_5(CH_3)_5$), a titanasiloxane compound, earlier studied by Ester Inga Eyjólfsdóttir under the supervision of Prof. Ingvar H. Árnason. A second subject are syntheses of novel organosilicon compounds towards what we believe to be a suitable precursor for 1,3,5-trisilabenzene. Thirdly a series of reactions intended to form silacyclohexane derivatives, with the silicon atom bonded to the metal centre of a transition metal complex, is discussed, although the target compounds have as yet not been successfully isolated. Finally we describe the discovery of an efficient one-step synthesis of an interesting tricyclic titanasiloxane, previously available in a low yield through a three step synthesis. As these subjects, although with a common theme, are not closely related, each will be covered somewhat separately. The two more extensive research topics are introduced in the next sections but introductions to the other subjects can be found in their corresponding chapters.

## 1.1 Alcoholysis of a titanasiloxane

In 2003 it was found, as a result of the attempted recrystallization of the titanasiloxane compound $Cp^{xpm}Ti(\mu\text{-}O_3)[(^t Bu)Si{-}CH_2]_3$ ($Cp^{xpm} = C_5H_4(p\text{-}C_6H_5Me)$) from $CDCl_3$ by the addition of methanol, that an unexpected alcoholysis occurred leading to the formation of a dimeric structure (Scheme 1.1).[2] It turned out that the bond between the titanium centre and the $Cp^{xpm}$ moiety had been broken and the dimer formed consisted of two titanium centres with octahedral coordination and two bridging methoxy ligands. In other positions the titanium was coordinated by the $[(^t Bu)Si(O){-}CH_2]_3$ moiety and a methanol molecule.

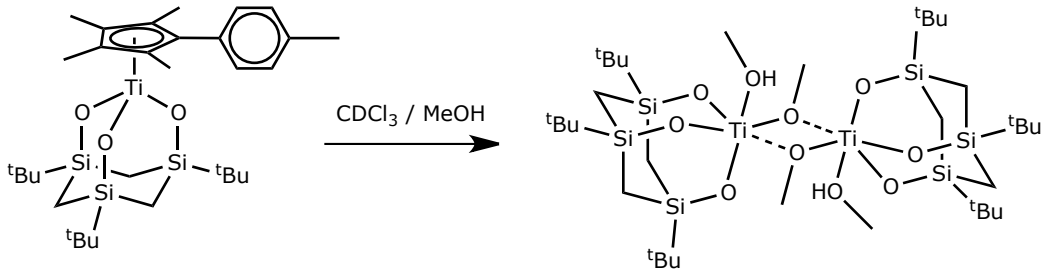


*Scheme 1.1: The reaction that occurred upon an attempt grow crystals of $Cp^{xpm}Ti(\mu\text{-}O_3)[(^tBu)Si{-}CH_2]_3$ from $CDCl_3$ by adding a small amount of MeOH.*

To better investigate this type of alcoholysis and the subsequent dimer formation, experiments were set up utilizing a related titanasiloxane complex, $Cp^*Ti(\mu\text{-}O_3)[(^tBu)Si{-}CH_2]_3$ (**1**), in which the $Cp^{xpm}$ group has been exchanged for $Cp^*$ (pentamethylcyclopentadienyl).[3] This research is covered extensively in Ester Inga Eyjólfsdóttir's M.Sc. thesis from 2008 titled *Synthesis, analysis and reactions of novel titanasiloxane complexes*, but the main results will be summarized in short here to provide the foundation for my discussion on the subject.

Several different samples were prepared containing **1** and an alcohol in a deuterated solvent. A few different samples contained MeOH as the alcoholysing agent but varied in other respects. Catalysis was attempted in two samples with the addition of MeONa in one case and NaOH in another. A single sample was set up with 80:20 mixture of MeOH-$d_4$ and $C_6D_6$ as the solvent with the intent of confirming or disproving that a chlorinated solvent was essential to the reaction (the $C_6D_6$ was added as **1** proved insoluble in MeOH, but solubility of the compound remained very low in the mixture). In addition to MeOH, three other aliphatic alcohols of differing bulkiness (EtOH, $^i$PrOH and $^t$BuOH) were tested as alcoholysing agents as well as phenol.

Dimer formation was observed in the case of MeOH and EtOH. In the case of $^i$PrOH a reaction occurred but was inconsistent with the type of dimer formation observed for the smaller alcohols and a trigonal bipyramidal structure was suggested for the product. No reaction was observed in the case of $^t$BuOH. A reaction occurred in the sample with PhOH as the alcoholysing reactant, forming what was expected to be a dimer although another set of peaks, possibly belonging to a trigonal bipyramidal complex, appeared as well. The structure of the products from the reaction with PhOH has not been conclusively determined. In short, it was found that the bulkiness of the alcohol was an important factor, as a dimer was not formed in the case of $^i$PrOH and no reaction was observed for the $^t$BuOH. The attempts to catalyse the reaction by MeONa and NaOH resulted in decomposition and the experiment with a chlorine free solvent failed. An unsolved mystery in the reactions where the dimeric structures were formed was the fate of the $Cp^*$ group once it had come free from

the titanium centre, as free $HCp^*$ could not be detected in the NMR spectra.

My research concerning this type of alcoholysis is covered in Chapter 2.

## 1.2 A precursor for 1,3,5-trisilabenzene

### 1.2.1 Silaaromatics: The Beginning

Silicon containing aromatic heterocycles have been the subject of research for many years now. Due to the similarities and differences between carbon and silicon these compounds are interesting research topics to better understand the nature of aromaticity, amongst other things. As benzene is the quintessential aromatic, syntheses of benzene analogues with one or more silicon atoms substituted for carbon (so called silabenzenes) have been sought for a long time.

The first report of a successful silabenzene synthesis and characterisation was in 1980,[4] when Maier et al. succeeded in the synthesis of monosilabenzene, although evidence of intermediacy had been reported earlier.[5] The compound was formed by flash pyrolysis and captured in an argon matrix at 10 K, but immediately became undetectable upon thawing of the matrix. Five years later Maier et al. reported an analogous synthesis of 1,4-disilabenzene, again captured in an argon matrix at 10 K.[6] The synthesis of more stable silabenzene compounds, that could be handled at room temperature, was however made elusive by the extreme reactivity of the silicon center.

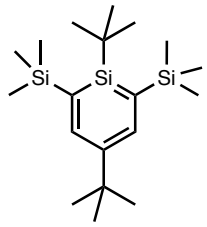


*(a)*

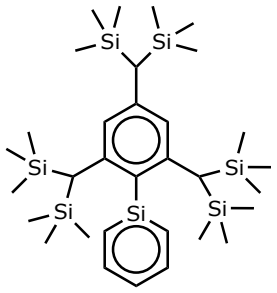


*(b)*

*Figure 1.1:*
*(a) Märkl and Schlosser's 2,6-bis(trimethylsilyl)-1,4-di-tert-butylsilabenzene, stable below $-100\,°C$ in a special solvent.*

*(b) Tokitoh et al.'s 1-Tbt-silabenzene, stable at RT.*

The first report of a "stable" silabenzene came from Märkl and Schlosser in 1988.[7] They had attempted kinetic stabilization through the addition of bulky substituents, synthesizing 2,6-bis-(trimethylsilyl)-1,4-di-*tert*-butylsilabenzene (Fig. 1.1a), but the compound was still only stable below $-100\,°C$, and it's stability apparently owing to coordination of the silicon by a Lewis base from the solvent it was kept in (Trapp mixture: THF/$Et_2O$/pet. ether, 4:1:1).[7–10] Märkl and Schlosser describe their surprise at the fact that what they believe to be highly stabilizing bulky groups are not sufficient to provide stability at room temperature. It would later come to light that much bulkier groups are required for adequate stabilization.

The first synthesis of a silaaromatic that can, unambiguously, be called stable was reported in 1997 by Tokitoh et al., who had synthesized 2-silanaphthalene stabilized by the extremely bulky Tbt group (Tbt = 2,4,6-tris[bis(trimethylsilyl)methyl]phenyl) linked to the silicon atom.[11] A second stable 2-silanaphthalene was reported in 1999[12] stabilized by the

even bulkier, although related, Bbt group (Bbt = 2,6-bis[bis(trimethylsilyl)methyl]-4-[tris-(trimethylsilyl)methyl]phenyl). A stable monosilabenzene didn't enter the arena until the year 2000, 20 years after the first reported synthetic evidence of such a compound.[8] The kinetic stabilization was again achieved through substitution by Tbt (Fig. 1.1b). Since then the research group of Prof. Norihiro Tokitoh at Institute for Chemical Research (ICR), Kyoto University have succeeded in synthesizing other silaaromatics utilizing the Tbt group for kinetic stability.[13–15]

### 1.2.2 Trisilabenzene — is it possible?

The first report of a polysilabenzene came from Rich and West in 1982.[16] They performed trapping reactions that provided evidence for the existence of hexamethyl-1,4-disilabenzene as an intermediate. The first isolation of a disilabenzene molecule was, as mentioned above, the characterisation of 1,4-disilabenzene frozen in an argon matrix, performed by Maier et al. in 1985. Ando et al. reported intermediacy of a 1,4-disilabenzene derivative formed by mild photochemical valence isomerization of 1,4-disila(Dewar-benzene) in 2000,[17] but no stable polysilaaromatics had yet been synthesized. Recently some more stable molecules with two silicon atoms substituted for carbon have been reported: A 1,2-disilabenzene derivative in 2007[18] and a 1,4-disilabenzene derivative in 2012.[19] In this latest example, Roesky et al. were able to isolate and analyse the compound crystallographically. But what about silaaromatics with three silicon atoms within the ring structure?

In 1992 Bjarnason and Arnason reported the detection of a ligand with the formula $C_3H_6Si_3$ in gas-phase reactions of transition metal ions and cyclopentadienyl transition metal ions with 1,3,5-trisilacyclohexane.[20] Although the formula was determined unambiguously, it's structure as 1,3,5-trisilabenzene was only speculative. However, theoretical studies of trisilabenzenes have suggested that the formation of 1,3,5-trisilabenzene is thermodynamically feasible.[21,22] In fact the 1,3,5-isomer of trisilabenzene has been described as an interesting synthetic target on the grounds of suggested high stabilization from aromaticity.[22] Baldridge et al. reported from their theoretical studies of this isomer, that a planar $D_{3h}$ geometry was consistently found, along with uniform bond delocalisation and suggestions of high aromaticity. They found that 1,3,5-trisilabenzene had ISE (isodesmic stabilization energy) and HSE (homodesmotic stabilization energy) values of 87% and 102% that of benzene, respectively. In comparison the corresponding values for monosilabenzene are 76% and 77% that of benzene.[22]

Although theoretical indications of high thermodynamic stabilization from aromaticity are certainly encouraging, experience has shown that synthesis and isolation can still be hard to achieve. As with other silaaromatics, trisilabenzene is expected to require highly bulky substituents for sufficient kinetic stabilization. We set out to develop a suitable synthetic

pathway, with a stable 1,3,5-trisilabenzene as the target compound. This portion of my research was conducted under the supervision of Dr. Yosiyuki Mizuhata, assistant professor at Norihiro Tokitoh's lab at ICR, Kyoto University. Chapter 3 covers our trials towards the synthesis of 1,3,5-trisilabenzene.

# 2 Alcoholysis of 1

We set out to further explore the type of alcoholysis reactions described in the Introduction. Previous research had given fairly unequivocal results concerning the effect of the steric bulk of the alcohol but we wanted to probe the effect of temperature and light on the rate of reaction when using MeOH as the alcoholysing agent. Secondly we wanted to examine whether the reaction was affected by the acidity of the alcohol. This factor is most easily explored by employing phenols as the alcoholysing agents because different substituents in the *para* position affect changes in the acidity of the hydroxyl group without disturbing the steric bulk around it significantly. In addition to these factors we set out to synthesize the dimer formed, in the case of MeOH, in a larger amount than before to obtain better NMR data for the pure compound and hopefully also shed some light on the fate of the $Cp^*$ group once it has been cleaved from the Titanium centre, as it was not detected in the spectra in previous experiments.

## 2.1 General information

Great care was put into the preparation of the chemicals for these reactions as they were expected to be ongoing for 2 years and any mistakes in preparation might not be realized until too late. MeOH p.a. was obtained from Merck, dried over $CaH_2$ and used freshly distilled. $CDCl_3$ was dried over $CaCl_2$ and distilled onto molecular sieves.

A mother solution containing $Cp^*Ti(\mu\text{-}O_3)[(^t\text{Bu})Si{-}CH_2]_3$ (**1**) (236.6 mg, 0.45 mmol) along with MeOH (1.45 mL, 36 mmol) and $CDCl_3$ (11.8 mL) was prepared under inert atmosphere. After thorough mixing to ensure a homogeneous solution, four portions of this solution were withdrawn and placed in NMR tubes. The solutions were frozen in liquid nitrogen, and the tubes evacuated and sealed off. The rest of the mother solution was placed in a glass ampoule which was sealed in a manner analogous to the NMR tubes. The ampoule, along with one of the NMR samples prepared (1a), was kept at room temperature (RT) and shielded from light. The intention was for this NMR sample to act as a window to what was going on in the larger ampoule without having to break its seal until the reaction had progressed far enough for a fair amount of the dimeric product to be obtainable. The other three NMR samples were placed in different conditions to monitor the effect of temperature and light. One sample was kept at RT, but exposed to natural light (1d) through a window. The other two were shielded from light by wrapping them in aluminium foil and kept at different temperatures.

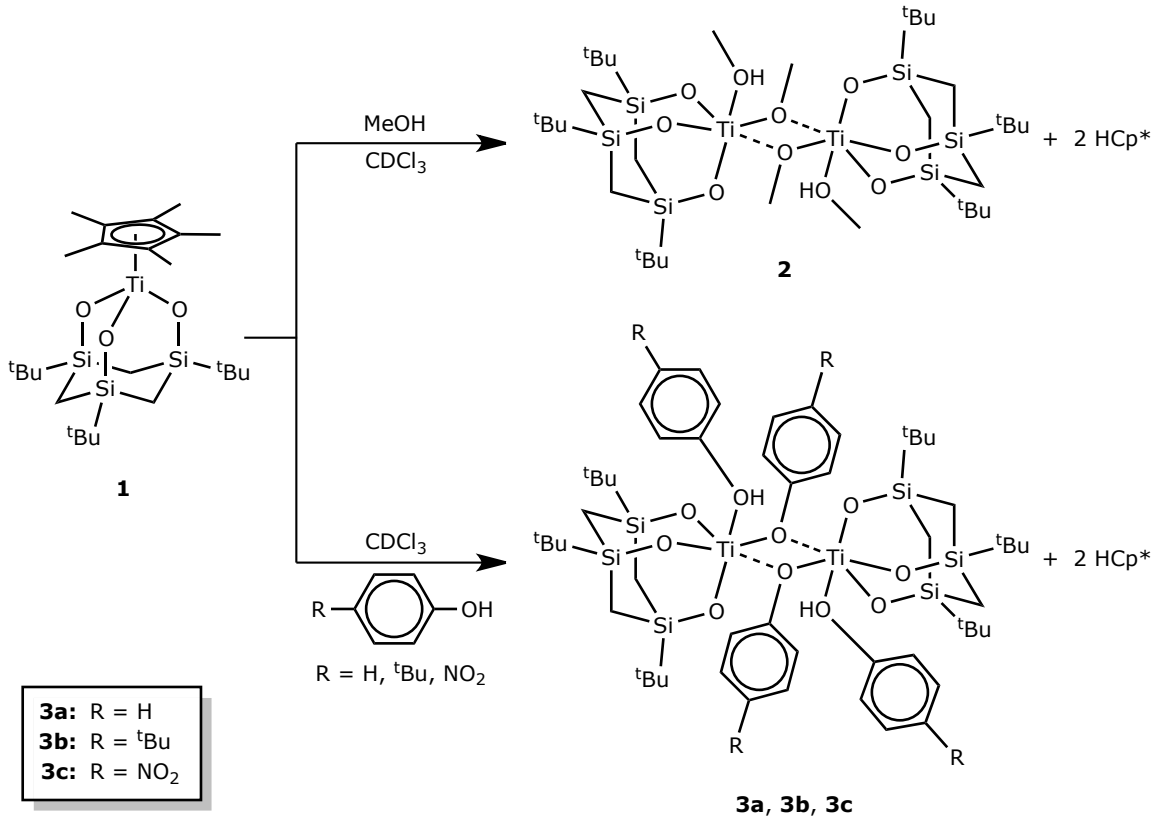


*Scheme 2.1: The expected dimeric products from the reactions of **1** and different alcohols.*

One was placed in a heating cabinet at 50 to 60 °C (1c) and one in a refrigerator at 4 to 10 °C (1b). These samples and their conditions are listed in Table 2.1 and Scheme 2.1 shows the expected product (**2**).

Three samples were prepared with phenols as the alcoholysing agents, one with unsubstituted phenol (2a) and two phenols with substituents in the *para* positions. The two substituted phenols were chosen so as to have one with an electron donating substituent (*para*-tertbutylphenol, 2b) and one with an electron withdrawing substituent (*para*-nitrophenol, 2c). The plan was to use $CDCl_3$ as solvent in all of these samples but in the case of *para*-

*Table 2.1: The samples prepared for study of the reaction of **1** with MeOH. As all these samples were extracted from the same mother solution they were initially identical: All had $CDCl_3$ as the solvent and a reactant ratio of 75 MeOH:**1**.*

| Sample No. | Temperature | Conditions |
|---|---|---|
| 1a | RT | shielded from light |
| 1b | 4 to 10 °C | shielded from light |
| 1c | 50 to 60 °C | shielded from light |
| 1d | RT | exposed to light |

*Table 2.2: The samples prepared for study of the reaction of **1** with phenols. All samples were kept at the same conditions, at room temperature and shielded from light.*

| Sample No. | Reactant | Reactant $pK_a$[a] | ROH:**1** | Solvents |
|---|---|---|---|---|
| 2a | PhOH | 9.99 | 16[b] | $CDCl_3$ |
| 2b | *p*-$^t$BuPhOH | 10.23 | 16[c] | $CDCl_3$ |
| 2c | *p*-($NO_2$)PhOH | 7.15 | 16[b] | $CDCl_3$/acetone-$d_6$ |

[a] $pK_a$ values are from CRC Handbook of Chemistry and Physics[23]
[b] obtained from integration of $^t$Bu peaks of **1** and aromatic protons of the phenol.
[c] obtained from integration of $^t$Bu peaks of both reactants.

nitrophenol its solubility proved too low so a few drops of acetone-$d_6$ were added as well. The samples prepared are described in Table 2.2 and Scheme 2.1 shows the expected dimeric products (**3a**, **3b** and **3c**).

$^1$H NMR spectra of the seven samples described above were measured approximately once a month for the first 400 days but more scarcely after that when very little change was observed.

### 2.1.1 Notes on the NMR spectra

All spectra reported in connection with these experiments were recorded on a 400 MHz spectrometer at RT. The signals that are most conveniently utilized for monitoring the transformation from the original adamantane shaped complex to the dimeric structure are the $^1$H NMR signals of the endocyclic protons. These are two distinct doublets with centers at −0.62 and −0.35 ppm (in samples 1a-1d, the exact shift varies in other samples) and coupling constants around 13 Hz (Figure 2.1). When alcoholysis and dimerization occur a new set of $H_{ax}$ and $H_{eq}$ peaks, stemming from the dimer, arise downfield from the ones for **1**. These are doublets with centres at −0.52 and −0.13 ppm and couplings constants close to 13 Hz. Thus as the reaction progresses this new set of doublets should appear and increase in ratio to the signals from **1**.

## 2.2 Results

To simplify comparison with results obtained in previous research on the subject we will adopt the same method of determining the extent of reactions as was described in Eyjólfsdóttir's thesis.[3] To obtain a ratio between the products and reactants, the peaks for comparable signals in the original complex and the formed dimer are integrated. This could mean integration of signals for $H_{ax}$, $H_{eq}$ or $^t$Bu. Defining $A_2$ and $A_1$ as the integral areas of the peaks

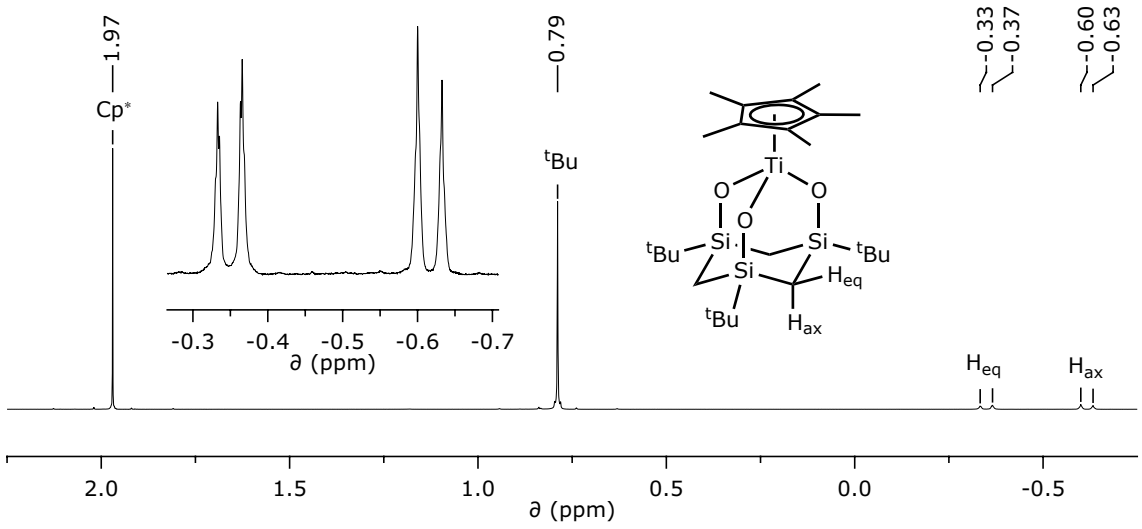


*Figure 2.1: $^1H$ NMR spectrum of **1** in $CDCl_3$/MeOH (mother solution). The expansion provides a clearer picture of the two doublets belonging to the protons of the trisilacyclohexane ring. Note that in the compound's spectrum in neat $CDCl_3$ (before the addition of MeOH) the signals have different chemical shifts. (A $^1H$ NMR spectrum of **1** in neat $CDCl_3$ can be found in Appendix A)*

for the dimer and **1**, respectively, the ratio of the dimer to **1** from integration, $r_{int}$, becomes:

$$r_{int} = \frac{A_{\mathbf{2}}}{A_{\mathbf{1}}} \tag{2.1}$$

Setting the integral of the peaks stemming from **1** to 1 enables us to read $r_{int}$ directly from the integral of the dimer's signal:

$$A_{\mathbf{1}} = 1 \quad \Rightarrow \quad r_{int} = A_{\mathbf{2}}$$

As each dimeric structure contains twice as many of the integrated groups as the original complex, the molar ratio of the dimer in a mixture with **1**, $r_{mol}$, is actually only half the ratio from the integration:

$$r_{mol} = \frac{r_{int}}{2} = \frac{A_{\mathbf{2}}}{2} \tag{2.2}$$

Taking this into account we calculate the mole fraction of the formed dimer, $\chi_{\mathbf{2}}$, setting the sum of the mole fractions of dimer and **1** to 1.

$$\chi_{\mathbf{2}} = \frac{\frac{A_{\mathbf{2}}}{2}}{1 + \frac{A_{\mathbf{2}}}{2}} = \frac{A_{\mathbf{2}}}{2 + A_{\mathbf{2}}} \tag{2.3}$$

This mole fraction is expressed in percentages in the text.

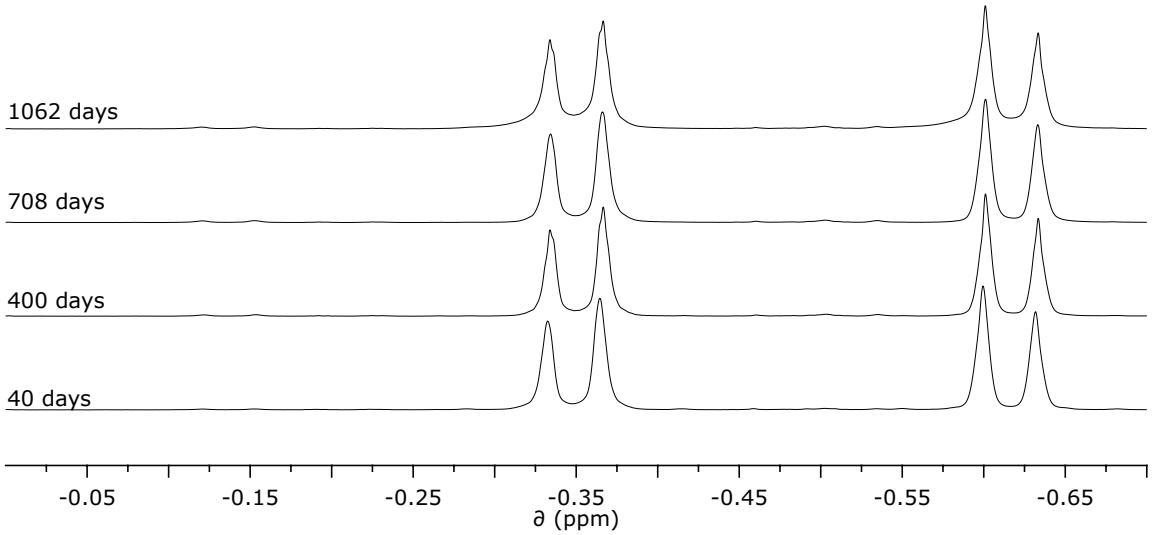


*Figure 2.2: Stacked $^1H$ NMR spectra of sample 1a at 40, 400, 708 and 1062 days. These spectra clearly show very little change, although a faint set of peaks assignable to the dimer can be seen at $-0.14$ and $-0.52$ ppm. Figure 2.3 shows this set of peaks more clearly.*

### 2.2.1 Sample 1a

As mentioned earlier this sample had a dual purpose, serving as a reference for the other samples as well as being informative of the changes taking place in the larger ampoule, which was kept at the same conditions. Based on previous results we expected noticeable transformation from the original complex to the dimer within a few weeks from the preparation of the samples. Previous experiments with comparable ratios of the reactants resulted in a 56% mole fraction of **2** in 378 days. Our results were radically different with the mole fraction reaching only 0.9% in 400 days and 2.4% in 1062 days. As considerable care was taken in the preparation of these samples, we found it unlikely that these results were caused by initial contamination of the sample. In addition, NMR spectra of the initial solution show no signs of contaminants. Contamination after the sample's preparation is practically impossible as the tube was sealed off. In light of this there are two conceivable explanations for the discrepancy in results: There may have been a substance present in the samples in previous experiments that is missing from our samples, or the dissimilarity is caused by a difference in storing conditions. No known contaminants were precent in previous experiments, but as the same care may not have been taken to eliminate all traces of water from the alcohol as in this case, the existence of trace amounts of water is not inconceivable.

### 2.2.2 Sample 1b

This sample was wrapped in aluminium foil and kept at 4 to 10 °C in a refrigerator. At the first and second measurements from the mixing of the reactants (at 40 and 76 days,

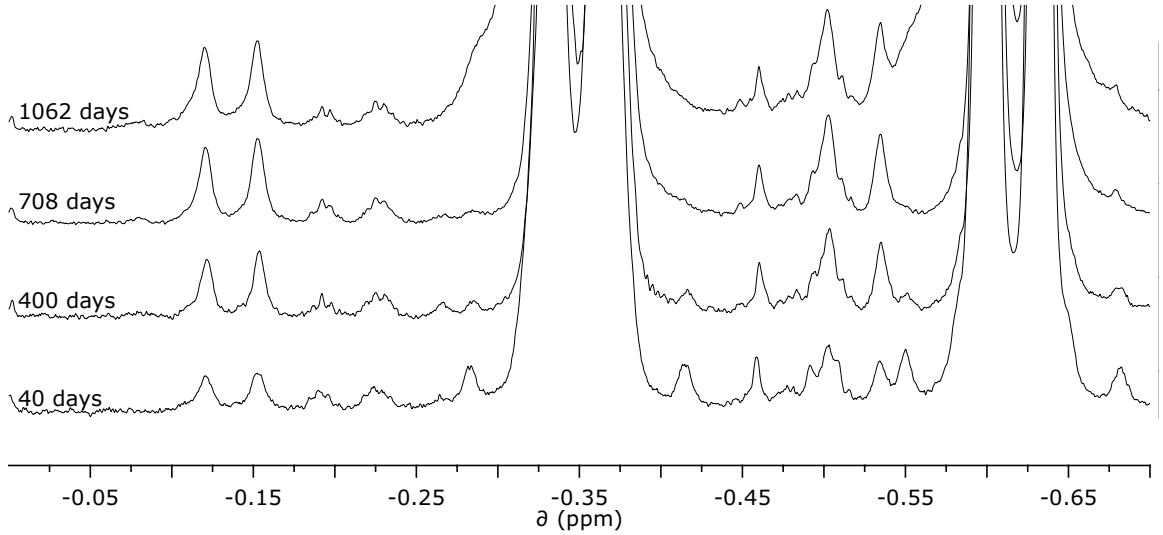


*Figure 2.3: Signals from **2** in $^{1}H$ NMR spectra of sample 1a.*

respectively) the sample's spectra showed no significant signs of a change. However, at the third measurement, after 124 days of reaction, drastic changes were found in the spectrum. At this point nothing remained of the signals assignable to **1** but two sets of peaks had arisen downfield, one at the chemical shifts expected for **2** and another set of two doublets at −0.44 and −0.07 ppm. The compound giving rise to these peaks has not been identified, but signals at these chemical shifts have been recorded before in a single sample with comparable reactant ratios and the same solvent. That sample did differ from ours in that it was kept at RT and showed gradually increasing signals for the dimer and the unidentified compound during the 56 days it was monitored.[24] As in previously measured spectra where a reaction between **1** and MeOH has taken place, the spectra recorded of this sample from the third measurement (124 days) and onward show no sign of $Cp^*$ bonded to the titanium centre. There are however a large number of smaller peaks visible in the area between 0.3 and 1.8 ppm that were not present in the sample's spectra before the reaction and among those peaks are signals that can be assigned to $HCp^*$ (Fig. 2.4). Integration reveals the ratio of these signals to the signals assigned to **2** to be consistent with $Cp^*$ dissociating from the metal centre, forming $HCp^*$, during dimer formation.

The sample was kept in the same conditions long after this dramatic change had occurred and measured at regular intervals, but as the spectrum recorded after 1062 days of reaction (Figures 2.5 and 2.6) shows, no further changes were observed.

### 2.2.3 Sample 1c

This sample was kept in a heating cabinet at 50 to 60 °C. Like samples 1a and 1b it was shielded from light by wrapping it in aluminium foil. The formation of **2** is somewhat more

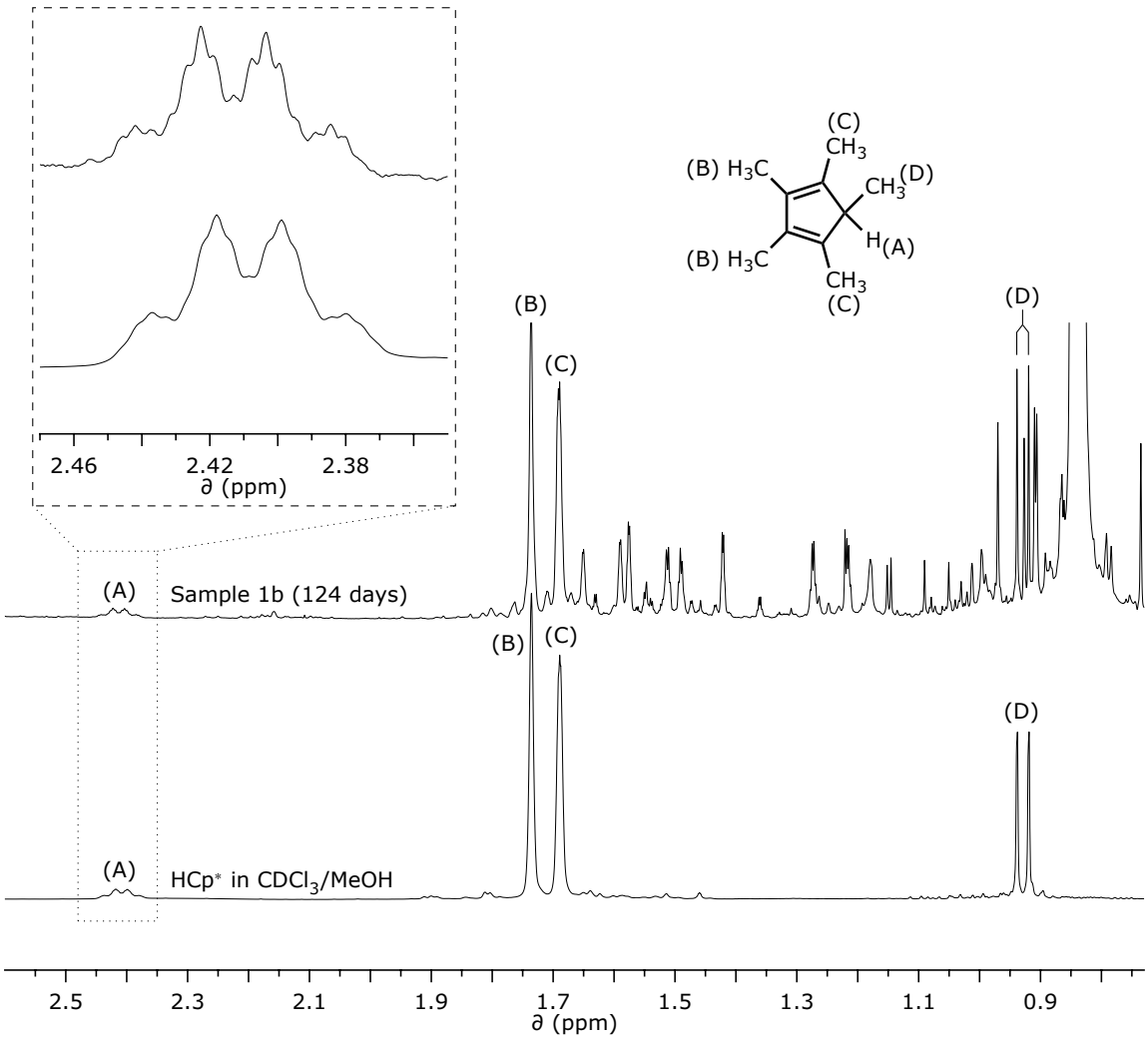


*Figure 2.4: Proof of $HCp^*$ in a $^1H$ NMR spectrum of sample 1b. The lower spectrum is recorded of $HCp^*$ in a mixture of $CDCl_3$ and MeOH. As the MeOH ratio in the two samples was not exactly the same, chemical shifts are slightly different. To make the comparison of signals easier, the lower spectrum has been shifted* 0.02 *ppm to the right.*

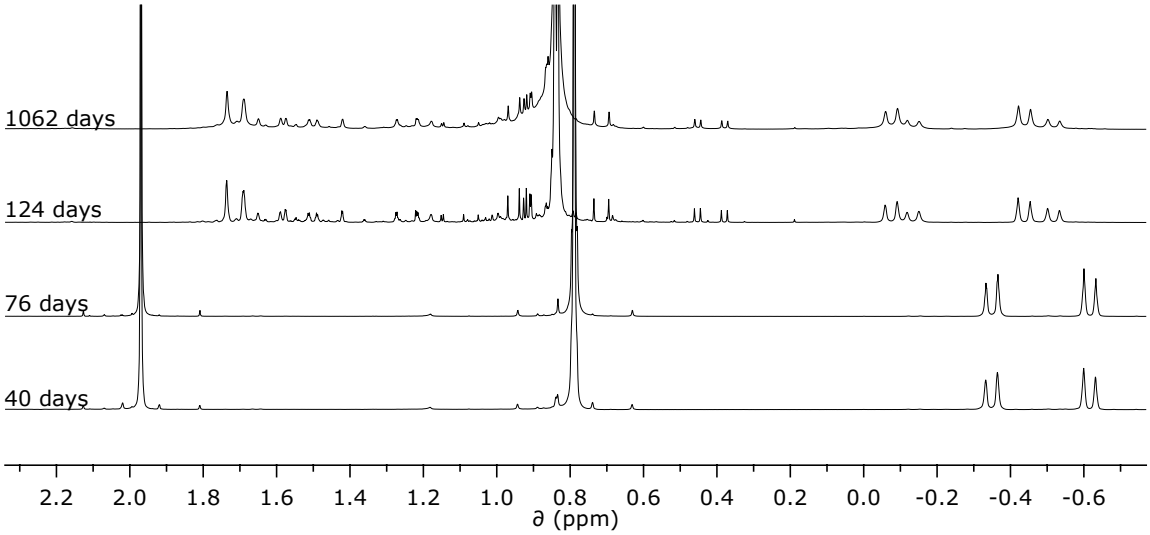


*Figure 2.5: Stacked $^{1}H$ NMR spectra of sample 1b at 40, 76, 124 and 1062 days.*

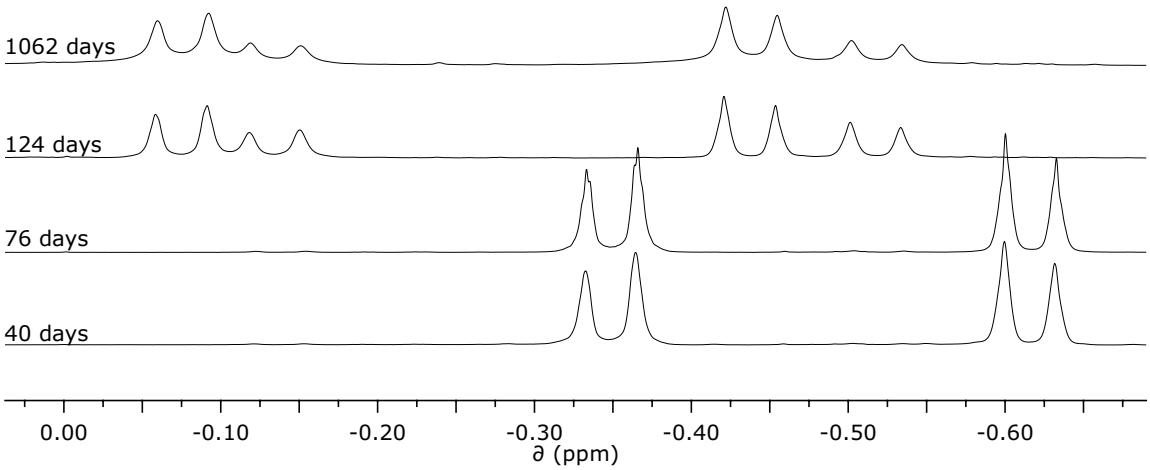


*Figure 2.6: Stacked $^{1}H$ NMR spectra of sample 1b at 40, 76, 124 and 1062 days.*

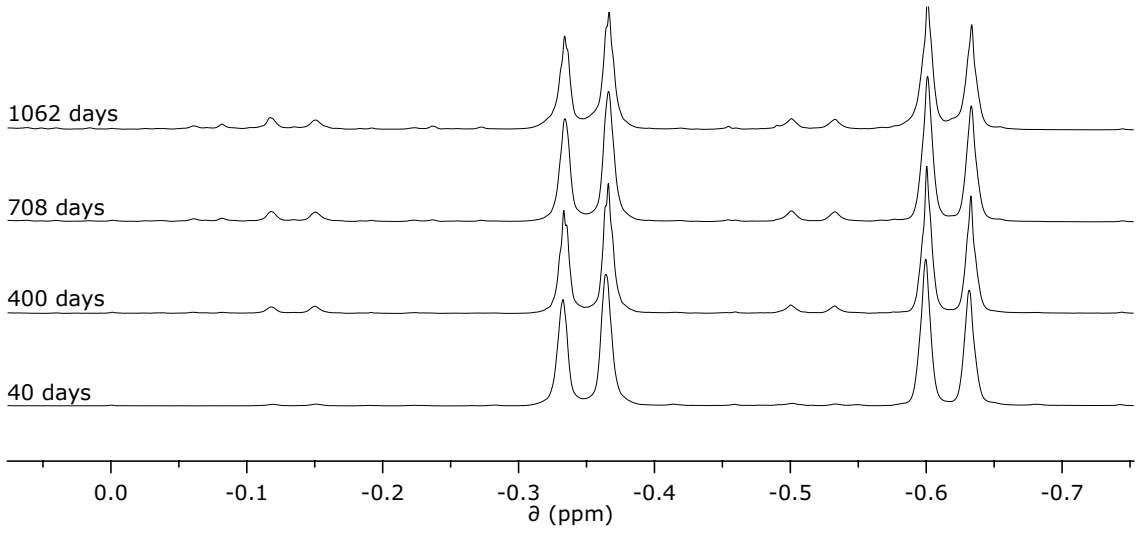


*Figure 2.7: Stacked $^{1}H$ NMR spectra of sample 1c at 40, 400, 708 and 1062 days. Although the changes here are less than dramatic, they are incontrovertibly clearer than in the case of 1a.*

rapid here than in the reference sample (1a), although it remains far below the values obtained in previous research, reaching only 2.9% in 400 days and 3.2% in 1062 days. Despite these changes being modest in comparison with previous results the faster reaction rate in this sample than the reference is indisputable. This difference can even be clearly witnessed by simple visual comparison of the stacked spectra for samples 1a (Fig. 2.2) and 1c (Fig. 2.7).

### 2.2.4 Sample 1d

This sample was the only one not wrapped in aluminium foil. It was kept near a window in the lab and was thus exposed to natural light. Already at the time of the first measurement, 40 days after the preparation of the samples, this sample showed vast decomposition of **1**. The large number of small peaks immediately visible in the measured spectrum led to the dismissal of this sample as a failure and clear indication of the reactions intolerance to exposure to light. It was only upon revising this spectrum during the work on this thesis that I realized the rejection of this data as informative had been a mistake. The disintegration of **1** is indeed undeniable and there is an appreciable number of small peaks from 0.3 to 1.8 ppm visible in the spectrum which did not exist before. However, as discussed above, this is also the case for sample 1b and upon closer inspection the two samples are quite comparable (Fig. 2.8). The same two sets of pairs of doublets exist in sample 1d after 40 days as in sample 1b after 124 days (Fig. 2.9). Additionally these signals appear in almost equal ratios (**2**:unknown compound integrates as 40:60 in 1b and 42:58 in 1d). Peaks assignable to $HCp^{*}$ are visible in these spectra as in the case of 1b. These newly discovered facts have a great impact on the conclusions that can be drawn from this research.

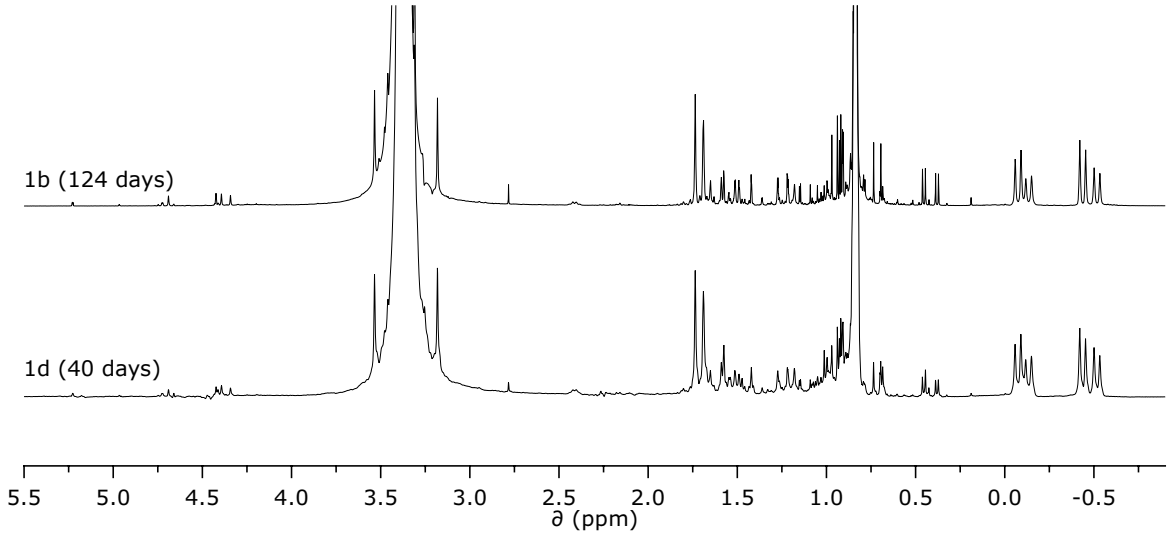


*Figure 2.8: Comparison of $^{1}H$ NMR spectra of samples 1b and 1d after 124 days and 40 days of reaction, respectively.*

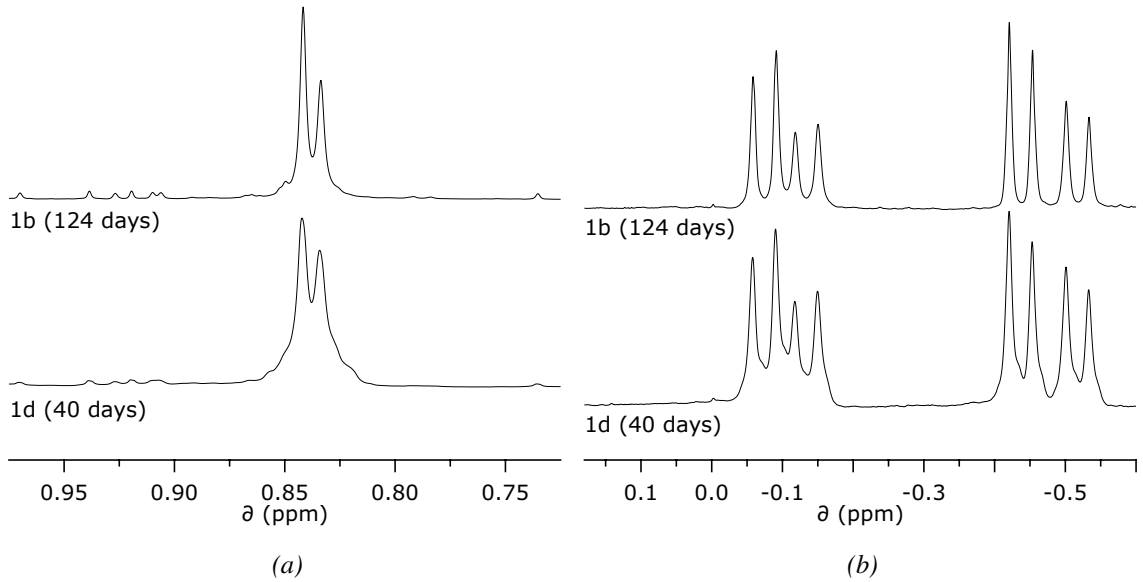


*Figure 2.9: A closer look at the $H_{eq}$, $H_{ax}$ (b) and $^{t}Bu$ (a) signals of samples 1b and 1d after 124 days and 40 days of reaction, respectively.*

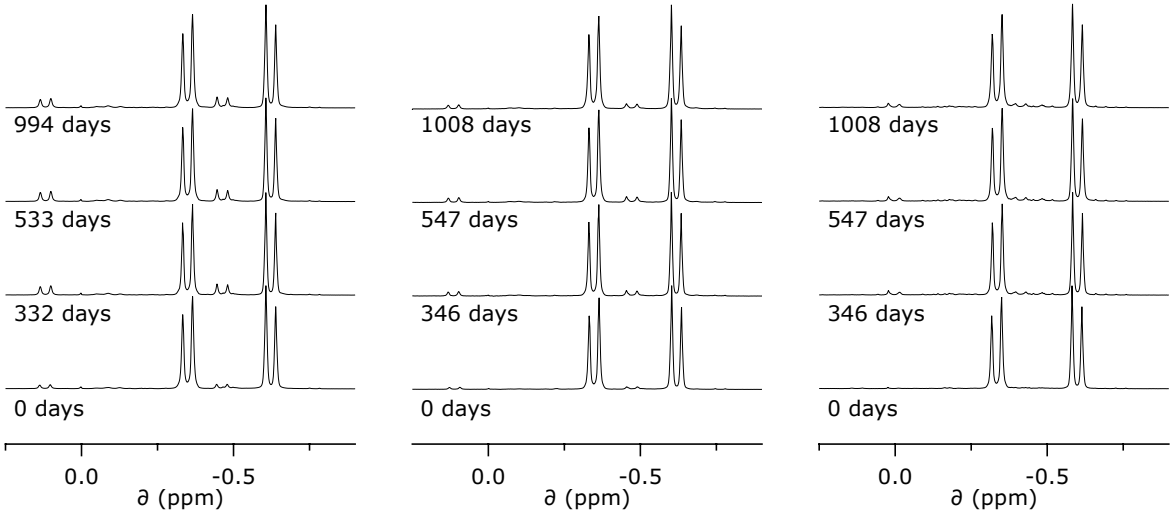


*(a) Sample 2a* *(b) Sample 2b* *(c) Sample 2c*

*Figure 2.10: Comparison of $^1H$ NMR spectra of samples 2a-2c. The spectra show that the reaction of **1** with the phenols, although in all cases slow compared to previous results with PhOH, is notably faster with unsubstituted PhOH than the substituted ones. Note that signals from product formation are already visible in the first measurement of samples 2a and 2b.*

### 2.2.5 Samples 2a-2c

The samples containing the different phenols were kept at the same conditions as sample 1a and the larger ampoule of the MeOH alcoholysis experiment. In short, the changes that took place in these samples were unimpressive. The sample containing unsubstituted phenol as the reactant showed more conversion than the other two, with the signals previously assigned to **3a** reaching 5.5% in less than a 100 days. After that, however, the ratio stabilized and did not exceed that value throughout the measuring period. Despite this very slow reaction throughout the research period, an interesting thing to note here is the immediate onset of the reaction as the first spectra of all three samples, recorded on the same day as the samples were prepared and sealed, showed signs of reaction, although in the case of 2c these signals were extremely faint.

One factor that is notably different in samples 2a-2c compared to those containing MeOH as a reactant, is the emergence of a second signal in the Cp* area which grows in proportion (15:3) to the $H_{ax}$ and $H_{eq}$ signals previously assigned to dimers. This is a singlet signal and therefore does not fit the spectrum of HCp*. This is an indication that the compounds being formed are not the expected dimers (**3a**-**3c**) but rather compounds where the titanium is still coordinated to the Cp* as well as being part of the adamantane-like cage.

## 2.3 Discussion

The meaning of our results described above was, to some degree, a mystery to us for a good while. It is only with the recent discovery concerning the fate of sample 1d, the one exposed to light, that an explanation for the differences between our results and those obtained in earlier research in actuality began to take shape.

A special storage vessel was prepared for the samples that were not being kept at special temperature conditions. This vessel housed samples 1a, 2a, 2b and 2c along with the larger ampoule containing the MeOH stock solution. The vessel consisted of a plastic cylinder with a screw cap and was lined with aluminium foil which could be folded over the top of the vessel's contents before screwing the cap on. These samples were thus kept at conditions extremely well shielded from light. The remaining two samples that we intended to shield from light, samples 1b and 1c, were also wrapped in aluminium foil, but with the tops of the NMR tubes exposed. Both these samples were kept in places where they should not experience much light in any case, in a refrigerator and heating cabinet, respectively. The heating cabinet was not used for anything other than this research throughout the monitoring period and thus was kept closed, except for the removal of the sample for measurements and for its replacement. The refrigerator is used by four lab members making that sample more likely to be exposed to light. Thus it can be concluded that in addition to the different temperature conditions experienced by sample 1b it may have had considerably more light exposure than samples 1a and 1c, which it was being compared to. This fits well with the close likeness discovered between samples 1b and 1d. Additionally this might explain the difference between our results and those obtained previously with samples of comparable composition, as those samples, although partly sheltered from light, were only shielded by wrapping the lower portion of the NMR tubes in aluminium foil and were kept in an electrically lit room. However, as previously stated, we cannot rule out the presence of e.g. trace amounts of water in the samples during previous studies which may also have affected the reactions.

Deducing from the fact that, after only 40 days of reaction, nothing remained of unreacted **1** in the sample wilfully exposed to light and that a large portion ($\sim 60\%$) of the products formed did not have the intended dimeric structure, unhindered light exposure is not optimal for what we wanted to achieve. However, the results concerning the samples that were completely shielded from light, except around the time of measurement, show that an absolute lack of light exposure is detrimental to the rate of the reaction. So much so, that studying it under those conditions is very impractical. In light of these discoveries a suitable quantity of light exposure would need to be found to make further research into these reactions feasible. Only then could samples at different conditions with respect to other factors such as temperature be expected to yield meaningful data in a sensible time frame.

With all these factors taken into account there are some conclusions, excluding the effect

of light, that can be drawn from our data. Firstly, signals assignable to $HCp^*$ have been detected in the spectra of samples 1b and 1d, confirming that $HCp^*$ is indeed a byproduct of the dimer formation. Secondly, as samples 2a-2c were all kept at the exact same conditions, the faster reaction rate in sample 2a compared to the other two can be contributed to the difference in reactants. Thus it appears that using unsubstituted phenol does indeed result in a higher rate of reaction than the two *para* substituted phenols we tested (4-*tert*-butylphenol and 4-nitrophenol). We speculate that, despite the substituents being in the *para* positions, in the case of $^t$Bu the steric bulk may be sufficient to reduce the rate of reaction through steric hindrance, thus working against the increase in reaction rate that the higher $pK_a$ value could conceivably bring about. Thirdly, as the $Cp^*$ signals found increasing in ratio with those previously assigned to dimers in the spectra of samples 2a-2c are singlets, they can not be attributed to $HCp^*$. This is a strong indication that the products of these reactions are not dimeric. Lastly, as samples 1a and 1c were kept under similar conditions concerning exposure to light and 1c showed conversion ratio close to a third higher than 1a, it is likely that mild heating has a positive effect on the reaction rate.

# 3 Synthesis and analysis of derivatives of 4

As described in the Introduction, we set out to develop a synthetic pathway to 1,3,5-trisilabenzene. Our starting material was 1,3,5-trisilacyclohexane (**4**), synthesized by Nanna Rut Jónsdóttir as described in her M.Sc. thesis.[25] The idea was to obtain a compound with each of the ring's silicon atoms carrying two substituents: A halogen atom (chlorine or bromine) and a bulky group for kinetic stabilization. Such a compound should be suitable for reaction with a strong base to remove three equivalents of hydrogen halide and form an aromatic ring system. In such a pathway a suitable substituent needs to be found. It should be bulky enough to provide the much needed kinetic stabilization, but not so bulky as to prevent access by the base in the final step of synthesis. As **4** has three silicon centres the situation around the ring becomes much more crowded than in the case of e.g. monosilabenzene. In light of this the stabilizing substituent in this case needs to be considerably less bulky then the enormous Tbt group utilized in syntheses of the monosilaaromatics already described.

Several synthetic routes can be visualized from **4** to a 1,3,5-trisilabenzene with bulky substituents on the silicon atoms. The routes we decided to explore can be seen in Scheme 3.1 and routes and steps referenced hereafter in this chapter pertain to those outlined in said scheme. Although all three bulky substituents are denoted by a single symbol in the scheme and a compound with three identical substituents is desirable from an aesthetic viewpoint, compounds with a mixture of different substituents were of course considered as well.

## 3.1 Aryl substituted 4

### 3.1.1 1,3,5-Triaryl-1,3,5-trisilacyclohexane (5 & 6)

Our first synthetic trials belonged to Route 1, as put forward in Scheme 3.1. As per the first step of that route, we decided to attempt triple substitution of **4** with groups somewhat bulkier than phenyl but not too much so. On this basis we selected two aryl groups, mesityl (Mes) and 2,6-di(isopropyl)phenyl (Dipp), as suitable candidates (Fig. 3.1). Lithiated species are suitable reagents for the substitution of hydrogen bonded to silicon and so reactions were carried out where lithiated reagents were prepared *in situ* by reactions of $^{t}$BuLi with the corresponding bromides in cooled (−75 °C) THF solutions. These reagents were subsequently introduced into cooled (−75 °C) THF solutions of **4**. The reaction procedures are described

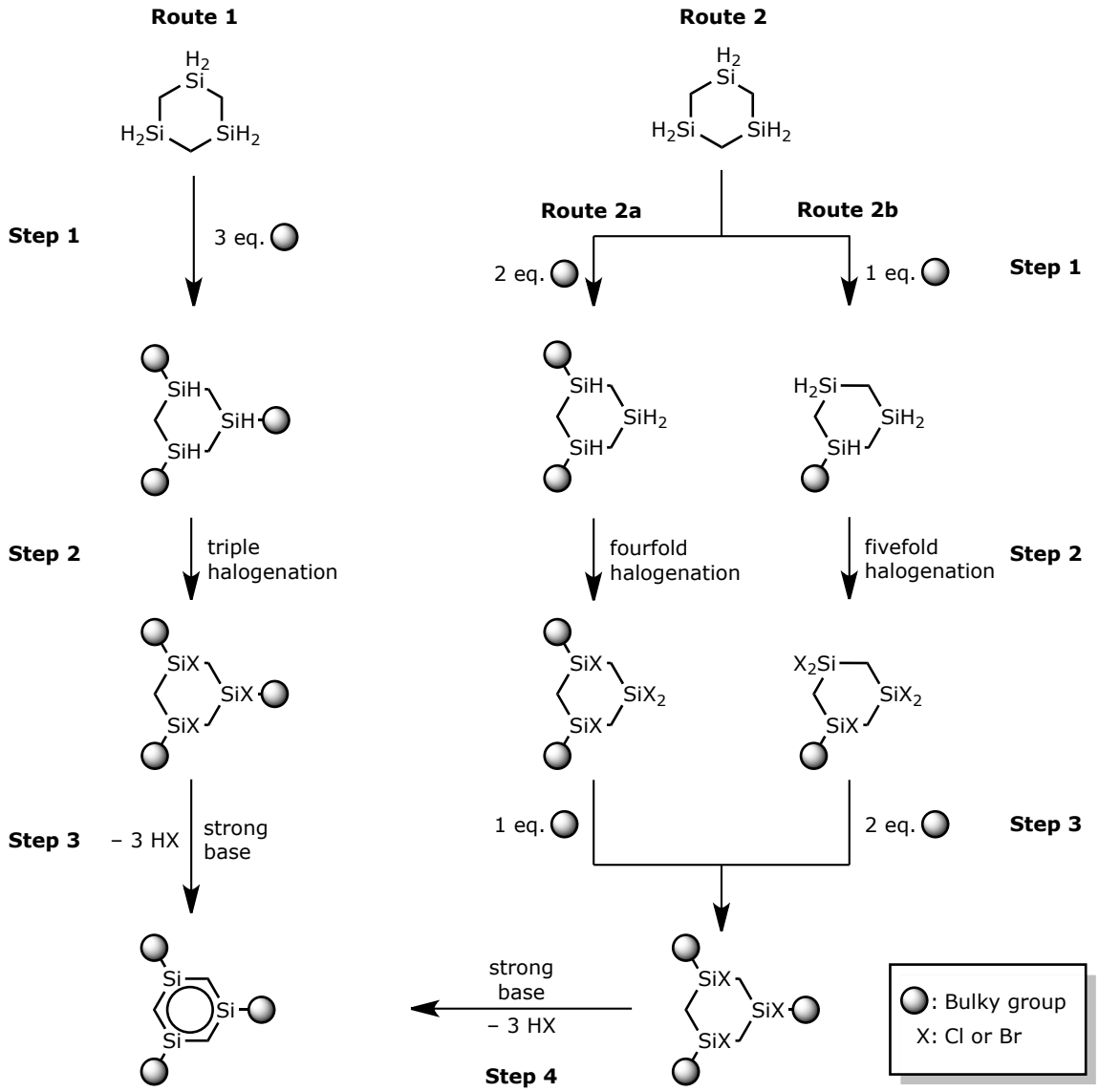


*Scheme 3.1: Several synthetic routes towards 1,3,5-trisilabenzene can be envisioned with 1,3,5-trisilacyclohexane (**4**) as starting material. This scheme outlines the routes we explored. The bulky groups, although denoted by a single symbol, could well be a mixture of different substituents.*

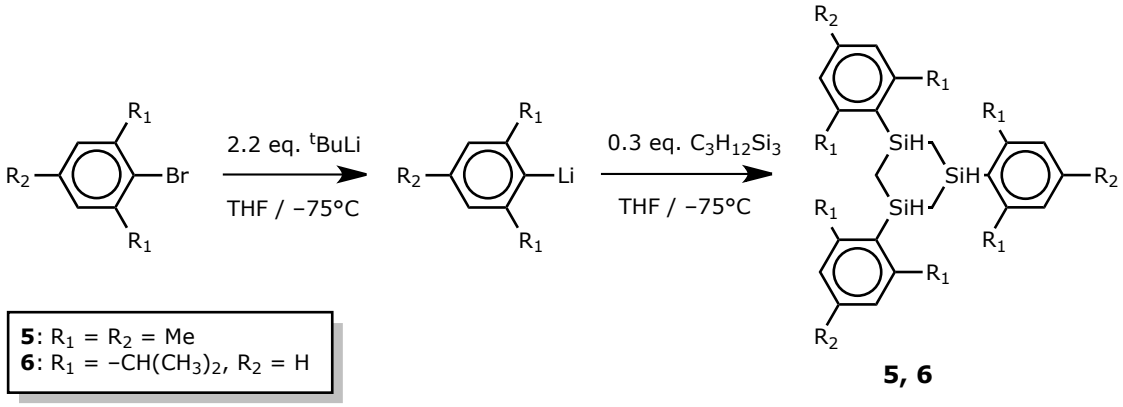


*Scheme 3.2: Syntheses of trisubstituted 1,3,5-trisilacyclohexane derivatives with aryl substituents (Mes, Dipp).*

in Scheme 3.2.

Mesitylbromide (MesBr) was obtained from Aldrich but 2-bromo-1,3-diisopropylbenzene (DippBr) was synthesized from 2,6-diisopropylaniline via Sandmeyer bromination.

The reactions of MesLi and DippLi with **4** yielded isomeric mixtures of 1,3,5-tri(Mes)-1,3,5-trisilacyclohexane (**5**) and 1,3,5-tris(Dipp)-1,3,5-trisilacyclohexane (**6**), respectively, in relatively high yields, although some decomposition of the DippLi reagent occurred forming 1,3-diisopropylbenzene (Dipb) and thereby lowering the yield of the Dipp derivative. The product mixtures in both cases contained a *cis,cis*-isomer as the major product, with *cis,cis*-1,3,5-tri(Mes)-1,3,5-trisilacyclohexane (**5a**) accounting for ~ 70% of **5** but a larger ratio in the case of *cis,cis*-1,3,5-tris(Dipp)-1,3,5-trisilacyclohexane (**6a**), although the exact ratio could not be determined. Both compounds were characterized by NMR and single crystal X-ray analysis. Poor results from the attempted halogenation of **5**, which are outlined in Section 3.2.1, led to our decision to abandon mesityl as a viable substituent, at least when following Route 1.

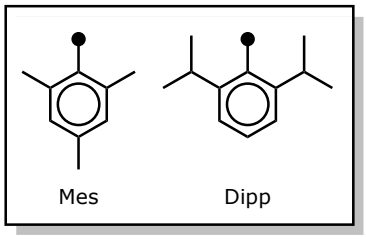


*Figure 3.1: The aryl groups chosen for Route 1.*

### 3.1.2 1-(Dipp)-1,3,5-trisilacyclohexane (7)

An attempt was made to synthesize 1,3-bis(Dipp)-1,3,5-trisilacyclohexane as per Route 2a, Step 1. As the formation of **6** had proceeded well, care was taken not to exceed a reactant ratio of 2:1 for DippLi:**4**, to prevent contamination of the product by the formation of the tris-derivative. During workup it became apparent that the intended compound had not been formed although no unreacted **4** remained (Scheme 3.3). The crude reaction product was found to contain a mixture of Dipb and 1-Dipp-1,3,5-trisilacyclohexane (**7**), a product expected from Step 1 in Route 2b. The formation of Dipb in this reaction further underlines the

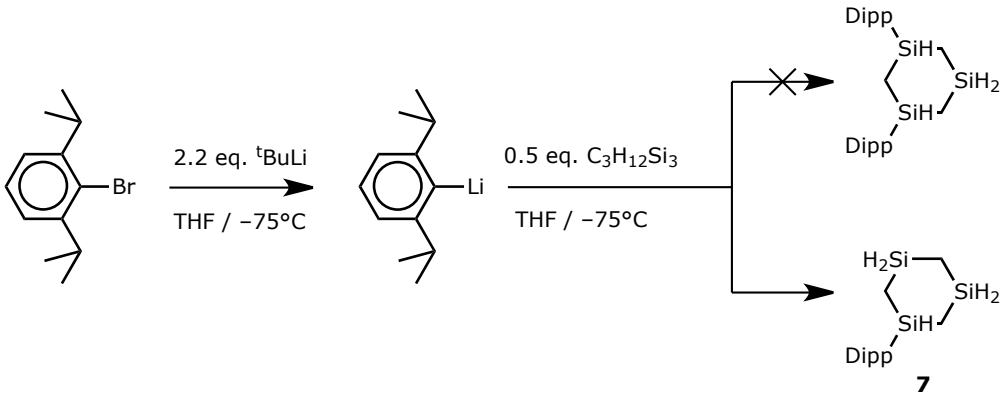


*Scheme 3.3: An attempt to produce 1,3-bis(Dipp)-1,3,5-trisilacyclohexane as per Route 2a, Step 1 (Scheme 3.1) resulted in the formation of 1-Dipp-1,3,5-trisilacyclohexane (**7**) – a product expected from Route 2b, Step 1.*

short lifetime of the DippLi reactant already mentioned. After this result we also attempted the selective synthesis of **7**, lowering the DippLi:**4** ratio to 1.1:1, which resulted in less than full conversion of **4**.

The main product, **7**, was isolable from the Dipb side product by HPLC (high performance liquid chromatography), ultimately giving ~32% yield of the pure compound. Additionally we managed to form crystals suitable for X-ray crystallographic analysis of **7** by sublimation upon mild heating (~ 45 °C) under vacuum, however the crystals proved quite delicate and partly dissolved in the oil used to cut the crystals to a size suitable for analysis. In spite of this a crystal structure was obtained for the compound. In addition to crystallographic analysis the compound was characterized by NMR spectroscopy.

## 3.2 Halogenation of derivatives of 4

Several attempts were made at the halogenation of the different derivatives of **4** described above, with varying degrees of success. The following subsections cover our halogenation trials.

### 3.2.1 Attempted bromination of 5

The first reaction, belonging to the halogenation step (Step 2) in Scheme 3.1, that we attempted, was the bromination of **5** by elemental bromine in hexane (Scheme 3.4). The product of this reaction was a complex mixture. Analysis by $^1$H NMR suggested that bromination of the methyl groups in *ortho* positions on the Mes substituents had occurred. This was confirmed with DEPT-135 measurements showing signals for several different $CH_2$ groups (Appendix F). As previously mentioned this vulnerability of the mesityl group's *ortho*-position methyl groups towards halogenation led us to abandon mesityl as a suitable substituent for

Route 1.

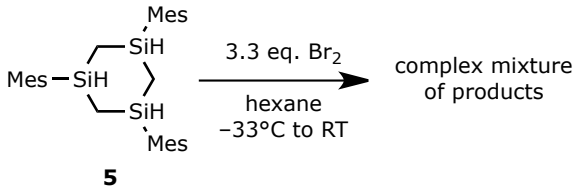


*Scheme 3.4: The procedure for our attempt at the bromination of **5**.*

### 3.2.2 Attempted bromination of 6

Two methods were explored for the bromination of **6** (Scheme 3.5). The first attempt was by reaction with N-bromosuccinimide (NBS) in benzene at RT. This reaction resulted in complete dissociation of **6** at the Si−C bond between the Dipp substituent and the silicon atoms in the ring, giving DippBr as the main product. As this result could conceivably be attributed to the excessive speed of introduction of the NBS (it was introduced in a single dose), a second attempt was made with several precautions being taken to prevent the contact of **4** with NBS from occurring too rapidly. This reaction was carried out by adding the NBS in small portions to a solution of **6** in hexane at 0 °C. The cooling as well as NBS's poor solubility in hexane was thus intended to soften the reaction conditions making the cleavage of the Si−C bond less likely. $^{1}$H NMR analysis of the reaction's products revealed more than one Si−H signal as well as signs of DippBr, indicating incomplete bromination of the silicon atoms and cleavage of the Si−C bond, respectively.

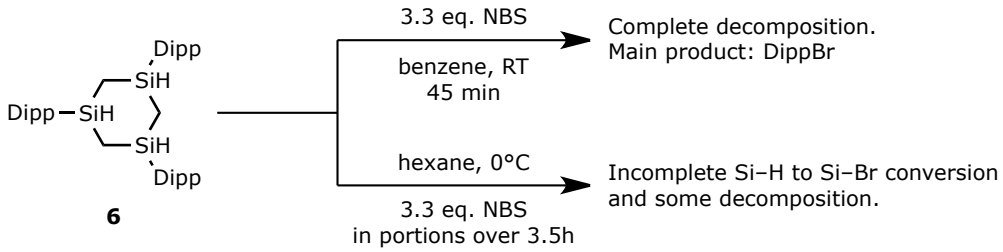


*Scheme 3.5: Bromination trials of **6**.*

These problems with the bromination of **6** may be caused by simple steric problems. Examination of a space filling model of the compound (Fig. 3.2) clearly reveals a congested situation. Taking into consideration that the covalent radius of a bromine atom is more than five times that of hydrogen (1.21Å and 0.23Å, respectively[23]), corresponding to an almost 150-fold volume, the triply brominated compound would be extremely congested.

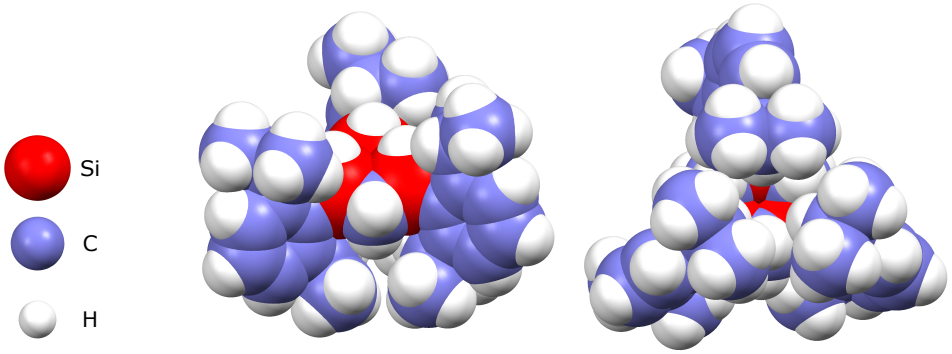


*(a) "Top" view* *(b) "Bottom" view*

*Figure 3.2: A space filling model of **6** from X-ray analysis. When viewed from the "top" (a) the congestion around the Si–H is clearly visible. Aquiring more space on that side is however impossible because of the buttressing effect of the isopropyl groups on the other side. This becomes apparent when the molecule is viewed from the "bottom" (b).*

### 3.2.3 Attempted bromination of 7

In light of the predicted congestion of a tribrominated derivative of **6** the idea arose to perform full bromination (fivefold) of **7** as per Route 2b, Step 2, and subsequently substitute two of the bromine atoms, one on each dibrominated silicon, for a group less bulky than Dipp. This could mean a less bulky aryl group (e.g. Mes), phenyl or even smaller groups such as *tert*-butyl. To this end the bromination of **7** was attempted with NBS in hexane at 0 °C with the NBS introduced in small doses over several hours (Scheme 3.6). Analysis of the product mixture revealed incomplete conversion from Si–H to Si–Br. In light of more promising results with chlorination, as outlined hereafter, no further attempts were made at the bromination of **7**.

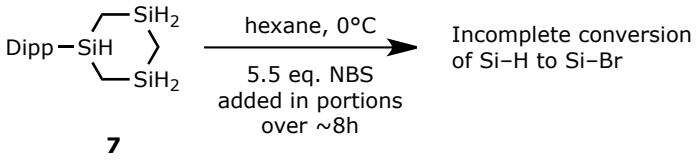


*Scheme 3.6: Procedure for the attempted bromination of **7**.*

### 3.2.4 Chlorination of 6

As brominations of **6** had proved difficult, presumably because of steric forces as outlined above, we decided to attempt chlorination instead. Two different methods of chlorination were trialled with one giving significantly better results than the other.

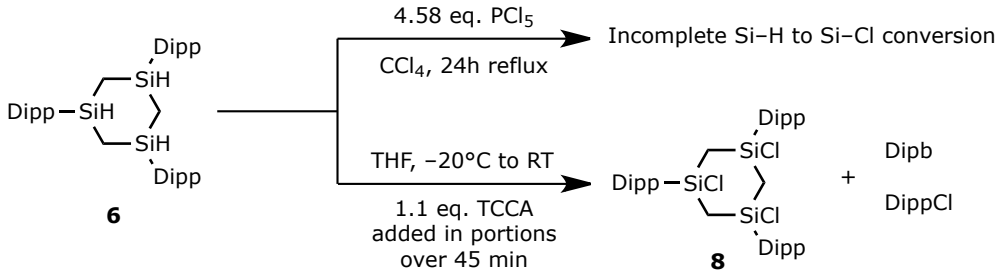


*Scheme 3.7: Procedure for the chlorination of **6**. Reaction of **6** with TCCA yielded **8**.*

## Chlorination by $PCl_5/CCl_4$

For the chlorination of **6** we chose a procedure previously successful in the chlorination of several silanes,[26,27] some of them with quite bulky substituents, e.g. trimesitylsilane and even tridurylsilane (duryl = 2,3,5,6-tetra(methyl)phenyl). By this procedure the chlorination should take place in a refluxing solution of the silane in tetrachloromethane along with phosphorus(V)chloride. $^1$H NMR analysis of the product mixture revealed unreacted Si−H as well as a complicated pattern of signals in the region of the side chain methyl groups of Dipp, indicating that some of the desired product may have formed but full conversion had not been achieved. Additionally some decomposition occurred during workup rendering the residue virtually insoluble in hexane, benzene, chloroform and THF. This may have been a result of insufficient quenching of unreacted $PCl_5$. As a different chlorination method proved more successful, this procedure was abandoned.

## Chlorination by TCCA

A second procedure tested for the chlorination of **6** utilizes trichloroisocyanuric acid (TCCA) as the chlorinating agent. TCCA which is produced in vast amounts (>100 000 $^t/_{year}$ worldwide of TCCA and its monosodium salt combined in 2002[28]) mainly for disinfection of swimming pools and for water treatment, has three chlorine atoms all of which are readily available for reaction. It has been noted that despite the proven usefulness of this compound as a reagent in the chlorination of several types of compounds (e.g. cyclic ethers, alkenes, ketones[29]), for some reason it has neither gained much prominence in organic chemistry laboratories nor been covered in organic chemistry textbooks.[28] Varaprath and Stutts, in 2007, reported its effectiveness (>90% yield in most cases) in the chlorination of several silanes and siloxanes, among which were compounds like diethoxyphenylsilane and the relatively crowded triphenylsilane.[29]

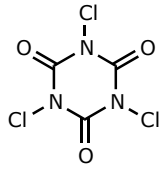


*Figure 3.3: TCCA.*

The procedure consist of TCCA, in a slight excess, being added in portions to a solution of the silane. Using THF as solvent, as we did, requires the solution to be cooled to −20 °C to restrain the exothermic reaction and prevent chlorination of the solvent. When the addition

of TCCA is complete the solution is allowed to warm up to RT. The desired products can be isolated from the excess TCCA and the cyanuric acid by removal of the polar THF and extraction by hexane in which these impurities are insoluble.

Using the method described above **6** was reacted with TCCA (Scheme 3.7). Analysis of the product mixture revealed full conversion from Si−H to Si−Cl, producing 1,3,5-trichloro-1,3,5-tris(Dipp)-1,3,5-trisilacyclohexane (**8**). The desired product was, however, contaminated with a compound having NMR signals consistent with DippCl as well as a very small amount of Dipb. Purification by recrystallization and HPLC has been attempted but resulted in an extremely low yield of almost pure **8** and decomposition, respectively.

## 3.3 Attempted synthesis of 1,3,5-trisilabenzene

In light of a rapidly closing timeframe on my research period in the Tokitoh laboratory we decided to attempt the final reaction of the most successful synthetic route we had come up with, despite the fact that the precursor (**8**) had not yet been successfully purified. This meant the reaction of **8** with a strong base as per Route 1, Step 3. Two trials were performed, both utilizing lithium diisopropylamide (LDA) as the base but with different solvents and at different temperatures (Scheme 3.8). The product mixtures of these trials were analysed by $^{1}$H NMR, $^{13}$C NMR and $^{29}$Si NMR but no signals assignable to the intended aromatic product could be detected in any of the spectra.

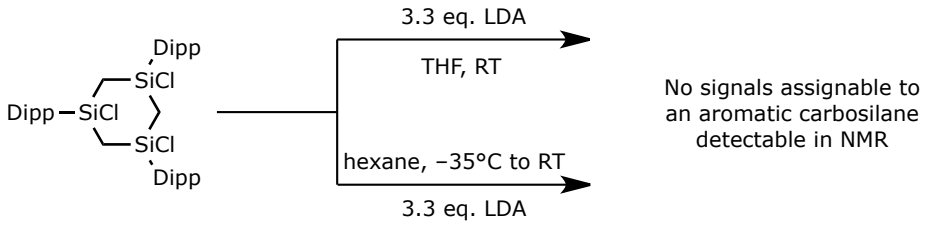


*Scheme 3.8: The two methods trialled so far for the production of 1,3,5-trisilabenzene by the reaction of **8** with a strong base.*

## 3.4 Summary

A suitable pathway has been established for the synthesis of **8** which is probably a well suited precursor for 1,3,5-trisilabenzene. Two main jobs remain concerning this compound: One is to find a suitable method for the purification of **8** and secondly to find the right combination of solvents, base and conditions to achieve the formation of an aromatic system. The previous syntheses of aromatic carbosilanes performed by the Tokitoh group required much fine tuning of the reaction conditions before the intended products were obtained. This

is despite the fact that in the case of monosilaaromatics unsaturation already exists in the precursors and only one double bond needs to be formed to achieve aromaticity. In light of this it is unsurprising that these initial trials on the final step of our synthetic pathway did not lead to the formation of 1,3,5-trisilabenzene as this requires the simultaneous or consecutive formation of three Si−C double bonds. However, the initiation of an aromatic system is a powerful force and, as has been noted in the introduction, theoretical examinations predict 1,3,5-trisilabenzene to be planar and highly aromatic. Interference by the contaminants in the precursor may well be a hindrance to the successful outcome of the reaction and successful purification of **8** is therefore a crucial obstacle to overcome.

A different approach to the routes we described in Scheme 3.1 might be using hexachlorinated **4** (1,1,3,3,5,5-hexachloro-1,3,5-trisilacyclohexane) as the starting material. In point of fact, the last step of the synthesis of **4** is the hydrogenation of the hexachlorinated compound. Thus one might skip the last step of that synthesis and proceed with the chlorinated trisilacyclohexane. This method would then "only" require the substitution of three chlorine atoms for a Dipp group to form **8**. Presumably an analogous method to the one described in Scheme 3.2 could be used for this step, exchanging **4** for the hexachlorinated variant. One would expect the steric bulk of the Dipp groups sufficient to ensure single substitution at each site, thus affording **8** in fewer steps than with our synthesis described above. However, owing to the apparent decomposition of some of the DippLi reagent in our reactions, some contamination by Dipb would be expected from this synthetic line as well, leaving the issue of successful purification of **8** as the most important obstacle to overcome at this stage.

## 3.5 Analyses of derivatives of 4

### 3.5.1 NMR spectroscopy

#### NMR analysis of **5**

As previously mentioned, the synthesis of **5** yielded a mixture of the isomers **5a** (*cis,cis*) and **5b** (*cis,trans*). Although some signals of the two compounds are similar enough to be indistinguishable from each other, in particular that of the methyl groups in *ortho* positions on the Mes substituents, other signals differ enough for them to be told apart. The signal from the aromatic protons is clearly formed by two overlapping peaks at 6.76 and 6.77 ppm (Fig. 3.4) and two sets of signals can also be seen for the protons on the silicon atoms, a clear triplet centred at 5.38 ppm from **5a** interspersed with a multiplet from **5b**. The clearest difference in signals stems from the methyl groups in *ortho* positions on the Mes substituent. The signal from **5a** is a single peak at 2.51 ppm, but **5b** gives different signals for the axially and equatorially positioned Mes groups, one on either side of the **5a** signal (Fig. 3.5).

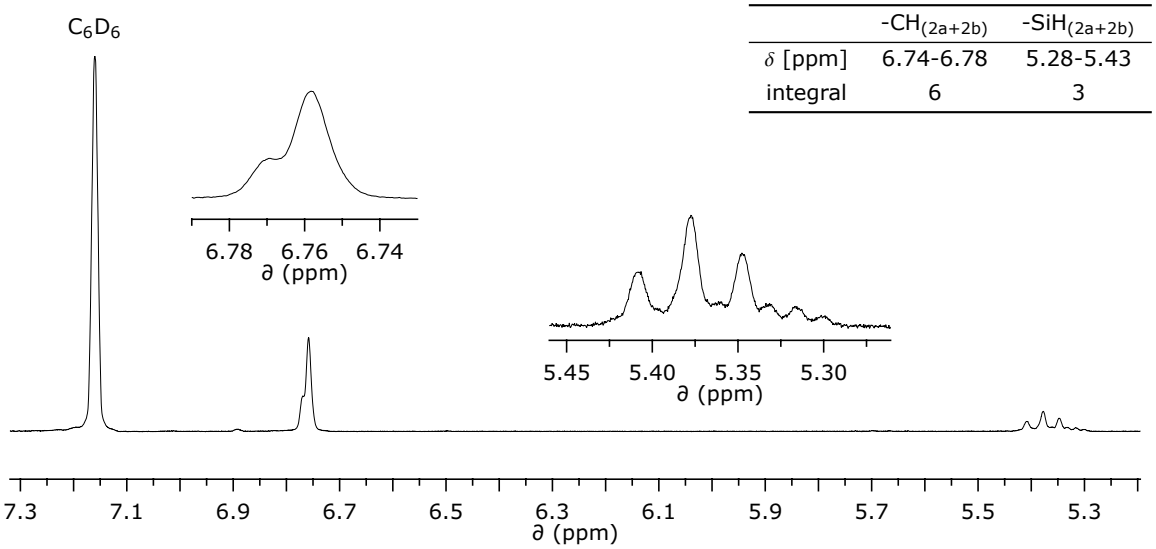


| | -CH(2a+2b) | -SiH(2a+2b) |
|---|---|---|
| δ [ppm] | 6.74-6.78 | 5.28-5.43 |
| integral | 6 | 3 |

*Figure 3.4: $^1H$ NMR spectrum of **5** in $C_6D_6$, higher region.*

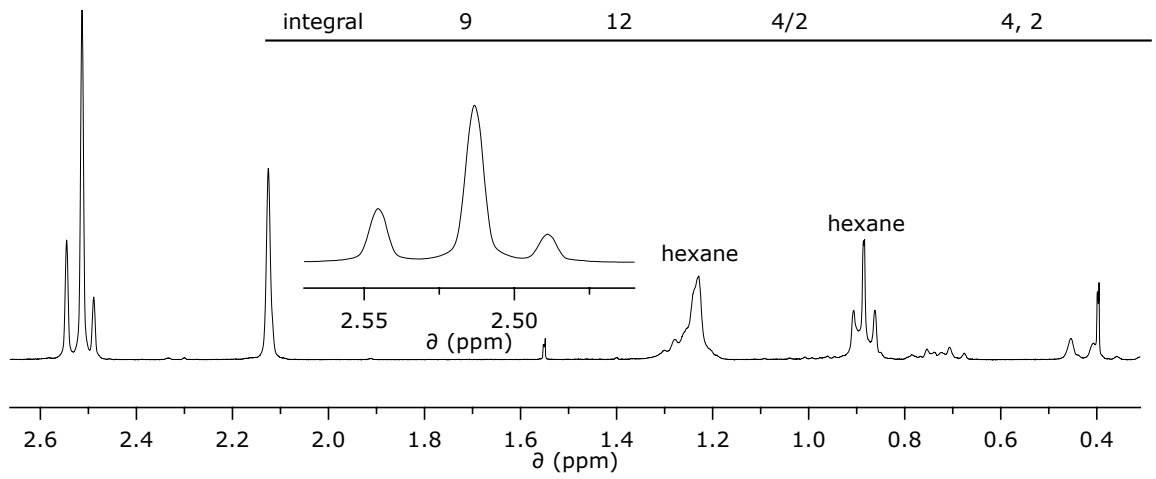


| | *p*-CH3 (2a+2b) | *o*-CH3 (2a) | *o*-CH3 (2b) ax/eq | –CH2–(2a+2b) |
|---|---|---|---|---|
| δ [ppm] | 2.13 | 2.51 | 2.55/2.49 | 0.28-0.48, 0.65-0.83 |
| integral | 9 | 12 | 4/2 | 4, 2 |

*Figure 3.5: $^1H$ NMR spectrum of **5** in $C_6D_6$, lower region.*

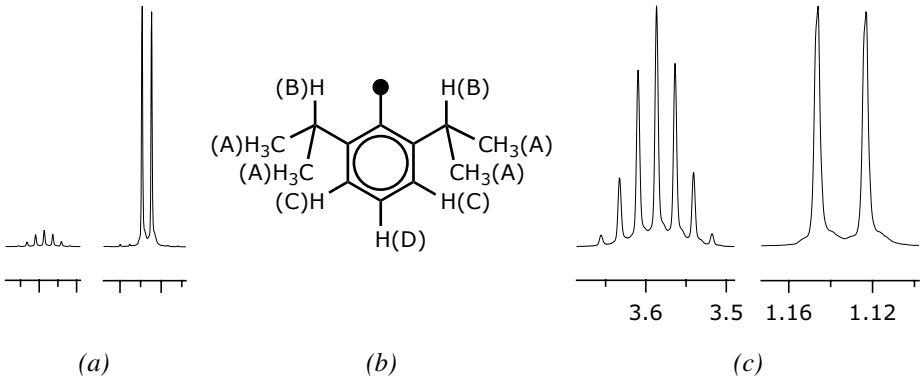


*Figure 3.6: The characteristic signals from the Dipp groups' $^{i}$Pr protons. The signals in this figure are taken from the $^{1}$H NMR spectrum of the DippBr synthesized as a precursor to our Dipp derivatives of **4**.*
*Part (a) shows the actual ratio of the signals from the single protons (B) on the $^{i}$Pr groups' secondary carbons, hereafter abbreviated as $^{i}$Pr(CH) (left) and the several protons (A) on the terminal carbons hereafter abbreviated as $^{i}$Pr($CH_3$) (right).*
*Part (b) shows the different proton regions in a Dipp group.*
*Part (c) shows the same signals as (a), magnified for a better demonstration of their shape.*

## On the Dipp containing compounds

The compounds described here that contain the Dipp group all exhibit very similar characteristic signals for the Dipp group. Rather than explaining the nature of these signals for each compound covered they will be briefly explained here. A Dipp group has 17 protons (Fig. 3.6) which can be divided into 4 groups: The 12 protons of the terminal carbons of the $^{i}$Pr groups, the 2 single protons on the $^{i}$Pr groups' secondary carbons, the 2 protons in *meta* positions and finally the proton in the *para* position. The first two give very characteristic signals in all of our compounds containing the Dipp group. Figure 3.6 shows examples of these signals which will hereafter be referred to as the $^{i}$Pr(CH) and the $^{i}$Pr($CH_3$) signals. As the signals of the aromatic protons are frequently distorted by the residual signals from the deuterated solvents ($CDCl_3$ and $C_6D_6$), less attention will be paid to them.

## NMR analysis of **6**

A $^{1}$H NMR spectrum of **6a** (Fig. 3.7) shows a triplet for the protons on the silicon atoms (C), the $^{i}$Pr(CH) signal is a septet at 3.58 ppm and the $^{i}$Pr($CH_3$) signal a doublet at 1.30 ppm. Signals stemming from the $-CH_2-$ protons in the trisilacyclohexane ring (D) as well as the Dipp's aromatic protons (E) are more complex. Some residual hexane is also visible in the spectrum along with a small water peak from the NMR solvent.

The $^{13}$C NMR spectrum (Fig. 3.8) shows the expected signals from **6a** along with signals

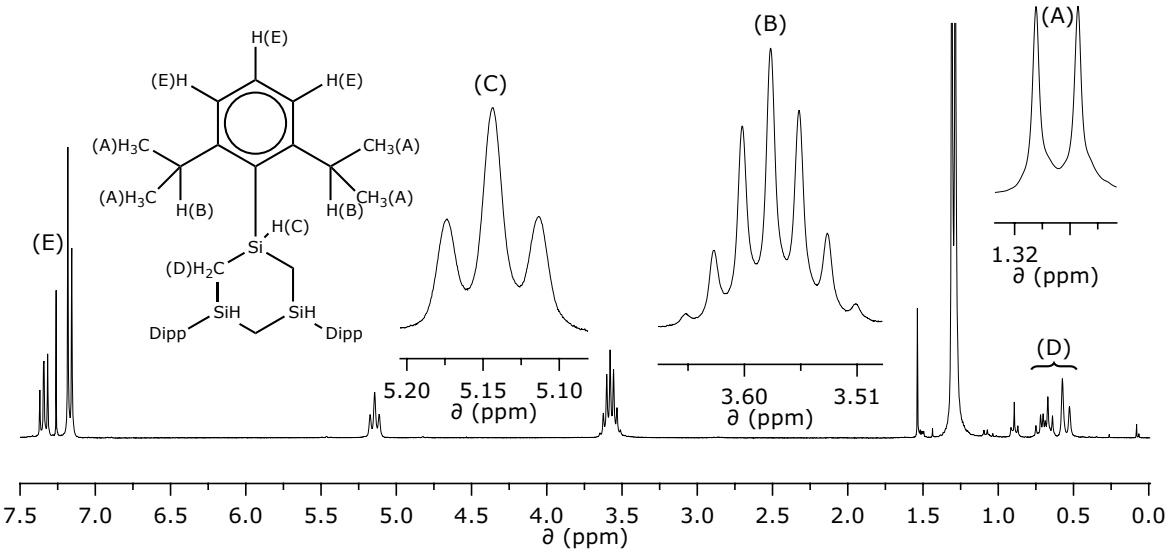


*Figure 3.7: $^{1}H$ NMR spectrum of **6a** in $CDCl_3$.*

from hexane. Peak positions were confirmed with DEPT-90 and DEPT-135 measurements.

## NMR analysis of **8**

Spectra of the product mixture from the formation of **8** revealed no remaining Si−H. However the product was contaminated by DippCl and other impurities in smaller amounts. Purification was attempted, but a completely pure sample of **8** has not yet been obtained. However, recrystallization yielded a very small amount of almost pure compound, enough to record a fairly distinct $^{1}$H NMR spectrum (Fig. 3.9).

Among noticeable changes from the $^{1}$H NMR spectrum of **6** is the chemical shift of the $-CH_2-$ signals from the silacyclohexane ring. In **6** these protons gave signals at around 0.5 to 0.75 ppm but in **8** these signals have shifted downfield to an area between 1.85 and 2.15 ppm. The $^{i}$Pr(CH) signal has also shifted downfield to 3.90 ppm compared to 3.58 ppm in **6**. The $^{i}$Pr($CH_3$) signals remains at roughly the same chemical shift although slightly shifted upfield. A more noticeable change in that signal is the clearer distinction between the isomers (*cis,cis* and *cis,trans*) as the signal is no longer a single doublet, although accurate analysis of the pattern is not possible due to distortion of the area by signals from hexane present in the sample. A small amount of DippCl is also still detectable in this sample as evidenced by its $^{i}$Pr($CH_3$) doublet at 1.14 ppm.

## NMR analysis of **7**

The reaction intended to form 1,3-bis(Dipp)-1,3,5-trisilacyclohexane was monitored by $^{1}$H NMR to ensure the highest possible yield. When the reaction had been ongoing for 14 h the $^{1}$H NMR spectrum of the reaction solution still showed clear signs of unreacted **4** as well

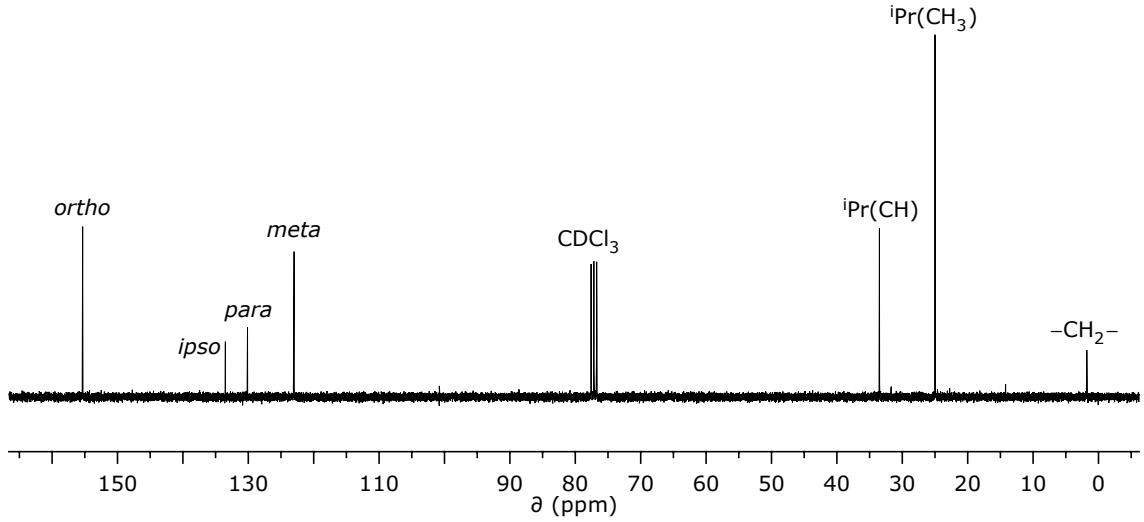


*Figure 3.8: $^{13}C\{^1H\}$ NMR spectrum of **6a** in $CDCl_3$.*

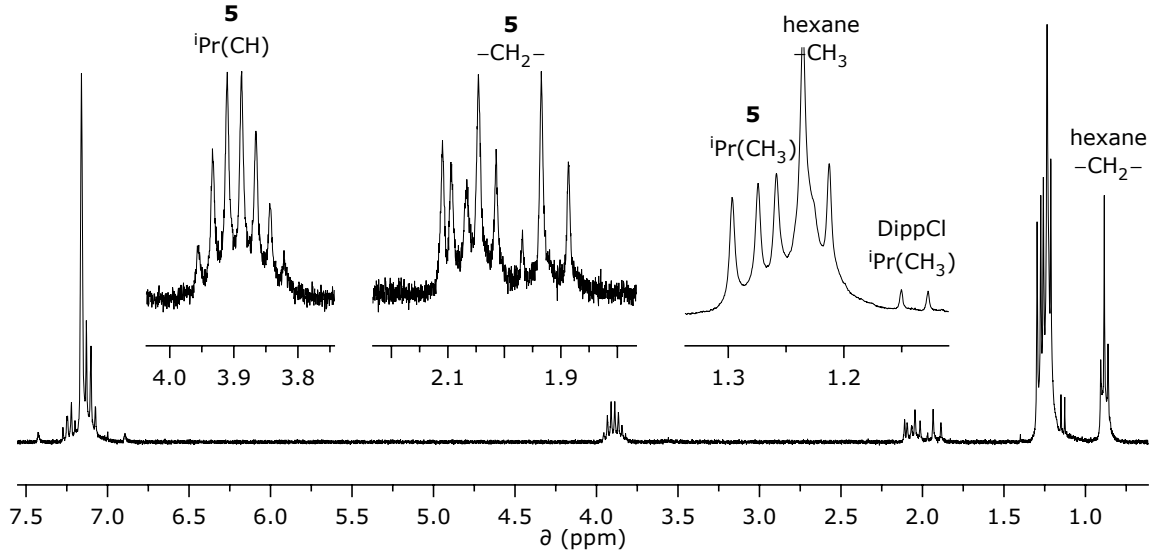


*Figure 3.9: $^1H$ NMR spectrum of **8** in $C_6D_6$. The $-CH_2-$ signals from the trisilacyclohexane ring as well as the $^iPr(CH)$ signal are shifted downfield compared to those in **6**. The $^iPr(CH_3)$ remains at a similar chemical shift as in **6**, but the signal is more complicated, presumably owing to the different isomers. Some contamination by hexane makes it difficult to provide a precise analysis of this area.*

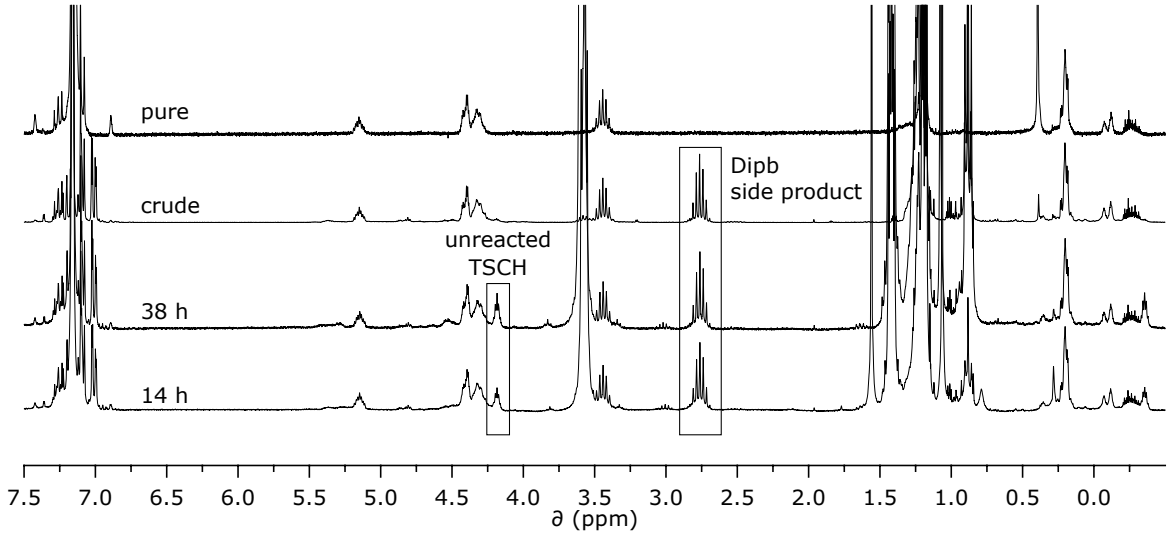


*Figure 3.10: $^1H$ NMR spectra of **7** in $C_6D_6$ showing the contents of the reaction solution at 14 and 38 h reaction time as well as the crude and purified product.*

as signals assigned to Dipb. As the Dipb could have been formed from the highly reactive DippLi after the extraction from the reaction vessel, meaning the reaction might still be ongoing, it was kept stirring for several more hours. Workup was initialised when no change in ratios was observed after 38 h from the beginning of the reaction. **7** was separated from the Dipb side-product by HPLC. Figure 3.10 shows comparison between the contents of the reaction solution at 14 h and 38 h reaction time as well as the crude and purified product. Figure 3.11 provides a closer look at the spectrum of the purified product, with the $^i$Pr(CH) signal at 3.44 ppm and the $^i$Pr($CH_3$) signal at 1.20 ppm.

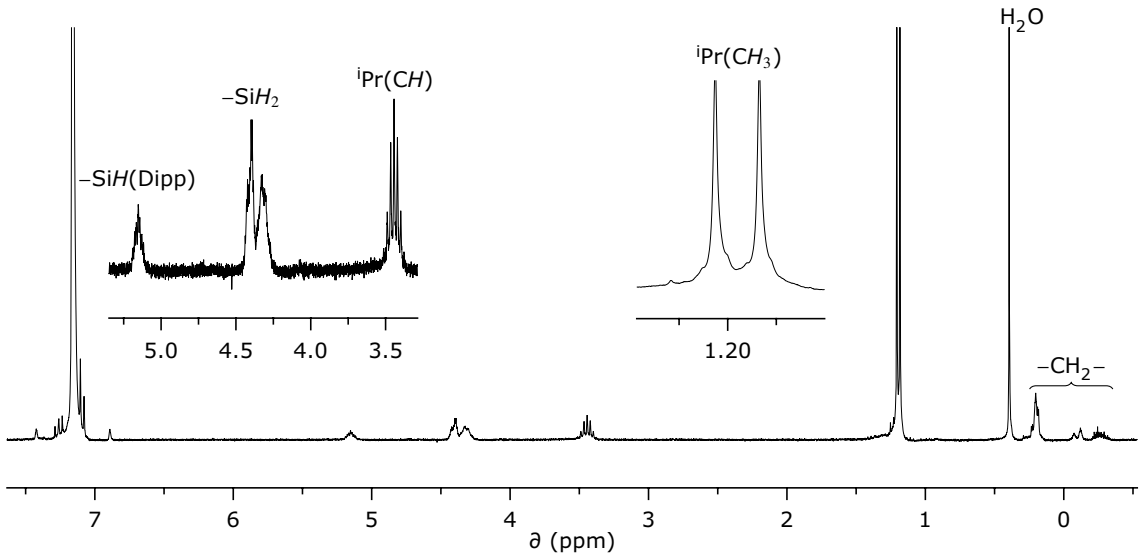


*Figure 3.11: $^1H$ NMR spectrum of **7** in $C_6D_6$ after purification by HPLC. A sharp peak at 0.40 ppm is due to water contamination of the NMR solvent.*

### 3.5.2 Crystallographic analyses

Crystallographic analyses were performed by Dr. Yosiyuki Mizuhata at ICR, Kyoto University.

#### Crystallographic analysis of **5**

A crystal of **5** was grown from a saturated solution in hexane. X-ray analysis confirmed the compound had the structure we set out to achieve with each silicon atom of the trisilacyclohexane ring connected to a hydrogen and a Mes group (Fig. 3.12). The compound crystallizes in a trigonal system and belongs to the space group $P3_1$ (#144). Each unit cell contains 3 molecules of **5** in three different orientations (Fig. 3.13). As mentioned earlier the crystal we analysed contained a mixture of *cis,cis* (**5a**) and *cis,trans* (**5b**) isomers with the former accounting for $\sim 70\%$ of the crystal. The *cis,cis* isomer crystallizes in a slightly twisted chair conformation with the Mes groups in typical equatorial positions and the Si−C bonds connecting the Mes groups to the ring forming 120° angles with the Mes groups' *ortho* carbons. The planes of the Mes groups form angles of 85, 61 and 84° with the plane formed by the silicon atoms in this chair form of the compound.

Due to the packing force of the mesityl groups the *cis,trans* isomer is forced into a distorted boat conformation. This leads to eccentric bond angles between the $C_{ipso}$−$C_{ortho}$ bonds of one of the Mes groups and the Si−$C_{ipso}$ bond connecting it to the trisilacyclohexane ring. Instead of the typical 120° of an $sp^2$ hybridized carbon the angles become 136 and 104°. Additionally, the orientation of the Mes groups relative to the plane of the silicon atoms is different from that in the other isomer, with the planes of the substituents forming angles of 62, 68 and 78° with said silicon plane. The two isomers are shown in Figure 3.12 along with a numbering scheme for selected atoms. Table 3.1 lists bond lengths, angles and torsion angles between the numbered atoms.

Crystal and data collection parameters, as well as detailed tables on bond lengths, bond to bond angles and torsion angles can be found in Appendix H.

#### Crystallographic analysis of **6**

Two crystallographic analyses were performed on **6**: One on a crystal containing both *cis,cis* and *cis,trans* isomers (**6a** and **6b**, respectively), and another on a pure sample of **6a**. **6** crystallizes in a triclinic crystal system in the space group $P\bar{1}$ (#2). It crystallizes as two independent molecules and each unit cell contains four molecules.

In the case of the isomeric mixture one of the two molecules was free of disorder and crystallized in a chair conformation with C−Si−C and Si−C−Si endocyclic bond angles in the range of 110 to 115°. The other molecule had disorders between chair (**6a**) and boat (**6b**)

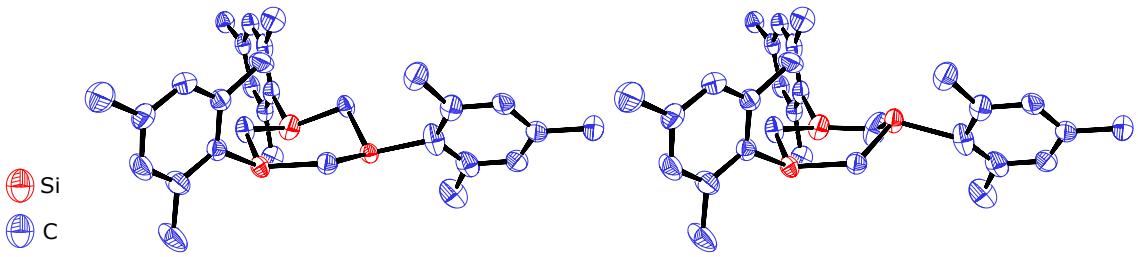


*(a) cis,cis-1,3,5-tri(Mes)-1,3,5-trisilacyclohexane (**5a**) – the major isomer of **5***

*(b) cis,trans-1,3,5-tri(Mes)-1,3,5-trisilacyclohexane (**5b**) – the minor isomer of **5***

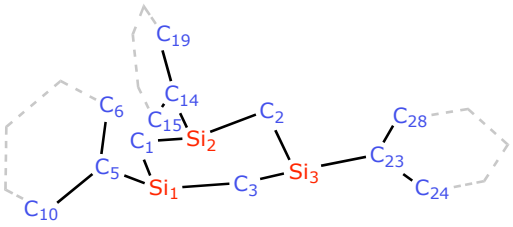


*(c) Numbering of atoms in **5a***

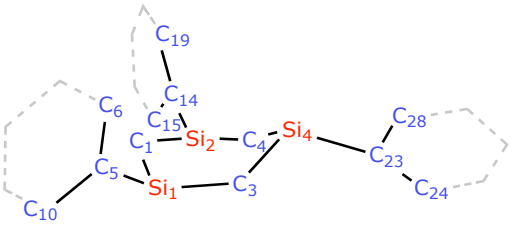


*(d) Numbering of atoms in **5b***

*Figure 3.12: The two isomers found in the crystal of **5**.*

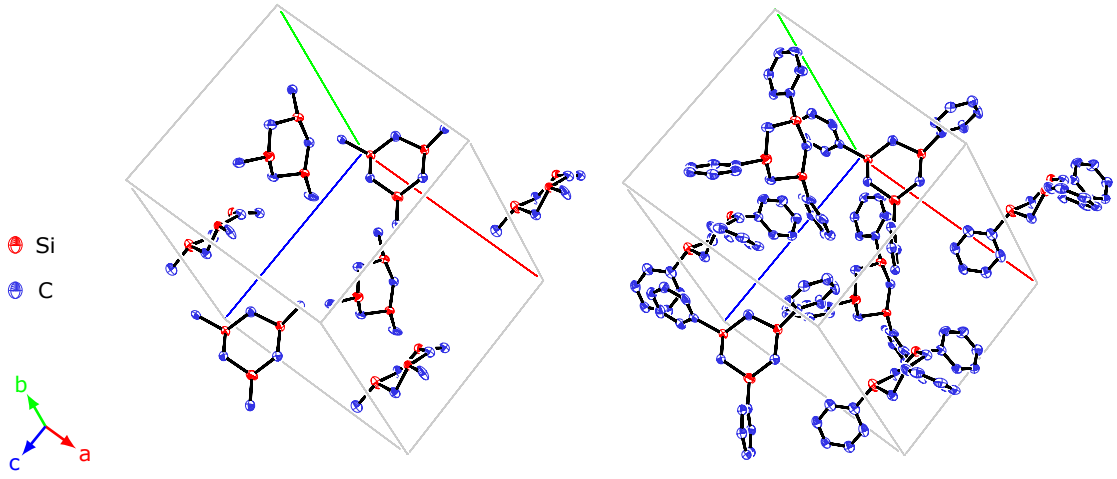


*(a)* *(b)*

*Figure 3.13: The trigonal unit cell of **5**. ORTEP drawing at 50% probability. Hydrogen is omitted for clarity. In part (a) all side group carbons, except the ipso carbons of the Mes groups are omitted as well, revealing the three different orientations of the molecules in the crystal. Part (b) omits the methyl carbons of the Mes groups but leaves the phenyl rings untouched for a more comprehensive visualization of the crystal structure. Irregularities stemming from the cis,trans isomer are omitted in both parts (a) and (b) (i.e. only **5a** is shown).*

*Table 3.1: Selected bond lengths, bond to bond angles and torsion angles from the crystallographic analysis of **5**. The numbering scheme for the molecule is given in Figure 3.12, subfigures (c) and (d).*

| **Bond lengths** [Å] | | **Angles** [°] | | **Torsion angles** [°] | |
|---|---|---|---|---|---|
| Si1–C1 | 1.872(3) | Si1–C1–Si2 | 116.22(18) | C1–Si1–C5–C6 | −68.2(3) |
| Si1–C3 | 1.878(3) | Si1–C3–Si3 | 118.48(17) | C1–Si2–C14–C19 | 64.0(3) |
| Si1–C5 | 1.885(3) | Si1–C3–Si4 | 115.10(18) | C2–Si2–C14–C19 | −56.2(4) |
| Si2–C1 | 1.868(3) | Si1–C5–C6 | 120.0(2) | C2–Si3–C23–C28 | 83.2(4) |
| Si2–C2 | 1.930(5) | Si1–C5–C10 | 123.0(2) | C3–Si1–C5–C6 | 58.5(3) |
| Si2–C4 | 1.710(18) | Si2–C2–Si3 | 108.4(3) | C3–Si3–C23–C28 | −41.0(4) |
| Si2–C14 | 1.901(3) | Si2–C4–Si4 | 113.8(10) | C3–Si4–C23–C28 | −89.1(4) |
| Si3–C2 | 1.872(6) | Si2–C14–C15 | 121.5(3) | C4–Si4–C23–C28 | 149.2(9) |
| Si3–C3 | 1.828(3) | Si2–C14–C19 | 119.8(3) | | |
| Si3–C23 | 1.895(4) | Si3–C23–C24 | 115.2(3) | | |
| Si4–C3 | 1.960(5) | Si3–C23–C28 | 126.4(3) | | |
| Si4–C4 | 1.90(2) | Si4–C23–C24 | 136.1(3) | | |
| Si4–C23 | 2.008(5) | Si4–C23–C28 | 103.8(3) | | |
| C5–C6 | 1.418(4) | C1–Si1–C3 | 113.79(15) | | |
| C5–C10 | 1.406(4) | C1–Si1–C5 | 109.19(15) | | |
| C14–C15 | 1.393(5) | C1–Si2–C2 | 105.6(2) | | |
| C14–C19 | 1.410(5) | C1–Si2–C14 | 112.96(15) | | |
| C23–C24 | 1.391(5) | C2–Si3–C23 | 110.5(2) | | |
| C23–C28 | 1.413(6) | C3–Si1–C5 | 111.53(15) | | |
| | | C3–Si3–C2 | 109.6(3) | | |
| | | C3–Si3–C23 | 114.37(15) | | |
| | | C3–Si4–C23 | 104.1(2) | | |
| | | C4–Si2–C1 | 121.2(6) | | |
| | | C4–Si2–C14 | 117.0(6) | | |
| | | C4–Si4–C3 | 112.2(8) | | |
| | | C4–Si4–C23 | 112.5(6) | | |
| | | C10–C5–C6 | 117.1(3) | | |
| | | C15–C14–C19 | 118.7(3) | | |
| | | C24–C23–C28 | 118.3(3) | | |

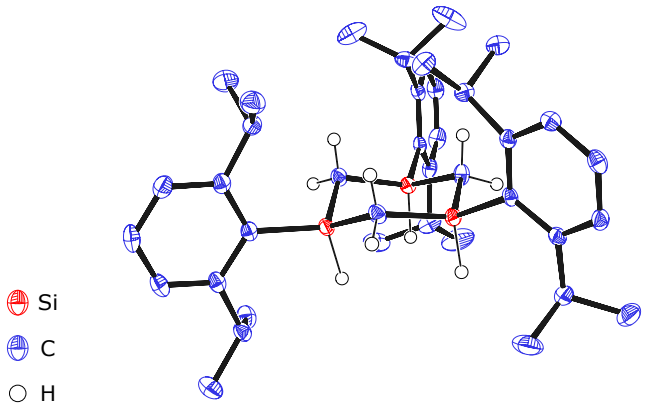


*Figure 3.14: Structure of **6a** as determined from X-ray crystallographic analysis. The figure shows one (Mole 1) of the two independent molecules found in the analysis of the crystal. ORTEP drawing at the 50% probability level. Hydrogen atoms on the Dipp groups are omitted for clarity.*

*Table 3.2: Selected bond lengths [Å] and angles [°] from the crystallographic analysis of **6a**.*

| **Element** | **Mole 1** | **Mole 2** |
|---|---|---|
| d(Si−C)endocyclic | 1.8691(17) - 1.8811(17) | 1.8719(18) - 1.8898(18) |
| d(Si−C)exocyclic | 1.8951(17) - 1.8979(17) | 1.8951(18) - 1.8978(18) |
| d(C−C)endocyclic | 1.373(3) - 1.430(2) | 1.374(3) - 1.525(2) |
| ∠(Si−C−Si) | 110.20(9) - 114.73(9) | 110.21(9) - 114.41(9) |
| ∠(C−Si−C) | 110.34(8) - 112.86(8) | 106.56(8) - 113.66(8) |
| ∠(Si−C−C) | 118.88(12) - 122.89(12) | 119.19(13) - 122.68(13) |
| ∠(C−C−C)endocyclic | 118.23(15) - 121.80(17) | 118.02(16) - 121.67(17) |
| τ(Si−C−Si−C)endocyclic | −46.84(12) - −57.46(11) | −41.45(13) - −60.47(11) |

with the chair conformation of **6a** accounting for ∼ 70%. Full refinement of the X-ray data proved difficult as the disorders in this crystal spread to the whole of one Dipp group making the two isomers difficult to divide.

The analysis of a pure sample of **6a** still revealed crystallization as two independent molecules, but now mostly free of disorders, although some variance was found in two isopropyl groups of one of the molecules. Both molecules display a chair conformation, one with endocyclic C−Si−C and Si−C−Si angles in the range of 110.2 to 114.7° (Mole 1) and the other in the range of 106.6 to 114.4° (Mole 2). Endocyclic Si−C bond lengths were in the ranges 1.869 to 1.881 Å (Mole 1) and 1.872 to 1.890 Å (Mole 2). Bond lengths from the silicon atoms to the *ipso* carbons of the Dipp substituents are in almost identical ranges in the two molecules from 1.895 to 1.898 Å. Selected bond lengths and angles within the two molecules are displayed in Table 3.2. Figures 3.14 and 3.15 show the structure of a single molecule and the unit cell of **6a**, respectively.

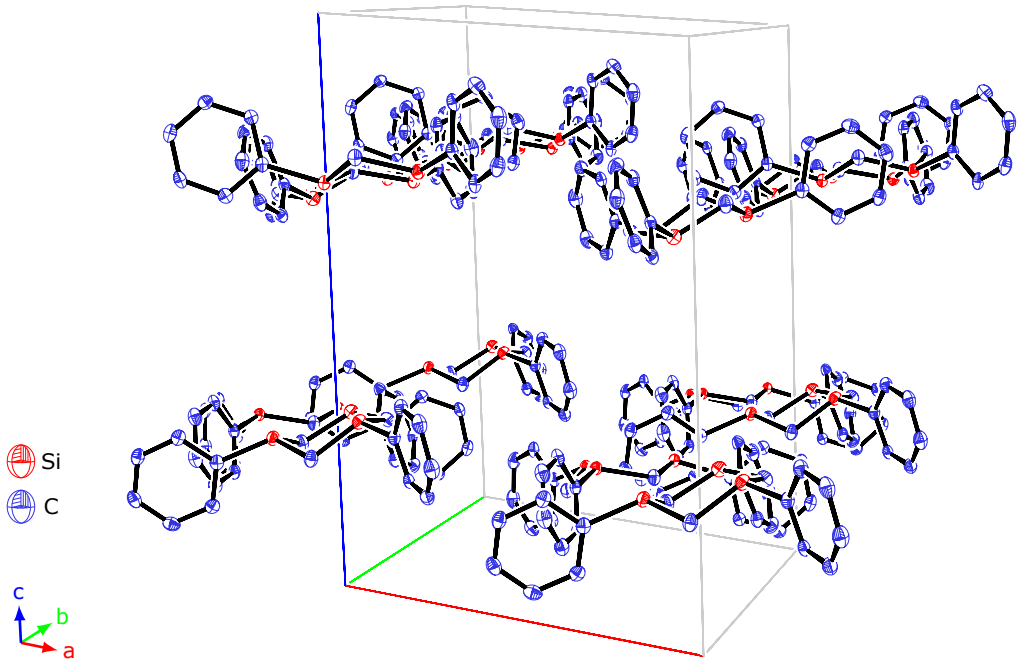


*Figure 3.15: The unit cell of **6a** as determined from X-ray crystallographic analysis. ORTEP drawing at the 50% probability level. Hydrogen atoms and the isopropyl groups on the Dipp substituents are omitted for clarity.*

## Crystallographic analysis of **7**

A crystal for X-ray analysis was obtained by sublimation from the product mixture of a reaction described in Scheme 3.3. As mentioned previously, the crystals turned out to be very delicate and difficult to handle, nevertheless the analysis was successful. **7** crystallizes in a monoclinic crystal system in the space group $P2_1/n$ (#14). As in the case of **6**, the compound crystallizes as two independent but very similar molecules with 8 molecules per unit cell. The compound crystallizes in a classic chair conformation with endocyclic C−Si−C bond angles in the range of 108 to 111° and Si−C−Si bond angles in the range of 112 to 115°. One would expect the ring structure in **6** to expand somewhat, due to the steric forces between the three Dipp groups, in comparison with **7** that has only one such substituent. This is indeed the case, as the TSCH (trisilacyclohexane) ring structure in **7** has noticeably shorter bonds than in **6**, with bond lengths varying from 1.834 to 1.870 Å. This is, however, not the case with the Si−$C_{ipso}$ bonds, with lengths of 1.904(5) Å (Mole 1) and 1.891(5) Å (Mole 2) falling on either side of the range observed in **6**. The planes of the Dipp substituents form angles of 70.5° (Mole 1) and 84.8° (Mole 2) with the planes formed by the silicon atoms in the TSCH structures they're connected to. The structure of a single molecule (Mole 1) and the unit cell can be found in Figures 3.16 and 3.17, respectively. Selected bond lengths and angles within the two molecules are displayed in Table 3.3.

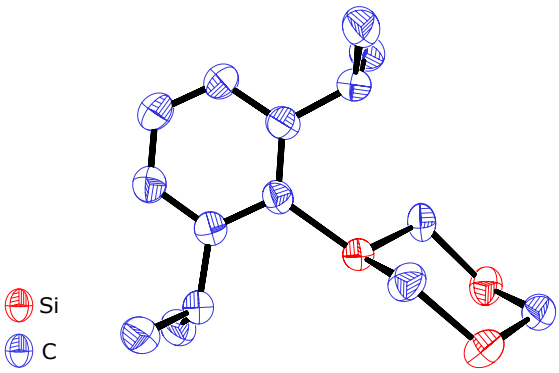


*Figure 3.16: Structure of **7** as determined from X-ray crystallographic analysis. The figure shows only one (Mole 1) of the two independent molecules found in the crystal. ORTEP drawing at the 50% probability level. Hydrogen atoms are omitted for clarity.*

*Table 3.3: Selected bond lengths [Å] and angles [°] from the crystallographic analysis of **7**.*

| **Element** | **Mole 1** | **Mole 2** |
|---|---|---|
| d(Si−C)endocyclic | 1.840(5) - 1.870(5) | 1.834(7) - 1.861(5) |
| d(Si−C)exocyclic | 1.904(5) | 1.891(5) |
| d(C−C)endocyclic | 1.356(6) - 1.415(6) | 1.371(8) - 1.399(6) |
| ∠(Si−C−Si) | 111.7(2) - 114.8(3) | 111.9(3) - 114.7(3) |
| ∠(C−Si−C) | 108.2(2) - 110.5(2) | 107.9(2) - 110.8(3) |
| ∠(Si−C−C) | 119.5(3) and 121.9(3) | 120.1(3) and 121.7(4) |
| ∠(C−C−C)endocyclic | 118.6(4) - 121.2(5) | 118.2(4) - 121.3(5) |
| τ(Si−C−Si−C)endocyclic | 50.9(3) - 58.5(3) | 49.7(4) - 57.5(4) |

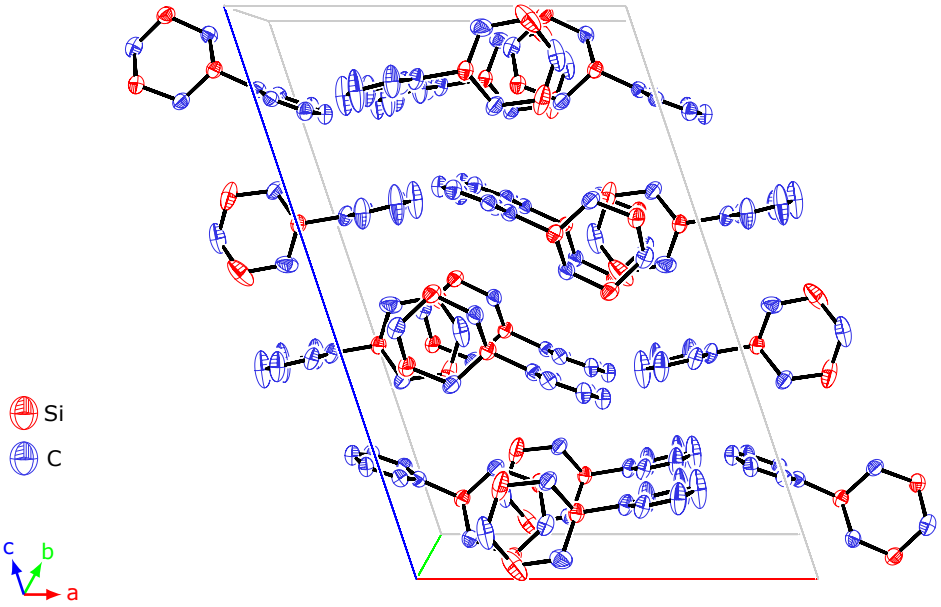


*Figure 3.17: The unit cell of **7** as determined from X-ray crystallographic analysis. ORTEP drawing at the 50% probability level. Hydrogen atoms and the isopropyl groups on the Dipp substituents are omitted for clarity.*

# 4 Syntheses and attempted isolation of silacyclohexane transition metal complexes

## 4.1 Introduction

In 1979 Klaus Hohenberger acquired his doctorate in chemistry from Universität Karlsruhe. His thesis describes research on transition metal complex derivatives of 1,3,5-trisilacyclohexane. He synthesized several different compounds with one or more silicon atoms of a 1,3,5-trisilacyclohexane bonded to transition metal complex moieties.[30] We set out to do similar syntheses, exchanging the trisilacyclohexane for monosilacyclohexane. We planned to synthesize a series of compounds with a few different transition metal complex moieties for precise characterization through e.g. X-ray analysis. The proposed method for such syntheses is the preparation of an alkali metal salt of the transition metal complex concerned, which is subsequently reacted with a monohalogenated (bromo or chloro) silacyclohexane to form the desired compound (Scheme 4.1).

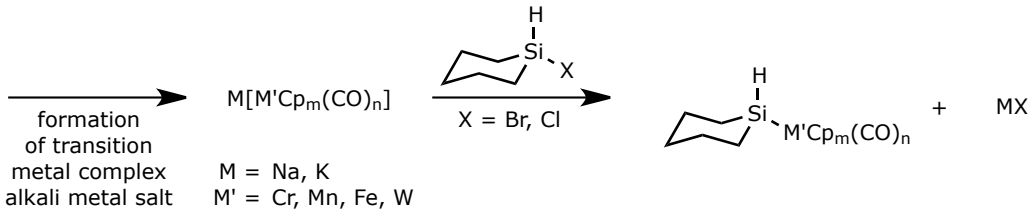


*Scheme 4.1: The reaction scheme towards the synthesis of transition metal complex substituted silacyclohexanes.*

## 4.2 Synthesis of transition metal complex alkali metal salts

Two different methods were used for the syntheses of the alkali metal salts of transition metal complexes. The first method (Scheme 4.2, method 1) consists of reacting the hexacarbonyl compound of a group 6 transition metal (Cr or W) with sodium cyclopentadienide (NaCp) forming the desired alkali metal salt and releasing carbon monoxide in the process. The other method utilizes sodium-potassium alloy to crack dimeric complexes yielding two equivalents of a complex alkali metal salt (Scheme 4.2, method 2).

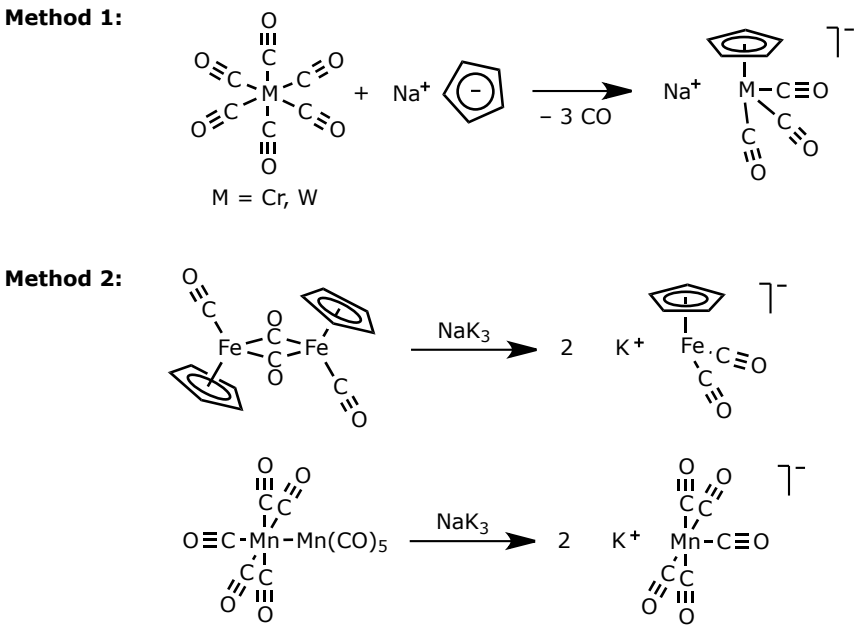


*Scheme 4.2: The two methods used for the syntheses of alkali metal salts of transition metal complexes.*

### 4.2.1 Preparation of precursors

#### Sodium cyclopentadienide

The NaCp required for the first method has traditionally been synthesized by reacting cyclopentadiene with sodium sand in THF. Sodium sand is prepared by placing sodium metal in a solvent with a high boiling point and heating with vigorous stirring until the molten sodium is beaten into small particles — sand. As the melting point of sodium (97.7 °C) is above the boiling point of THF (66 °C) the preparation of the sodium sand requires the use of a higher boiling solvent, commonly xylene, necessitating a solvent change. Additionally the other reactant, cyclopentadiene, undergoes dimerization with time and needs to be freshly cracked from dicyclopentadiene (DCPD). This somewhat cumbersome method for a simple reaction was made obsolete in 2003, when Roesky et al. reported an improved method for the synthesis of NaCp, requiring neither cracking of the precursor nor the production of sodium sand in a separate solvent.[31] In fact the new method requires no added solvent at all. Freshly cut sodium metal is simply placed in an excess of DCPD and the mixture refluxed at 160 °C. The heating both melts the metal and causes the retro-Diels–Alder reaction of DCPD forming cyclopentadiene, which immediately reacts with the molten sodium forming the desired NaCp and releasing $H_2$. NaCp precipitates from the solution as a white solid. When no sodium remains and the evolution of $H_2$ ceases the desired product can be isolated by filtering off the excess DCPD and washing the solid with pentane. Scheme 4.3 shows a simple comparison of the two methods of NaCp production. A small amount of the NaCp used for the first trials of the alkali metal salt formations was prepared using the “traditional” method

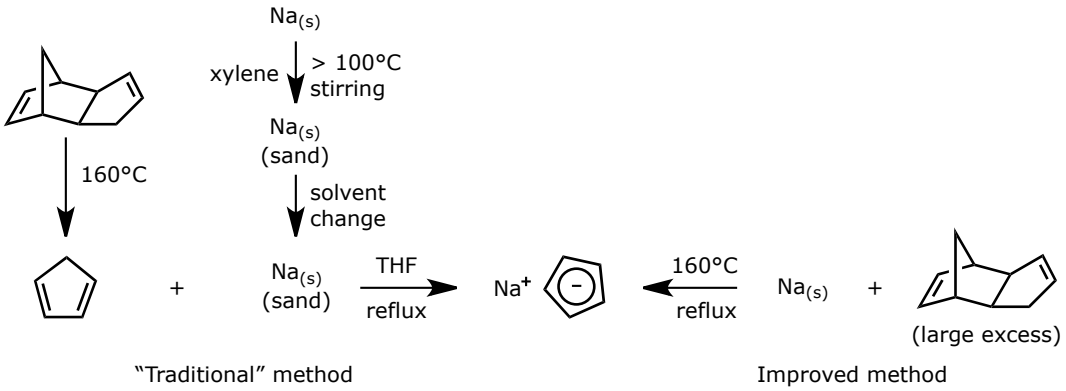


*Scheme 4.3: Two methods used for the syntheses of sodium cyclopentadienide (NaCp). The reaction was vastly simplified by the method reported by Roesky et al. in 2003.*

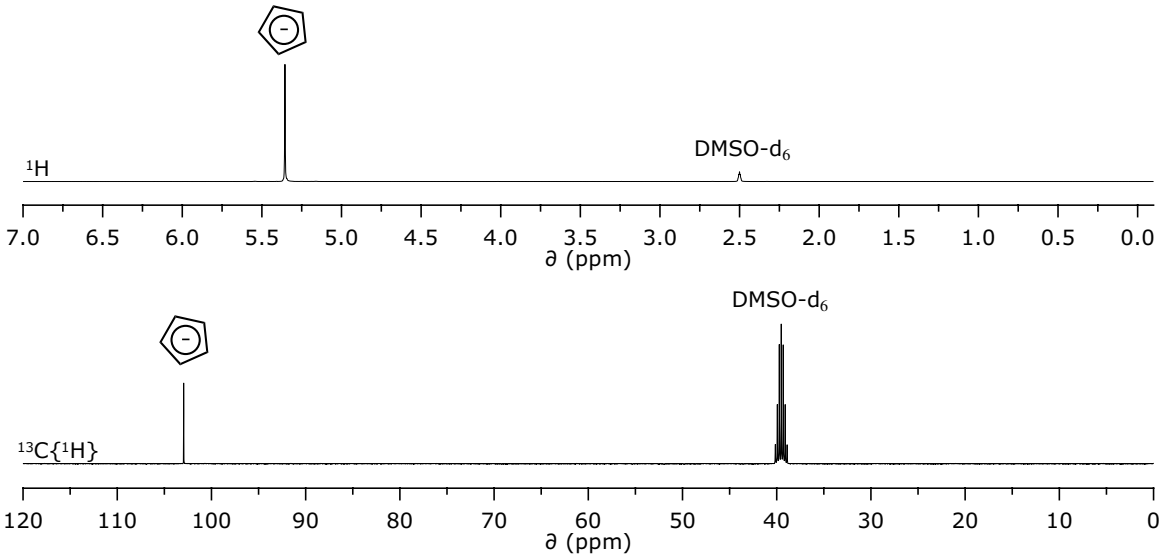


*Figure 4.1: $^{1}H$ and $^{13}C$ NMR spectra of NaCp in DMSO-$d_6$.*

but the bulk of the reactions was carried out with NaCp synthesized following the improved method. Despite an exceedingly straightforward workup the NaCp obtained through this synthesis is of high purity as evidenced by the NMR spectra (Fig. 4.1).

## Liquid sodium-potassium alloy

The sodium-potassium alloy required for Method 2 (Scheme 4.2) is made by weighing out the metals in a molar ratio of 1:2.8 sodium:potassium. The metals are then cut into small pieces and placed in a glass vial. Stirring the metal cuttings and applying pressure to them with a glass rod mixes the metals and liquefies the alloy. All these manipulations are carried out in a glove box under dry argon atmosphere and the alloy stored and handled under those conditions. The alloy is easily transferred between vessels via syringe or pasteur pipette. Another method for obtaining this alloy is heating a mixture of the metals gently in xylene

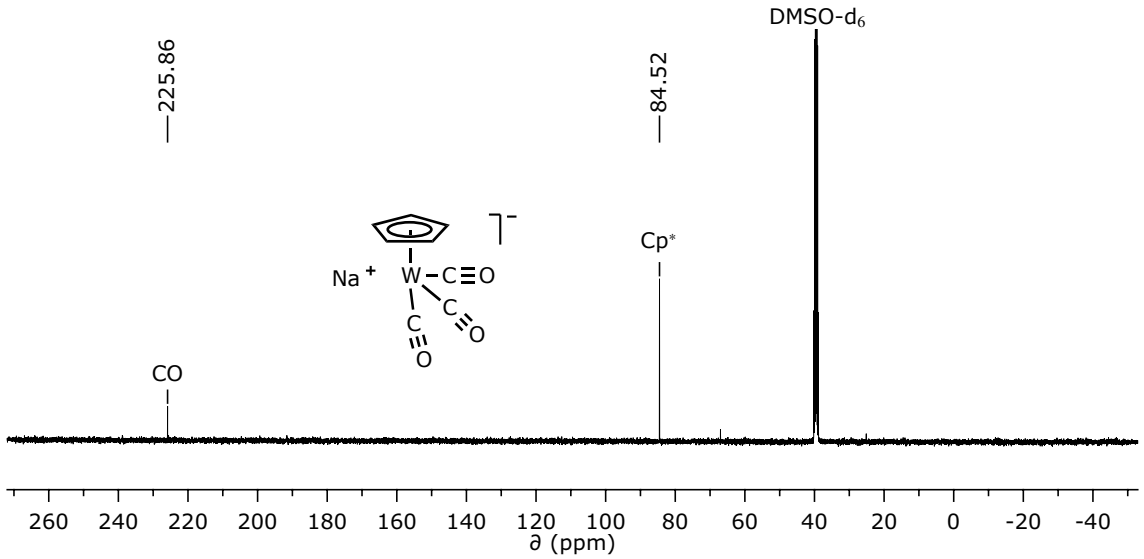


*Figure 4.2: $^{13}C$ NMR spectrum of $Na[(\eta^5\text{-}C_5H_5)W(CO)_3]$ in DMSO-$d_6$.*

until the metals coalesce.[32] Diglyme can be added to help keep the alloy in one globule and it can be kept in the solvent under inert atmosphere nigh indefinitely. Due to easy access to an inert atmosphere in a glove box the former method was chosen for convenience.

### 4.2.2 Results

The preparation of the sodium salts by Method 1 (Scheme 4.2) was based on procedures described in *Inorganic Syntheses* with an amendment from Hohenberger's thesis (using an excess of the carbonyl to ensure full conversion) and with the modification that an updated method was used for the production of NaCp as described above. In addition to these changes we consistently found that in order for full conversion of the NaCp to take place much longer reflux periods than described in these references is required. The suggested reflux time is 3 to 6 hours[34] but we found that reflux periods in excess of ten hours were often necessary. The complex anion containing tungsten proved easy to handle, even as a dry solid in the form of $Na[(\eta^5\text{-}C_5H_5)W(CO)_3]$, although all manipulations were of course carried out under inert atmosphere. The chromium variant proved more unstable and prone to decomposition. Figure 4.2 shows the $^{13}C$ NMR spectrum of the tungsten compound.

The handling of salts produced by the cleavage of dimeric complexes by $NaK_3$ posed some initial problems. Following the procedures described in Hohenberger's thesis[35] and sources cited therein,[32] solutions containing $K[(\eta^5\text{-}C_5H_5)Fe(CO)_2]$ were dried out to obtain the salt as a solid. This proved to be unsuitable as the $[(\eta^5\text{-}C_5H_5)Fe(CO)_2]^-$ anion ($Fp^-$) is extremely reactive and thus very difficult to handle. Some research into recent literature on the subject revealed that in order for $Fp^-$ to be stable for convenient storage and handling as a solid a much bulkier counter ion is required (e.g. $Ph_2C{=}O/K^+$).[36] In light of this we opted for using

the produced $Fp^-$ in solution in the next reaction without intermediate isolation. This does not pose a problem as the only contaminants left by the reaction, the excess of metal alloy, can be easily removed by filtration. The filtrate is then ready for use in the next reaction as the solvent, THF, was also deemed suitable for that step. The $NaK_3$ cleavage of $Mn_2(CO)_{10}$ was only attempted once and appeared to result in less than full conversion. Longer reaction time may be needed in this case.

## 4.3 Synthesis of 1-chloro-1-silacyclohexane

For reaction with the alkali metal salts 1-chloro-1-silacyclohexane was synthesized by classical methods using a two step synthesis involving a digrignard intermediate (Scheme 4.4). The use of a brominated compound for the initial step of this synthesis can lead to some formation of a brominated product through halogen exchange reactions. An NMR spectrum of the product of such a reaction, after purification by distillation, can be seen in Figure 4.3. 1-Chloro-1-silacyclohexane synthesized this way was used for some of the subsequent reactions, but for others we used pure 1-bromo-1-silacyclohexane synthesized by Þorvaldur Snæbjörnsson, an undergraduate in our lab. Pure 1-bromo-1-silacyclohexane is achieved by reacting a portion of 1-chloro-1-silacyclohexane (possibly containing some of the brominated product), like the one described above, with phenyl magnesium grignard, producing 1-phenyl-1-silacyclohexane. This is subsequently converted to 1-bromo-1-silacyclohexane by reaction with HBr.[37]

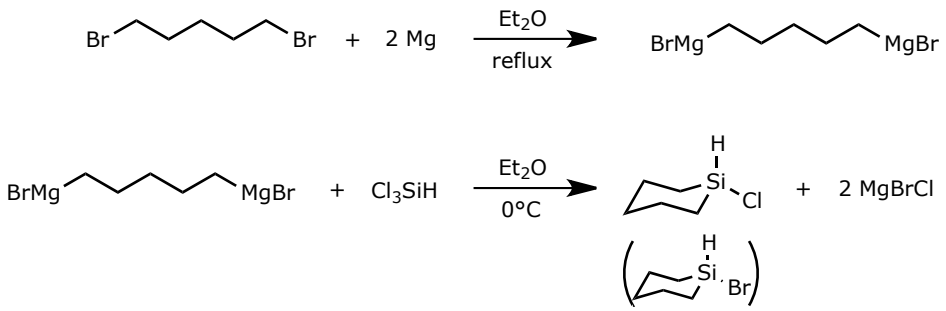


*Scheme 4.4: Procedure for the synthesis of 1-chloro-1-silacyclohexane involving the formation of a digrignard. Although the intended compound is the major product of this reaction, some 1-bromo-1-silacyclohexane is frequently formed due to halogen exchange reactions.*

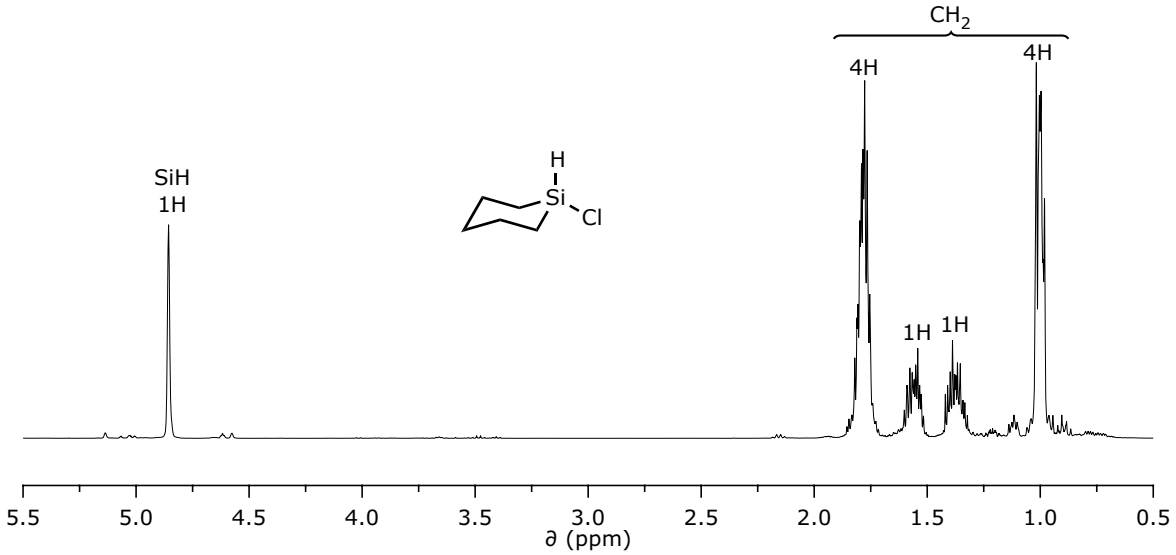


*Figure 4.3: $^{1}H$ NMR spectrum of 1-chloro-1-silacyclohexane in $CDCl_3$.*

## 4.4 Syntheses and attempts at the isolation of final products

Different methods were tested for the syntheses of the final products of this reaction series with varied results. Scheme 4.5 shows some examples of the methods tested. However the same problem arose in all cases where the intended products are likely to have been formed — isolation of the products proved exceedingly difficult. A major factor in these difficulties is the fact that the products were in all cases highly prone to sublimation and additionally lacked stability. In some cases changes in colour occurred mere minutes after introducing the compounds to an NMR solvent.

Although purification by sublimation is of course normally a desirable method, the extreme ease with which these compounds sublimate, in combination with the low yields from the reactions, resulted in only very small amounts being obtained. This may be due to a considerable portion of the products being lost during solvent evaporation. Additionally, when isolation was attempted by sublimation from the sticky residues, some residuals of the reaction solvents invariably condensed onto the cold finger along with the products making measured NMR spectra less effective in the analysis of the reaction products. Isolation has also been attempted through crystallization and slow evaporation of the solvent without positive results. Analysis by high resolution mass spectrometry was attempted but to no avail. When this is written no conclusive data exists as to the structure of the final products of these reactions, although colour changes to the reaction solutions as well as the colour of the solvent removed by condensation and NMR spectra of the reaction mixtures clearly indicate that a reaction has taken place.

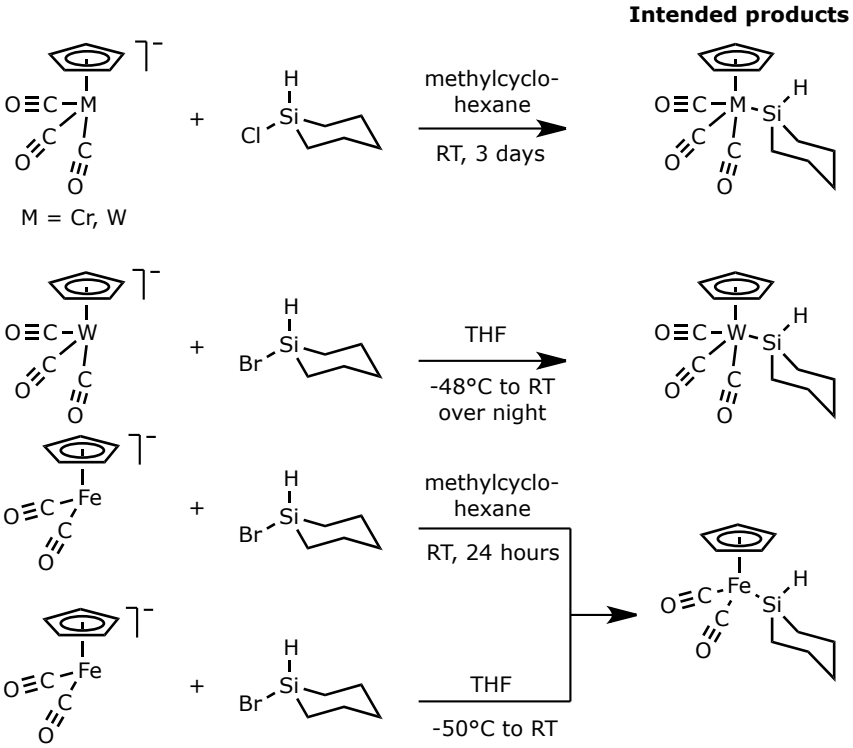


*Scheme 4.5: Examples of the methods trialled for syntheses of silacyclohexanes bonded with transition metal complex moieties.*

# 5 Other work

## 5.1 Improved synthesis of 11

In 2008 an attempt was made to synthesize $Cp^*Ti(\mu\text{-}O_3)[DisSi{-}O]_3$ (Dis = $-CH(SiMe_3)_2$), an adamantane shaped complex for use in alcoholysis experiments, by the reaction of a six-membered siloxane ring, $[DisSi(OH){-}O]_3$ (**9**), with $Cp^*TiCl_3$. Analysis of the products of this reaction revealed that the intended compound had not been formed, but rather an eight-membered ring (**10**) of titanium, silicon and oxygen ($Ti_2Si_2O_4$), with chlorine and $Cp^*$ as substituents on the titanium atoms and hydroxyl and Dis groups on the silicons, along with several side-products. In an attempt to methylate the titanium centres, **10** was reacted with MeLi. This reaction however also had an unexpected result as the intended methylation did not occur, but rather an unidentified intermediate was formed which subsequently rearranged into the tricyclic compound **11** (Scheme 5.1).

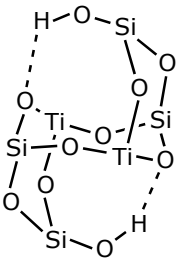

*Figure 5.1: The tricyclic core of **11** as determined from X-ray crystallographic analysis. (The compound's Dis and $Cp^*$ groups are omitted for clarity.)*

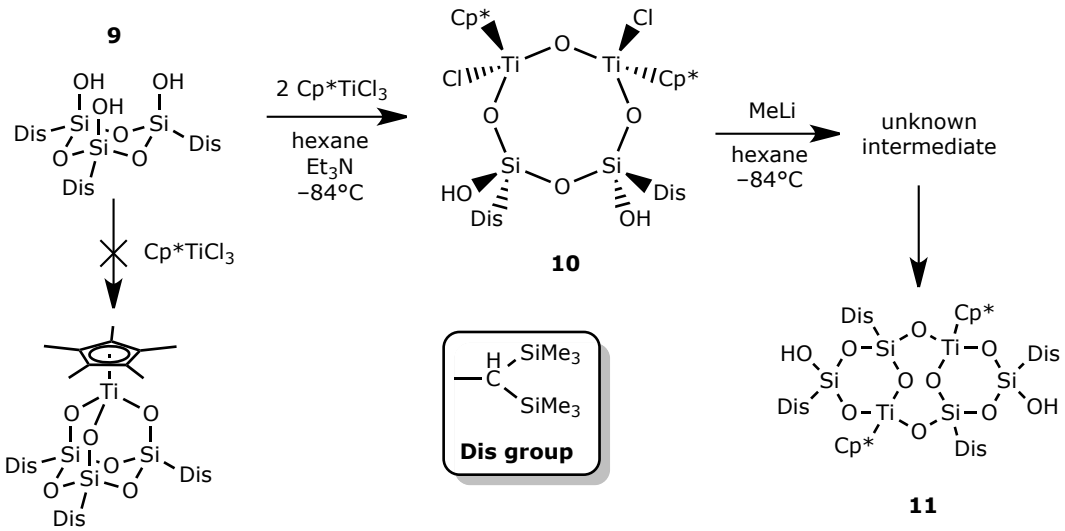


*Scheme 5.1: Formation of **11** via a two step synthesis, starting from **9**.*

High quality crystals of **11** were grown from a concentrated solution in hexane and subjected to single-crystal X-ray diffraction analysis. The analysis revealed that the three ring-structures of the compound, which belongs to the point group $C_i$ and crystallizes in the

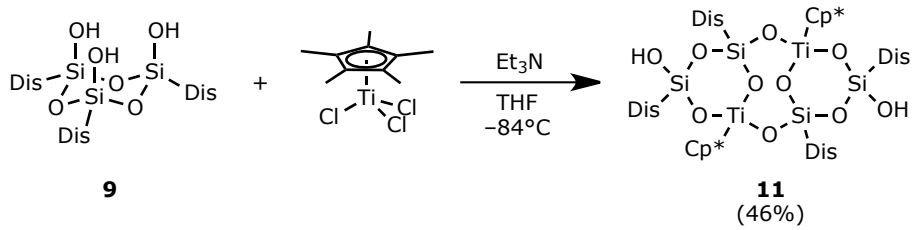


*Scheme 5.2: Formation of **11** via a single step synthesis, starting from **9**.*

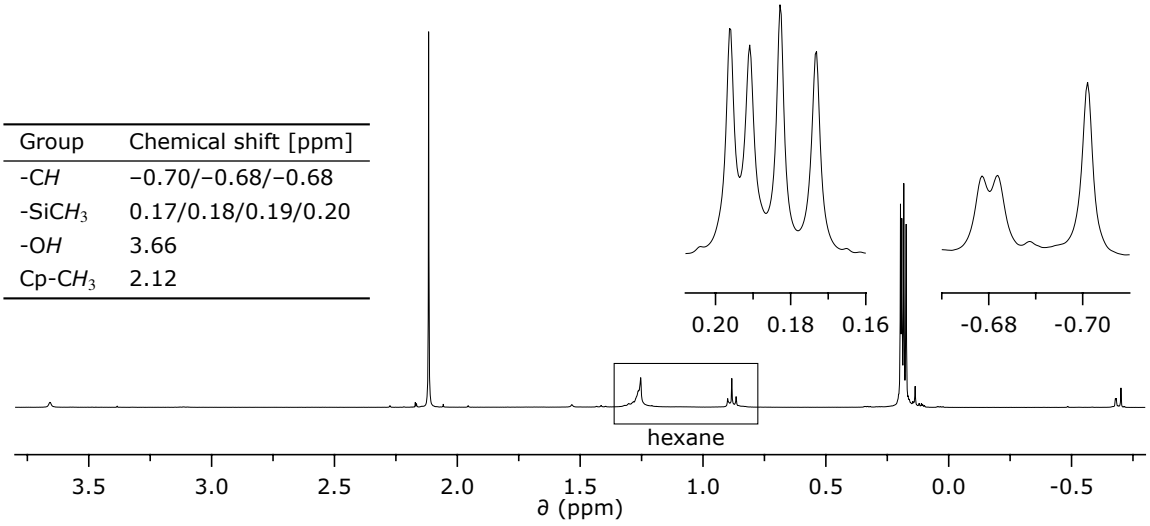


*Figure 5.2: $^1H$ NMR spectrum of **11** in $CDCl_3$. The compound is easily identified by the two distinct sets of peaks shown in the expanded portions of the spectrum.*

triclinic space group $P\bar{1}$, form a ball-like core through hydrogen bonding of the hydroxyl groups and oxygens within the ring structures (Fig. 5.1). It was also found that hexane was incorporated into the crystal lattice, with each unit cell containing one molecule of **11** and one molecule of hexane. In addition to the X-ray analysis, **11** was characterized by $^1$H NMR and MS measurements.[3]

We intended to have another go at the synthesis of $Cp^*Ti(\mu\text{-}O_3)[DisSi{-}O]_3$ by a very similar procedure, but exchanging hexane for THF as solvent. As before the adamantane complex was not among the products but instead we found that **11** had been formed in a considerable amount. Several trials were made at this synthesis eventually reaching a top yield of around 46% of pure **11** via fractional crystallization of the product mixture from hexane (Scheme 5.2). The products from our reactions were simply identified by $^1$H NMR spectroscopy as the structure of the compound had been elucidated by previous research. The $^1$H NMR spectrum of **11** shows two very distinct sets of peaks for the Dis groups: Four peaks at around 0.2 ppm for the methyl groups and three peaks close to −0.7 ppm for the −CH protons (Fig. 5.2). The formation of **11** by these two quite different routes indicates a high tendency for its emergence which in turn is evidence of the compounds stability under these conditions.

## 5.2 Temperature calibration of an NMR probe head

### 5.2.1 Introduction

Within my research group at University of Iceland, Science Institute considerable research has been conducted in conformational analysis of several different sila- and germaorganics with the heteroatom (or atoms) found in a six-membered ring structure. At normal conditions these compounds undergo ring flip at such a high rate that detecting individual signals from different conformers is impossible with NMR. As a result such conformational analyses rely on a technique called dynamic NMR (DNMR), in which a compound's NMR spectrum is measured at several different low temperatures and the change in peak width, and at the best of times the splitting of signals, are utilized to obtain information about the conformational tendencies of the compound in question.

This type of experiment requires an NMR probe head specially equipped to allow for the sample to be cooled to temperatures below 120 K. Such a probe head was previously available for use with a 250 MHz NMR spectrometer at the institute. However, when this spectrometer went out of commission the need arose to obtain a probe head with these capabilities fit for use with the NMR spectrometer currently in service at the institute. On this basis a broadband observe probe head with cooling capabilities was obtained from BRUKER and fitted to the Science Institute's Bruker AVANCE 400 NMR spectrometer late in 2010. The cooling of the probe head is controlled from software provided by the manufacturer and said software reports the temperature in real time. However, the temperature values reported by the equipment itself are not accurate enough for the type of DNMR experiments being conducted by our group. In light of this we conducted a special calibration of the NMR probe head to ascertain the relationship between the equipment's reported temperature and the actual temperature "experienced" by the NMR sample being measured.

### 5.2.2 Setup

To evaluate the temperature of the sample within the probe we used a type-K thermocouple, consisting of Chromel and Alumel wires which are insulated from one another except for two connection points at either end of the thermocouple. One of these points, the measuring point, was positioned in an NMR tube which then descended into measuring height within the probe head. The other point, the reference point, was connected to a digital multimeter (Keithley 175A Autoranging Multimeter) and its temperature monitored with a mercury thermometer (Fig. 5.3). The temperature of this refrence point ($T_{ref}$) in conjunction with the potential reported by the multimeter ($V_{thc}$) gives us the means to calculate the temperature of the measuring point ($T_{corr}$). Thus $T_{ref}$ and $V_{thc}$ are always recorded simultaneously.

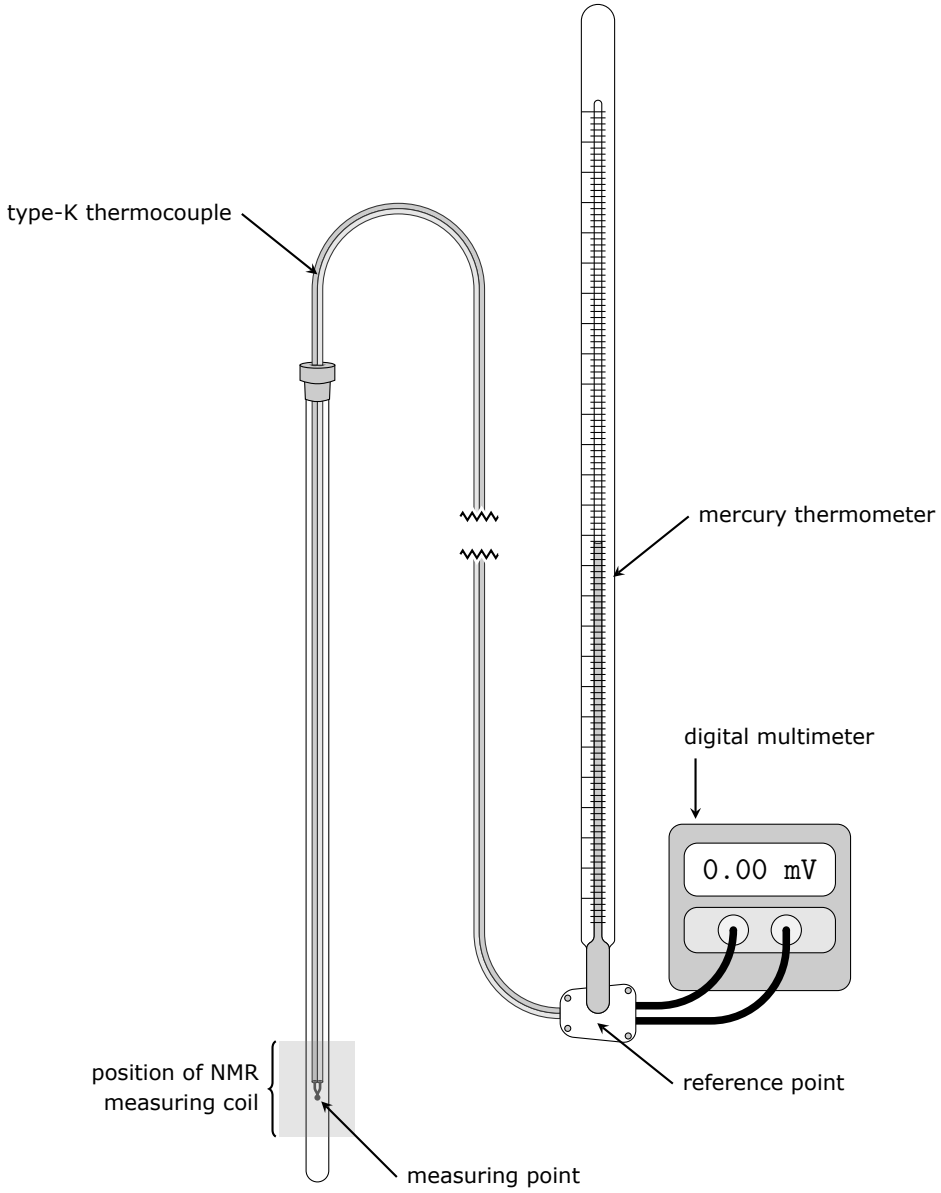


*Figure 5.3: Schematic of the setup we used for the calibration.*

*Table 5.1: Constants for calculations according to equations 5.1 and 5.2.*[23]

| | $-270\,^{\circ}\mathrm{C} \leq T \leq 0\,^{\circ}\mathrm{C}$ | | $0\,^{\circ}\mathrm{C} \leq T \leq 1372\,^{\circ}\mathrm{C}$ |
|---|---|---|---|
| $c_0$ | 0.000 000 000 0 | $h_0$ | $-1.760\,041\,368\,6 \cdot 10^{-2}$ |
| $c_1$ | $3.945\,012\,802\,5 \cdot 10^{-2}$ | $h_1$ | $3.892\,120\,497\,5 \cdot 10^{-2}$ |
| $c_2$ | $2.362\,237\,359\,8 \cdot 10^{-5}$ | $h_2$ | $1.855\,877\,003\,2 \cdot 10^{-5}$ |
| $c_3$ | $-3.285\,890\,678\,4 \cdot 10^{-7}$ | $h_3$ | $-9.945\,759\,287\,4 \cdot 10^{-8}$ |
| $c_4$ | $-4.990\,482\,877\,7 \cdot 10^{-9}$ | $h_4$ | $3.184\,094\,571\,9 \cdot 10^{-10}$ |
| $c_5$ | $-6.750\,905\,917\,3 \cdot 10^{-11}$ | $h_5$ | $-5.607\,284\,488\,9 \cdot 10^{-13}$ |
| $c_6$ | $-5.741\,032\,742\,8 \cdot 10^{-13}$ | $h_6$ | $5.607\,505\,905\,9 \cdot 10^{-16}$ |
| $c_7$ | $-3.108\,887\,289\,4 \cdot 10^{-15}$ | $h_7$ | $-3.202\,072\,000\,3 \cdot 10^{-19}$ |
| $c_8$ | $-1.045\,160\,936\,5 \cdot 10^{-17}$ | $h_8$ | $9.715\,114\,715\,2 \cdot 10^{-23}$ |
| $c_9$ | $-1.988\,926\,687\,8 \cdot 10^{-20}$ | $h_9$ | $-1.210\,472\,127\,5 \cdot 10^{-26}$ |
| $c_{10}$ | $-1.632\,269\,748\,6 \cdot 10^{-23}$ | $h_{10}$ | $1.185\,976 \cdot 10^{-1}$ |
| | | $h_{11}$ | $-1.183\,432 \cdot 10^{-4}$ |

### 5.2.3 Relationship between the temperature and potential of the thermocouple

#### The basic relationship

The formulas giving the relationship between potential and temperature are:[38]

$$E = c_0 + c_1 T + c_2 T^2 + c_3 T^3 + \ldots c_{10} T^{10} \qquad -270\,^{\circ}\mathrm{C} \leq T \leq 0\,^{\circ}\mathrm{C} \tag{5.1}$$

$$E = h_0 + h_1 T + h_2 T^2 + h_3 T^3 + \ldots h_9 T^9 + h_{10} e^{h_{11}(T-126.9686)^2} \qquad 0\,^{\circ}\mathrm{C} \leq T \leq 1372\,^{\circ}\mathrm{C} \tag{5.2}$$

Where $E$ denotes the potential in mV, $T$ represents the temperature in degrees Celsius and the other components are constants listed in Table 5.1. These formulas assume a reference point at 0 °C. Since our reference point is at variable temperature above 0 °C, a correction has to be made to the value of the potential as displayed by the multimeter before the correct temperature can be calculated.

#### Concerning our setup

Since the temperature of our reference point, $T_{ref}$, is above 0 °C it lowers the value of the measured potential, $E_{read}$, by a number of mV equal to that of $E_{ref}$, the potential displayed by the thermocouple with reference point at 0 °C and measuring point at $T = T_{ref}$. Based on this we calculate the value of $E_{ref}$ from the value of $T_{ref}$ for each measurement, using equation 5.2, and add it to the measured potential to obtain $E_{corr}$, the potential actually caused by the deviation of the measuring point's temperature from 0 °C:

$$E_{corr} = E_{read} + E_{ref} \tag{5.3}$$

*Table 5.2: Values of constants needed for equation 5.4.*

| $p_0$ | $p_1$ | $p_2$ | $p_3$ | $p_4$ | $p_5$ | $\mu$ | $\sigma$ |
|---|---|---|---|---|---|---|---|
| 184.31 | 54.024 | 6.2902 | −0.63813 | −1.2534 | 0.39864 | 196.72 | 52.967 |

Having found the value of $E_{corr}$ we plug it into the corresponding equation (5.1 or 5.2) and solve for $T$ to obtain $T_{corr}$, the actual temperature of the measuring point.

### 5.2.4 Results

Calculations based on the descriptions above were carried out in MATLAB®. A function was written to calculate $T_{corr}$ from input values of $E_{read}$ and $T_{ref}$ on the basis of equations 5.1, 5.2 and 5.3. Additionally an m-file for running our collected data through this function and calculating $T_{corr}$ for each obtained measurement was written. All values obtained through measurements and calculations can be found in Table 5.3. The MATLAB® files and data document can be found in Appendix L.

Plotting the obtained values of $T_{corr}$ as a function of $T_{NMR}$ and fitting the plotted data to a 5th degree polynomial (5th degree gave the best fit from linear through 9th degree) yields the following type of equation:

$$T_{calc}\,[K] = p_0 + p_1 z + p_2 z^2 + p_3 z^3 + p_4 z^4 + p_5 z^5 \qquad ; \qquad z = \frac{T_{NMR}\,[K] - \mu}{\sigma} \tag{5.4}$$

The values of the constants $p_0$ through $p_5$ as well as $\mu$ and $\sigma$ can be found in Table 5.2. The plotted data can be seen in figure 5.4 along with the fit.

Examining the data in Table 5.3 one can see that, using the 5th degree fit, the deviation of $T_{calc}$ from the correct temperature value, $T_{corr}$, never exceeds 0.4 °C. On the basis of this we consider the fit an acceptable approximation and intend to use equation 5.4 along with the values from Table 5.2 to calculate corrected temperature values from the temperature reported by the NMR instrument.

*Table 5.3: All measured and calculated temperature values along with the measured potential of the thermocouple. $T_{NMR}$ represents the probe head temperature reported by the instrument itself, $V_{thc}$ is the electric potential measured at the reference point of the thermocouple, $T_{ref}$ is the temperature of the refrence point of the thermocouple, $T_{corr}$ is the actual temperature of the measuring point of the thermocouple as calculated from $T_{ref}$ and $V_{thc}$ and $T_{calc}$ is the temperature calculated from the value of $T_{NMR}$ using equation 5.4.*

| $\boldsymbol{T_{NMR}}$ **[K]** | $T_{NMR}$[°C] | $V_{thc}[mV]$ | $T_{ref}$[°C] | $\boldsymbol{T_{corr}}$ **[K]** | $T_{corr}$[°C] | $\boldsymbol{T_{calc}}$ **[K]** | $T_{calc}$[°C] |
|---|---|---|---|---|---|---|---|
| **289.8** | 16.7 | −0.07 | 18.6 | **289.9** | 16.8 | **289.9** | 16.8 |
| **272.5** | −0.6 | −0.89 | 19.0 | **269.7** | −3.4 | **269.7** | −3.4 |
| **259.5** | −13.7 | −1.48 | 19.0 | **254.5** | −18.6 | **254.6** | −18.6 |
| **249.6** | −23.6 | −1.90 | 18.6 | **243.0** | −30.1 | **243.0** | −30.1 |
| **240.5** | −32.7 | −2.27 | 18.2 | **232.6** | −40.5 | **232.5** | −40.7 |
| **229.1** | −44.1 | −2.75 | 18.2 | **219.3** | −53.9 | **219.4** | −53.7 |
| **220.4** | −52.8 | −3.08 | 18.0 | **209.6** | −63.5 | **209.6** | −63.5 |
| **209.8** | −63.4 | −3.48 | 18.1 | **198.0** | −75.2 | **198.0** | −75.1 |
| **200.3** | −72.9 | −3.80 | 18.2 | **188.3** | −84.8 | **188.0** | −85.2 |
| **189.4** | −83.8 | −4.17 | 18.2 | **176.6** | −96.5 | **177.0** | −96.2 |
| **181.0** | −92.2 | −4.41 | 18.0 | **168.5** | −104.7 | **168.8** | −104.3 |
| **170.7** | −102.5 | −4.65 | 17.5 | **159.6** | −113.5 | **159.3** | −113.9 |
| **161.0** | −112.2 | −4.91 | 17.8 | **150.8** | −122.3 | **150.6** | −122.5 |
| **151.0** | −122.2 | −5.16 | 18.0 | **141.9** | −131.3 | **141.9** | −131.3 |
| **140.5** | −132.7 | −5.40 | 18.0 | **132.5** | −140.6 | **132.7** | −140.5 |
| **130.0** | −143.2 | −5.63 | 18.0 | **123.1** | −150.1 | **123.1** | −150.1 |
| **123.0** | −150.2 | −5.78 | 17.8 | **116.2** | −156.9 | **116.2** | −156.9 |
| **122.9** | −150.3 | −5.78 | 17.8 | **116.2** | −156.9 | **116.1** | −157.0 |

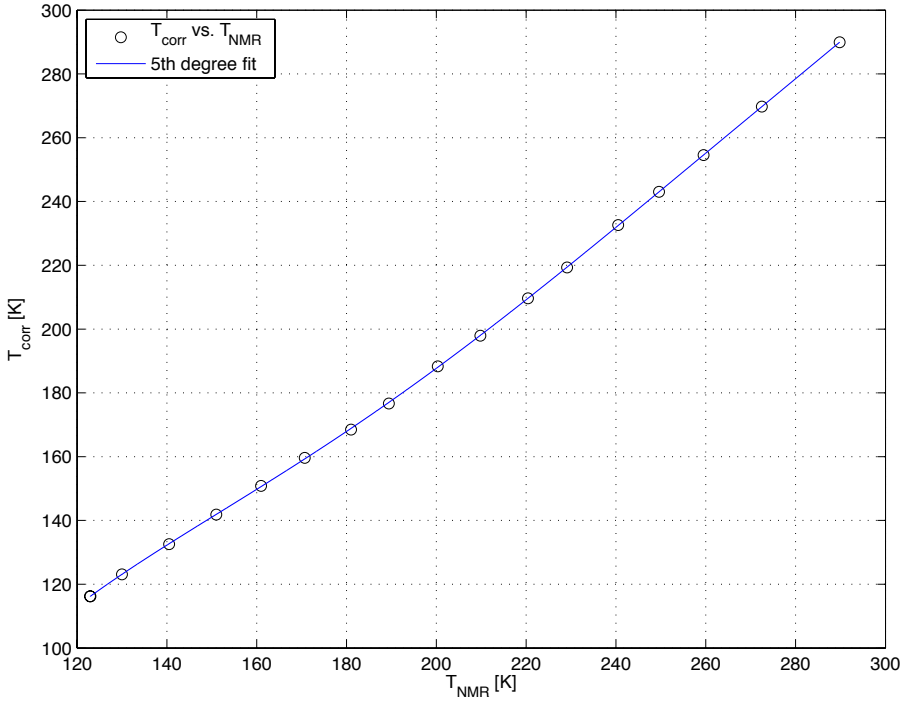


*Figure 5.4: Plot of $T_{corr}$ vs. $T_{NMR}$ as circles with the 5th degree fit to the data displayed as a solid line.*

# 6 Summary

Various experiments were performed during my period as an M.Sc. student in the chemistry department of the University of Iceland Science Institute, with varying degrees of success. Considerable progress has been made on some projects undertaken during these studies but others leave quite a few questions for future researchers.

Experiments were set up to probe the effects of temperature and acidity on alcoholysis reactions of **1**, an adamantane titanasiloxane compound. In addition we hoped to solve mysteries, remaining from previous research, regarding the side products of the reactions through the syntheses of a larger amount of product than had previously been achieved. Unfortunately some of the questions we set out to answer remain unanswered as this is written, as our reactions failed to proceed at the expected rate. None of the experiments run during this research resulted in a sufficient extent of reaction for unambiguous conclusions to be drawn from the amount of products formed as a function of time. However, we confirmed the formation of $HCp^*$ as a byproduct of dimer formation and made unexpected discoveries concerning the substantial effect of light exposure on these reactions which need to be taken into account should further attempts be made at research in this area. Additionally, we found that the products of the reaction of **1** with phenols are most likely not dimers, as previously assumed.

The synthesis of a precursor to a kinetically stabilized 1,3,5-trisilabenzene was sought through two different routes starting from 1,3,5-trisilacyclohexane (**4**). We described the establishment of a successful three step synthetic route to 1,3,5-trichloro-1,3,5-tris(Dipp)-1,3,5-trisilacyclohexane (**8**), a compound that we believe fits the criteria for a precursor to a kinetically stable 1,3,5-trisilabenzene. The next step to be taken along this path is the development of an effective method to purify this precursor compound, contaminated by a 1,3-diisopropylbenzene byproduct, and thus obtaining a sample suitable for the pinnacle of this subject of research — the formation of the aromatic system.

We attempted the syntheses of transition metal complexes containing metal centres bonded to cyclopentadienyl, carbonyl and silacyclohexane moieties. Three different alkali metal salts (Na, K) of complex anions of chromium, tungsten and iron were synthesized. Several attempts were made at the syntheses and analyses of the target compounds. Despite clear signs that reactions took place, possibly forming the intended products, isolation of these compounds was unsuccessful and no conclusive analyses exist to confirm their structure.

The final chapter describes two other projects I worked on during my time in the Árnason

lab: The first one is the improved synthesis of a large tricyclic titanasiloxane compound, **11**, previously formed during earlier research in the Árnason group. The latter is the calibration of the institution's NMR spectrometer's probe head with cooling capabilities, from which the data is used to perform corrections to temperature values reported by the spectrometer during DNMR experiments in connection with the group's conformational analyses of sila- and germaorganics.

# Experimental section

## General comments

All manipulations, unless otherwise noted, were carried out under inert atmosphere (dry $N_2$(g) in some cases, dry Ar(g) in others) using standard Schlenk techniques. All glassware was dried in an oven at 120 °C prior to use, and evacuated while hot.

All solvents for reactions were dried prior to use. Halogen free solvents (hexane, pentane, diethyl ether, THF, toluene) were dried over sodium wire or by equivalent methods and used freshly distilled. Solvents containing halogens (chloroform, dichloromethane, tetrachloromethane) were distilled from $CaCl_2$ or $CaH_2$.

Deuterated solvents for NMR-measurements were kept over molecular sieves. Deuterated chloroform for alcoholysis experiments was dried over anhydrous calcium chloride and distilled onto molecular sieves. Deuterated benzene for measurements of air and moisture sensitive compounds in the quest for a trisilabenzene precursor was passed over a potassium mirror and kept under dry argon atmosphere in a glove box.

$[CpFe(CO)_2]_2$, $Mn_2(CO)_{10}$ and $W(CO)_6$ were purchased from ABCR, $SiCl_3H$ from Fluka, 1,5-dibromopentane from ACROS organics, *tert*-butyllithium from Kanto Chemical Co., Inc., iodine from May and Baker Ltd., mesitylbromide, magnesium shavings, 4-*tert*-butylphenol, 4-nitrophenol, and $Cr(CO)_6$ from Aldrich and $CaCl_2$ (anhydrous) from Merck. All these chemicals were used without further purification. Methanol for alcoholysis experiments was obtained from Merck, dried over $CaH_2$ and used freshly distilled. Triethylamine was purchased from Merck, dried over $CaH_2$ and distilled onto molecular sieves for storage. Celite and silica gel for SCC (short column chromatography) were purchased from Wako Pure Chemical Industries. 1,3,5-trisilacyclohexane was synthesized by Nanna Rut Jónsdóttir, $Cp^*TiCl_3$ by Dr. Már Björgvinsson, 1-bromo-1-silacyclohexane by Þorvaldur Snæbjörnsson, some of the 2-bromo-1,3-diisopropylbenzene (DippBr) used was synthesized by Dr. Eiko Mieda, pure NBS was prepared by Dr. Takahiro Sato from commercially available NBS, $Cp^*Ti(\mu\text{-}O_3)[(^t\text{Bu})Si{-}CH_2]_3$ and $[DisSi(OH){-}O]_3$ were synthesized by Ester Inga Eyjólfsdóttir.

$^1$H NMR (400 MHz or 300 MHz), $^{13}$C NMR (101 MHz or 76 MHz) and $^{29}$Si NMR (59 MHz) spectra were measured on a Bruker AVANCE 400 MHz and a JEOL JNM-AL300 spectrometers. Spectra were measured at room temperature, unless otherwise noted. In $^1$H NMR spectra, signals from residual $CHCl_3$ in $CDCl_3$ (7.26 ppm) and from residual $C_6D_5H$ in $C_6D_6$

(7.16 ppm) were used as references. In $^{13}$C NMR spectra, signals due to $CDCl_3$ (77.16 ppm) and $C_6D_6$ (128.06 ppm) were referenced.[39] $^{29}$Si NMR spectra were measured using INEPT (insensitive nuclei enhanced by polarization transfer) techniques with TMS (tetramethylsilane) as an external standard.

Mass spectra were recorded by Dr. Sigríður Jónsdóttir at the University of Iceland Science Institute on a micrOTOF-Q spectrometer.

X-ray analyses were carried out by Dr. Yoshiyuki Mizuhata at the Institute for Chemical Research (ICR) at Kyoto University, Kyoto, Japan.

# Experimental

## Experiments concerning alcoholysis reactions

**Reaction of $Cp^*Ti(\mu\text{-}O_3)[(^tBu)Si{-}CH_2]_3$ (1) with MeOH (Samples 1a-1d):** Adamantane complex $Cp^*Ti(\mu\text{-}O_3)[(^tBu)Si{-}CH_2]_3$ (**1**) (236.3 mg, 0.447 mmol) was dissolved in $CDCl_3$ (11.8 mL) in a glass ampule. MeOH (1.45 mL, 1.15 g, 35.8 mmol) was added via syringe and the solution thoroughly mixed. Four portions were withdrawn from the solution and placed in four NMR tubes with sealable glass tops. All five samples were degassed, frozen in liquid nitrogen and the vessels evacuated and sealed. The samples' $^1$H NMR spectra were measured approximately once a month for the first 400 days but more scarcely after that when very little change was observed. $^1$H NMR (400 MHz, $CDCl_3$): $\delta$ = −0.62 (d, $^2J_{H_{ax}\text{-}H_{eq}}$ = 13.03 Hz, 3H, $H_{ax}$), −0.35 (d, 3H, $H_{eq}$), 0.79 (s, 27H, $CH_3$[**1**]), 1.97 (s, 15H, $Cp^*$), 3.35 (s, 225H, $CH_3$[MeOH]), 3.38 (s, 75H, O*H*).
Other samples for the alcoholysis experiments were prepared in an analogous manner. Details on those samples can be found in Chapter 2.

## Experiments towards a 1,3,5-trisilabenzene precursor

**1,3,5-Tri(Mes)-1,3,5-trisilacyclohexane (5):** To a stirred, cooled solution (−78 °C) of MesBr (525.6 mg, 2.64 mmol) in THF (10 mL), $^t$BuLi (5.81 mmol, 3.77 mL 1.54 M in n-pentane) was added via gas-tight syringe. After 35 minutes the reaction flask was moved to an ice-water bath and allowed to warm to 0 °C. The resulting light yellow solution was transferred via a silicon tube to another flask containing a stirred, cooled solution (−70 °C) of 1,3,5-trisilacyclohexane (105.8 mg, 0.799 mmol) in THF (15 mL). Stirring was continued and the solution allowed to warm slowly up to RT over night. The reaction solution underwent several changes in colour until it reached RT: At −50 °C a white precipitate was visible, at −30 °C the solution was yellow/reddish and at RT the following day it had a blue/greyish tint. A TLC (thin layer chromatography) check of the reaction mixture run in hexane showed a single dot at low $R_f$ (∼0.2).

Workup was started under argon in a glove box. Co-evaporation with hexane was used to remove any traces of the THF. The residue was then treated with hexane again and the resulting solution filtered through celite on a sintered glass filter and the solvent removed to yield the crude product as a sticky white solid. As NMR measurements of the crude reaction products, before and after exposure to air, indicated the product was stable, workup was continued in air.

The crude product was redissolved in hexane and run through a column packed with a small amount of silica gel to remove all traces of inorganic salts, yielding 1,3,5-tri(Mes)-1,3,5-trisilacyclohexane (**5**) (329.1 mg, 85%). The isolated product was made up of *cis,cis*-1,3,5-tri(Mes)-1,3,5-trisilacyclohexane (**5a**) and *cis,trans*-1,3,5-tri(Mes)-1,3,5-trisilacyclohexane (**5b**) in ratios of ~70% and ~30%, respectively.

For clarity, NMR information for the two isomers will be supplied separately although taken from the same spectrum.
*cis,cis*-1,3,5-Tri(Mes)-1,3,5-trisilacyclohexane (**5a**) $^{1}$H NMR (300 MHz, $C_6D_6$): $\delta$ = 0.28 - 0.82 (m, 6H, C$H_2$), 2.13 (s, 9H, C$H_3$ *para*), 2.51 (s, 18H, C$H_3$ *ortho*), 5.38 (t, 3H, Si*H*), 6.76 (br s, 6H, C*H*).
*cis,trans*-1,3,5-Tri(Mes)-1,3,5-trisilacyclohexane (**5b**) $^{1}$H NMR (300 MHz, $C_6D_6$): $\delta$ = 0.28 - 0.82 (m, 6H, C$H_2$), 2.12 (9H, C$H_3$ *para* on $Mes_{ax}$ and $Mes_{eq}$), 2.49 (s, 6H, C$H_3$ *ortho* on $Mes_{ax}$), 2.55 (s, 12H, C$H_3$ *ortho* on $Mes_{eq}$), 5.36 (m, 3H, Si*H*), 6.74 - 6.78 (6H, C*H*).

**Attempted synthesis of 1,3,5-tribromo-1,3,5-tri(Mes)-1,3,5-trisilacyclohexane:** Bromine (110 µL, 344 mg, 2.15 mmol) was introduced via syringe to a stirred solution of 1,3,5-tri(Mes)-1,3,5-trisilacyclohexane (**5**) (317 mg, 0.650 mmol) in hexane (14 mL) at −32 °C. Upon the addition the clear and colourless solution turned orange. The solution was stirred while the cooling bath slowly warmed up. When the temperature of the cooling bath reached 5 °C the bath was removed. Upon warming, the solution's colour became lighter and at room temperature (an hour after the removal of the cooling bath) the solution was light yellow. An additional hour of stirring made no difference to the solution's colour, but a white suspended solid seemed to be forming. The solution was left stirring over night. A TLC run in hexane revealed a mixture of products. The solvent was pumped off revealing a mixture of oily and solid residues. NMR measurements ($^{1}$H, $^{13}$C, DEPT) revealed bromination of the mesityl groups' *ortho* position methyl groups. Procedure abandoned.

**2,6-Di(isopropyl)phenylbromide:** This synthesis and workup was performed in air. A three-necked flask was fitted with a high performance mechanical stirrer on the middle neck. Through a side neck, 48% $HBr_{(aq)}$ (175 mL, 3.22 mol) and diisopropylaniline (50 mL, 47.5 g, 0.289 mol) were introduced and the solution cooled to 0 °C. A solution of sodium nitrite (22.25 g, 0.322 mol) in water (100 mL) was then added dropwise to the solution during the

course of an hour. Upon the completed addition powdered copper metal (1.46 g) was added to the solution. The cooling was then removed, a side neck on the flask fitted with a reflux condenser and the solution heated at reflux for 2 h.

The crude product was co-distilled with water from the reaction mixture and approximately half of it worked up as follows: The crude reaction products were placed in a separatory funnel and extracted with chloroform ($4 \times 50$ mL). The combined extracts were washed with 3 M NaOH ($3 \times 50$ mL) and brine ($2 \times 50$ mL). The resulting solution was dried over $MgSO_4$, filtered and the solvent removed via evaporation, yielding 10 g of a yellow oil. A TLC run in hexane revealed the desired product as a colourless dot at high $R_f$ (0.74). The impurities could be seen as yellow dots at very low $R_f$ (0 - 0.06).

Integration of an NMR-spectrum suggested the crude products contained 80-85% of the desired product, which was isolated by SCC on a column of 60 mm diameter packed with ca. 5 cm of wet silica gel using hexane as fluent. Evaporation of the solvent yielded the product as a clear and colourless oil (7.94 g). $^1$H NMR (300 MHz, $C_6D_6$): $\delta$ = 1.13 (d, $^3J_{HH}$ = 6.85 Hz, 12H, C$H_3$), 3.59 (hept, $^3J_{HH}$ = 6.85 Hz, 2H, C$H$[$^i$Pr]), 6.92 - 7.10 (3H, C$H$[phenyl]).

**1,3,5-Tris(Dipp)-1,3,5-trisilacyclohexane (6):** To a stirred, cooled solution (−75 °C) of DippBr (527 µL, 617.3 mg, 2.560 mmol) in THF (10 mL), $^t$BuLi (5.63 mmol, 3.66 mL 1.54 M in n-pentane) was added via a gastight syringe. After 25 minutes the reaction flask was moved to an ice-water bath and allowed to warm up to 0 °C. The resulting solution was transferred via silicon cannula to a cooled solution (−78 °C) of 1,3,5-trisilacyclohexane (102.7 mg, 0.776 mmol) in THF (12 mL). The reaction flask was kept in the cooling bath and allowed to warm up slowly to RT over night and left stirring for a whole day (this was incidental and is not required).

The reaction was worked up in air. When workup was started the reaction mixture contained a fair amount of a white solid. A TLC of the reaction mixture run in hexane showed two dots, one at $R_f \sim 0.20$ and another at $R_f \sim 0.85$. The high $R_f$ dot turned out to belong to 1,3-diisopropylbenzene formed upon the decomposition of some of the DippLi. This may be due to DippLi having a relatively short lifetime in THF solution at 0 °C.

THF was pumped off and subsequently three small amounts of hexane added and pumped off to ensure complete removal of the polar solvent. The residue was treated with several small portions of hexane which were then filtered through celite compressed on a sintered glass filter. The filtrate was run through a column packed with a small amount of silica gel to remove all traces of inorganic salts. SCC may also be utilized to separate the desired product from the 1,3-diisopropylbenzene side product.

The desired product (357.4 mg, 0.583 mmol, 75%) was obtained as an isomeric mixture of

*cis,cis*-1,3,5-tris(Dipp)-1,3,5-trisilacyclohexane (**6a**) and *cis,trans*-1,3,5-tris(Dipp)-1,3,5-trisilacyclohexane (**6b**). The exact isomeric ratio could not been determined, as the two isomers give very similar NMR-signals. It is however apparent that a vast majority of the compound is in the *cis,cis* form. $^{1}$H NMR (300 MHz, $CDCl_3$): $\delta$ = 0.50 - 0.77 (6H, C$H_2$), 1.30 (d, $^{3}J_{HH}$ = 6.76 Hz, 36H, C$H_3$), 3.58 (sept, 6H, C$H$[$^{i}$Pr]), 5.14 (t, $J_{HH}$ = 8.96 Hz, 3H, Si$H$), 7.12 - 7.39 (3H, C$H$[phenyl]). $^{13}$C{$^{1}$H} NMR (76 MHz, $CDCl_3$): $\delta$ = 1.79 ($C$H$_2$), 24.99 ($C$H$_3$), 33.50 ($C$H[$^{i}$Pr]), 123.00 ($C$H[meta]), 130.12 ($C$H[para]), 133.51 ($C$[ipso]), 155.33 ($C$[ortho]).

**1-Dipp-1,3,5-trisilacyclohexane (7):** To a stirred, cooled solution (−70 °C) of DippBr (359 µL, 420.1 mg, 1.74 mmol) in THF (6 mL), $^{t}$BuLi (3.83 mmol, 2.49 mL 1.54 M in n-pentane) was added via a gastight syringe. After a few minutes the reaction flask was moved to an ice-water bath and allowed to warm up to 0 °C. The resulting solution was transferred via silicon cannula to a cooled solution (−68 °C) of 1,3,5-trisilacyclohexane (205.9 mg, 1.56 mmol) in THF (10 mL). The reaction flask was kept in the cooling bath and allowed to warm up slowly to RT over night and left stirring for 38 h. Twice during this period samples were withdrawn from the solution for $^{1}$H NMR measurements. As product/reactant ratios were the same at 14 h and 38 h it can be assumed that the extra stirring time was unproductive. Significant decomposition of the DippLi reactant occurred leaving unreacted 1,3,5-trisilacyclohexane, lowering the yield of **7** and contaminating the product with Dipb. Workup was performed in air. The solvent was pumped off and 4 small portions of hexane added and removed in succession. The residue was treated with hexane and the resulting solution filtered through celite on a sintered glass filter. Filtration was repeated as a solid precipitated in the filtrate, most likely from the reaction of unreacted 1,3,5-trisilacyclohexane with moisture from the air. The resulting solution was run through a short plug of silica gel in a column to remove inorganic material. Evaporation of the solvent left a clear colourless oil. NMR spectrum revealed a mixture of the intended product and Dipb. **7** was separated from the Dipb by HPLC yielding 144 mg (32%) of pure product as a clear and colourless oil which crystallized upon cooling. $^{1}$H NMR (300 MHz, $C_6D_6$): $\delta$ = −0.35 - −0.19/−0.15 - −0.05/0.14 - 0.30 (6H, C$H_2$), 1.20 (d, $^{3}J_{HH}$ = 6.76 Hz, 12H, C$H_3$), 3.44 (m, 2H, C$H$[$^{i}$Pr]), 4.22 - 4.48 (m, 4H, Si$H_2$), 5.15 (m, 1H, Si$H$), 7.05 - 7.31 (3H, C$H$[phenyl]).

**Attempted syntheses of 1,3,5-tribromo-1,3,5-tris(Dipp)-1,3,5-trisilacyclohexane:**

**Attempt 1:** To a stirred solution of 1,3,5-tris(Dipp)-1,3,5-trisilacyclohexane (**6**) (240 mg, 0.391 mmol) in benzene (11 mL) NBS (N-bromosuccinimide) (229 mg, 1.29 mmol) was added in a single dose. Within 2 minutes the solution turned dark orange. 10 minutes after the addition of NBS the colour had faded to yellow and a white suspended solid was visible. Half an hour after the introduction of NBS the solution was close to colourless and workup

was begun. NMR revealed breakage of the Si−$C_{ipso}$ bond resulting in DippBr as the major product.

**Attempt 2:** To a stirred solution of 1,3,5-tris(Dipp)-1,3,5-trisilacyclohexane (**6**) (103 mg, 0.168 mmol) in hexane (8.5 mL) at 0 °C, NBS (97.6 mg, 0.548 mmol) was added in several small portions over 3.5 h. When the addition was complete and the solution had been stirred at RT for 1 h, a TLC revealed a fair amount of unreacted **6**. A small portion of benzene (0.82 mL) was added to improve solubility and the solution stirred over night. NMR analysis of the products revealed incomplete conversion from Si−H to Si−Br as well as decomposition resulting in the formation of DippBr.

**1,3,5-Trichloro-1,3,5-tris(Dipp)-1,3,5-trisilacyclohexane (8):**

**Method A:** 1,3,5-tris(Dipp)-1,3,5-trisilacyclohexane (**6**) (92.5 mg, 0.151 mmol) and $PCl_5$ were placed in the reaction vessel which was fitted with a reflux condenser. Freshly distilled $CCl_4$ (4.2 mL) was added via syringe. Both reactants readily dissolved. The solution was kept at a steady reflux (oil bath set to 116 °C) for 24 h and subsequently left to stand at RT for another day. NMR measurements of the reaction solution revealed a mixture of products, the desired product probably among them along with a small amount of unreacted Si−H. Quenching of $PCl_5$ by the normal means (MeOH) is not feasible in the presence of reactive Si−Cl bonds and workup was attempted forthwith. During workup the product underwent a change. An ESI-MS (electrospray ionization mass spectrometry) spectrum of the compound formed showed only one identifiable pattern, that of an HCl adduct of the desired compound.

**Method B:** To a stirred solution of 1,3,5-tris(Dipp)-1,3,5-trisilacyclohexane (**6**) (236 mg, 0.385 mmol) in THF (3.5 mL) kept below −20 °C, TCCA (trichloroisocyanuric acid) (99.6 mg, 0.429 mmol) was added in 8 approximately equal portions during the course of 45 min. After the last addition the cooling bath was allowed to slowly warm up to RT. THF was removed by evaporation and 3 small portions of hexane added and removed in succession. The residue was treated with hexane and the resulting solution filtered through celite. Hexane was evaporated off leaving a fairly dry white solid (277.2 mg). NMR revealed a mixture of **8**, DippBr and Dipb with the desired product accounting for approximately 80% judging by integration. $^1$H NMR (300 MHz, $C_6D_6$): $\delta$ = 1.14 (d, $^3J_{HH}$ = 6.86 Hz, C$H_3$[$^i$Pr, DippBr]), 1.19 (d, $^3J_{HH}$ = 6.93 Hz, C$H_3$[$^i$Pr, Dipb]), 1.21/1.26/1.27/1.30 (C$H_3$[$^i$Pr, **8**]), 1.85 - 2.14 (C$H_2$[endocyclic, **8**]), 2.76 (m, C$H$[$^i$Pr, Dipb]), 3.56 (m, C$H$[$^i$Pr, DippBr]), 3.89 (m, C$H$[$^i$Pr, **8**]), 6.94 - 7.29 (C$H$[phenyl, Dipb+DippBr+**8**]). $^{29}$Si NMR (59 MHz, $C_6D_6$): $\delta$ = 11.05, 15.38.

**Attempted synthesis of 1,3,3,5,5-pentabromo-1-(Dipp)-1,3,5-trisilacyclohexane:** To a solution of 1-Dipp-1,3,5-trisilacyclohexane (**7**) (53.6 mg, 0.183 mmol) in hexane (4.7 mL)

at 0 °C, NBS was added in small portions over a period of 8 h and the solution then left stirring for 40 h. At the end of this period the solution had changed from yellow to reddish. The solvent was evaporated off and the reaction vessel introduced into the glove box. The residue was treated with hexane and the resulting solution filtered through celite on a sintered glass filter. Hexane was evaporated off the filtrate and a sample of the residue measured by NMR. Measurement revealed incomplete Si−H to Si−Br conversion.

**Attempted syntheses of 1,3,5-tris(Dipp)-1,3,5-trisilabenzene:**
**Attempt 1:** To a solution of 1,3,5-trichloro-1,3,5-tris(Dipp)-1,3,5-trisilacyclohexane (**8**) (55.3 mg, 0.070 mmol) in THF, LDA (lithiumdiisopropylamide) (24.9 mg, 0.232 mmol) was added in the solid state resulting in a yellow solution. The solution was stirred at RT for an hour, seemingly becoming more yellow in the first half hour. THF was evaporated off and three small portions of hexane added and evaporated off in succession. The yellowish white residue was treated with hexane and the resulting solution filtered through celite on a sintered glass filter. Hexane was evaporated off, leaving a yellow oil. NMR measurements revealed no signals assignable to the desired compound.
**Attempt 2:** To a solution of 1,3,5-trichloro-1,3,5-tris(Dipp)-1,3,5-trisilacyclohexane (**8**) (46.3 mg, 0.065 mmol) in hexane at −35 °C, LDA (lithiumdiisopropylamide) (23.1 mg, 0.216 mmol) was added in the solid state. Two small portions of THF were used two wash the LDA vial into the reaction solution. Around 50 min later the solution was removed from cooling. 50 min after that the solution, previously clear, appeared foggy. When no further change was observed 40 min later, the solvent was pumped off and two more small portions of hexane added and evaporated off. The residue was treated with hexane and the resulting solution filtered through celite on a sintered glass filter. Hexane was evaporated off leaving a yellow oil. NMR measurements revealed no signals assignable to the desired compound.

## Experiments towards silacyclohexane derivatives

**1-Chloro-1-silacyclohexane:** A solution of 1,5-dibromopentane (63.3 g, 275 mmol) in $Et_2O$ (150 mL) was added dropwise to magnesium shavings (14.7 g, 605 mmol) in $Et_2O$ (40 - 50 mL) at reflux. After the addition was completed, the mixture was heated at reflux for two hours and then stirred over night. The excess magnesium was separated from the desired di-Grignard by filtering the solution through glass wool into a dropping funnel. The resulting two-phased solution was then slowly added to a solution of trichlorosilane (36.7 g, 270 mmol) and $Et_2O$ (150 mL), while stirring at 0 °C. A lot of white reaction salt was formed during this reaction. After stirring over night, the $Et_2O$ was distilled off the reaction mixture and replaced by pentane. The reaction mixture was then filtered under nitrogen, the salt washed several times with pentane and then discarded. Distillation of the reaction mixture

at 95 to 113 °C and 250 to 335 torr, yielded chlorosilacyclohexane (14.9 g, 41%) with some impurities of bromosilacyclohexane due to halogen exchange reactions. $^{1}$H NMR (400 MHz, $CDCl_3$): $\delta$ = 0.86 - 1.15 (m, 4H, C$H_2$), 1.30 - 1.43 (m, 2H, C$H_{2(ax/eq)}$), 1.50 - 1.63 (m, 2H, C$H_{2(ax/eq)}$), 1.72 - 1.86 (m, 4H, C$H_2$), 4.86 (s, 1H, Si*H*). $^{13}$C{$^{1}$H} NMR (101 MHz, $CDCl_3$): $\delta$ = 14.92, 23.25, 29.19.

**Sodium cyclopentadienide:** Sodium metal (979.2 mg, 42.6 mmol) and dicyclopentadiene (25 mL) were placed in a round bottom flask fitted with a reflux condenser and the mixture heated at reflux for 5 h. At this point no sodium remained but a white solid had precipitated in a considerable amount. The solid product was separated from the liquid by filtering over a sintered glass filter. The solid was then washed with three portions of freshly distilled pentane, dried under vacuum and subsequently moved to a Schlenk tube for storage. The amount of product recovered from the filter was 3.67 g (98%). $^{1}$H NMR (400 MHz, DMSO-$d_6$): $\delta$ = 5.36 (s, C*H*). $^{13}$C{$^{1}$H} NMR (101 MHz, DMSO-$d_6$): $\delta$ = 102.95 (*C*H).

**Na[($\eta^5$-$C_5H_5$)W(CO)$_3$]:** Sodium cyclopentadienide (100.7 mg, 1.14 mmol) and hexacarbonyltungsten (433.4 mg, 1.23 mmol) were weighed into a two necked 50 mL round bottom flask under argon atmosphere in a glove box. The flask was brought out of the glove box and the central neck fitted with a reflux condenser connected to a Schlenk line. THF (20 mL) was introduced through the side neck via syringe and stirring initiated. The solution so prepared, which was brown and cloudy, was heated at reflux for 18 h (over night). Once the solution, still brown and cloudy, had cooled somewhat it was filtered over a sintered glass filter, resulting in a bright yellow filtrate, which was dried forthwith via evaporation under reduced pressure. Once the solvent had been removed the flask contained a mixture of the intended product, Na[($\eta^5$-$C_5H_5$)W(CO)$_3$] - a yellow solid, and unreacted W(CO)$_6$. The excess carbonyl was removed via sublimation leaving 355.8 mg (87%) of product. $^{1}$H NMR (400 MHz, DMSO-$d_6$): $\delta$ = 5.02 (s, C*H*). $^{13}$C{$^{1}$H} NMR (101 MHz, DMSO-$d_6$): $\delta$ = 84.52 (*C*H[Cp]), 225.86 (*C*O).

**Na[($\eta^5$-$C_5H_5$)Cr(CO)$_3$]:** Sodium cyclopentadienide (306 mg, 3.48 mmol) and hexacarbonylchromium (842 mg, 3.83 mmol) were weighed into a two necked 50 mL round bottom flask under argon atmosphere in a glove box. The flask was brought out of the glove box and the central neck fitted with a reflux condenser connected to a Schlenk line. THF (25 mL) was introduced through the side neck via syringe and stirring initiated. The solution so prepared, which was brown and cloudy, was heated at reflux for 25 h. Once the solution, still brown and cloudy, had cooled somewhat it was filtered over a sintered glass filter, resulting in a light yellow filtrate, which was dried forthwith via evaporation under reduced pressure. Once the solvent had been removed the flask contained a mixture of the intended product,

$Na[(\eta^5\text{-}C_5H_5)Cr(CO)_3]$ - a light yellow solid, and unreacted $Cr(CO)_6$. The excess carbonyl was removed via sublimation leaving 688 mg (88%) of product. The product is quite unstable when dry and immediately turns green on exposure to air.

**$K[(\eta^5\text{-}C_5H_5)Fe(CO)_2]$:**
**Method A:** In a 50 mL pear shaped Schlenk flask connected to a Schlenk line $[CpFe(CO)_2]_2$ (226.8 mg, 0.641 mmol) was dissolved in THF (21 mL) resulting in a dark purplish red solution. Sodium-potassium alloy ($NaK_{2.83}$, 452 mg, 3.38 mmol) was pipetted into the solution under inert atmosphere, the flask stoppered and the mixture stirred for roughly 6 h. The excess alloy along with a dark brown solid was filtered out yielding a blood red filtrate. The solvent was removed by evaporation under reduced pressure leaving a brownish red solid (184.8 mg, 0.855 mmol, 67%) which spontaneously combusted in air, which is consistent with the $Fp^-$ anions high reactivity. Analysis by IR spectroscopy was attempted, but the available setup for the IR equipment proved unsuitable for such a reactive compound. This solid was used in a subsequent reaction without conclusive analyses.
**Method B:** In a 50 mL pear shaped Schlenk flask connected to a Schlenk line $[CpFe(CO)_2]_2$ (393.5 mg, 1.11 mmol) was dissolved in THF (24 mL) resulting in a dark purplish red solution. Sodium-potassium alloy ($NaK_{2.83}$, 780 mg, 5.85 mmol) was pipetted into the solution under inert atmosphere, the flask stoppered and the mixture stirred for just under 6 h. The excess alloy along with a dark brown solid was filtered out yielding a blood red filtrate. This solution was used without further purification, assuming a yield of 70% based on referenced data[40] and our previous result (Method A).

**Attempted synthesis of $K[Mn(CO)_5]$:** In a 50 mL pear shaped Schlenk flask connected to a Schlenk line $Mn_2(CO)_{10}$ (407 mg, 1.04 mmol) was dissolved in THF (20 mL) resulting in a clear yellow solution. Sodium-potassium alloy ($NaK_{2.83}$, 836 mg, 6.26 mmol) was pipetted into the solution under inert atmosphere. Upon the addition of the alloy the solution darkened somewhat and was orange after about 5 min. The flask was stoppered and the mixture stirred for 3 h. The excess alloy was filtered out yielding a yellow/orange filtrate. The solvent was removed by evaporation under reduced pressure leaving solid residue of two colours most of which looked very similar to the starting material. Purification of this compound was not sought as the time of my research was up.

**Attempted synthesis of $C_5H_{11}Si[(\eta^5\text{-}C_5H_5)Cr(CO)_3]$:** In a 50 mL round bottom Schlenk flask, connected to a Schlenk line, $Na[(\eta^5\text{-}C_5H_5)Cr(CO)_3]$ (701 mg, 3.13 mmol) was suspended in methylcyclohexane (25 mL). 1-chloro-1-silacyclohexane (255 mg, 1.89 mmol) was added in a single dose via a micropipette. The solution was stirred at RT for 3 days followed by filtration over a sintered glass filter to remove unreacted material. The solvent

was removed completely via evaporation under reduced pressure leaving a dark brown sticky residue. Isolation of the desired compound from this residue was unsuccessful. Additionally, see *Note on the workup of these reactions* at the end of this section.

**Attempted syntheses of $C_5H_{11}Si[(\eta^5\text{-}C_5H_5)W(CO)_3]$:**

**Method A:** In a 50 mL round bottom Schlenk flask, connected to a Schlenk line, $Na[(\eta^5\text{-}C_5H_5)W(CO)_3]$ (206.9 mg, 0.581 mmol) was suspended in methylcyclohexane (9 mL). 1-bromo-1-silacyclohexane (99.2 mg, 0.554 mmol) was added in a single dose via a micropipette. The solution was stirred at RT for 3 days followed by filtration over a sintered glass filter to remove unreacted material. A reduction in volume of the filtrate was achieved by evaporation under reduced pressure. The solvent that was removed by this method had a yellow tint. NMR measurements of the solvent yielded no useful data. The solvent was then removed completely via evaporation leaving a dark brown, almost black, sticky residue. The flask was fitted with a cold finger and the residue heated mildly (hair dryer) under reduced pressure. A very small amount of damp yellow crystals deposited on the finger. The crystals were washed into a Schlenk tube with $CDCl_3$ and the resulting yellow solution transferred to an NMR tube. Analysis yielded inconclusive data and the sample started to change colour, turning orange in only a few minutes. A comparable reaction leading to similar results was performed exchanging only $CDCl_3$ for $C_6D_6$ but with the same results. Additionally, see *Note on the workup of these reactions* at the end of this section.

**Method B:** 1-bromo-1-silacyclohexane (93.7 mg, 0.523 mmol) was added via micropipette to a solution of $Na[(\eta^5\text{-}C_5H_5)W(CO)_3]$ (186.1 mg, 0.523 mmol) in THF (20 mL) at −50 °C and the solution allowed to slowly warm up to RT. As the solution got warmer it changed colour from the initial yellow to a foggy brown at −28 °C. The solution was kept stirring over night and the solvent then removed by evaporation under reduced pressure. The solvent removed clearly contained a dissolved compound as it was yellow. NMR measurements of the sticky dark residue yielded no conclusive data. Additionally, see *Note on the workup of these reactions* at the end of this section.

**Attempted syntheses of $C_5H_{11}Si[(\eta^5\text{-}C_5H_5)Fe(CO)_2]$:**

**Method A:** To a suspension of $K[(\eta^5\text{-}C_5H_5)Fe(CO)_2]$ (184.8 mg, 0.855 mmol) in methylcyclohexane (20 mL), 1-bromo-1-silacyclohexane (134 mg, 0.75 mmol) was added in a single dose via a micropipette and the mixture stirred at RT for 22 h. Following this period the solution was filtered to remove unreacted material and the filtrate dried by removing the solvent via evaporation under reduced pressure. The removed solvent's strong yellow colour suggested the presence of a solute. Sublimation from the sticky, almost wet, residue was attempted but without success. Additionally, see *Note on the workup of these reactions* at the end of this section.

**Method B:** A solution of K[($\eta^5$-$C_5H_5$)Fe(CO)$_2$] (336 mg, 1.55 mmol) (prepared by the method described in *K[($\eta^5$-$C_5H_5$)Fe(CO)$_2$], Method B* above) was added dropwise into a stirred solution of 1-bromo-1-silacyclohexane (265 mg, 1.48 mmol) in THF (17 mL) at −50 °C. Upon the completion of the addition the cooling was removed and the solution stirred for another 30 min. The solvent was removed via evaporation under reduced pressure, leaving a dark sticky, almost wet, residue in the reaction flask. The solvent removed was yellow, indicating the presence of a solute. Extraction of the solid residue did not lead to the isolation of the desired product. Additionally, see *Note on the workup of these reactions* at the end of this section.

### Note on the workup of these reactions

Following the methods described above, for the formation of transition metal complexes containing the silacyclohexane moiety, several attempts were made at extraction of the products from the solid residues with different solvents (hexane, pentane, toluene) and isolation of the products by crystallization through cooling or evaporation of solvent or a combination of the two. Additionally isolation from the removed solvents, containing solutes judging by their colour, was attempted through the same methods. None of these experiments resulted in the successful isolation of the desired compounds.

## Other reactions

**[($C_5Me_5$)Ti−O−Si(($Me_3Si)_2$CH)−O]$_2$[($\mu$−$O_2$)[Si(($Me_3Si)_2$CH)(OH)]]$_2$ (11):** In a 100 mL round bottomed Schlenk flask, (DisSi(OH)−O)$_3$ (45.4 mg, 0.067 mmol) was dissolved in THF (40 mL) under inert gas atmosphere at 20 °C and $Et_3N$ (37 µL) added to the solution with a micropipette. $Cp^*TiCl_3$ (22.8 mg, 0.079 mmol) was then added to the solution in a single dose with vigorous stirring. The dark orange solution was stirred over night and gradually became light yellow. THF was removed via condensation and the residue treated with *n*-hexane (50 mL). The precipitated salts were filtered off under inert atmosphere and fractional crystallization of the filtrate yielded the product (23.3 mg, 46%). The desired amount of crystallization was achieved when 4-5mL remained of the solvent, leaving side-products unprecipitated. $^1$H NMR (400 MHz, $CDCl_3$): $\delta$ = −0.70/−0.68/−0.68 (s, 4H, C*H*($SiMe_3)_2$), 0.17/0.18/0.19/0.20 (s, 72H, Si$CH_3$), 2.21 (s, 30H, Cp−$CH_3$), 3.66 (s, 2H, O*H*).

# Bibliography


[1] Greenwood, N.; Earnshaw, A. *Chemistry of the Elements*, 2nd ed.; Elsevier Butterworth Heinemann, 1997.

[2] Guðnason, P. I. Kísilinnihaldandi sexhringir. M.Sc. thesis, University of Iceland, 2003.

[3] Eyjólfsdóttir, E. I. Synthesis, analysis and reactions of novel titanasiloxane complexes. M.Sc. thesis, University of Iceland, 2008.

[4] Maier, G.; Mihm, G.; Reisenauer, H. P. *Angewandte Chemie International Edition in English* **1980**, *19*, 52–53.

[5] Barton, T. J.; Burns, G. T. *Journal of the American Chemical Society* **1978**, *100*, 5246–5246.

[6] Maier, G.; Schöttler, K.; Reisenauer, H. P. *Tetrahedron Letters* **1985**, *26*, 4079–4082.

[7] Märkl, G.; Schlosser, W. *Angewandte Chemie International Edition in English* **1988**, *27*, 963–965.

[8] Wakita, K.; Tokitoh, N.; Okazaki, R.; Nagase, S. *Angewandte Chemie International Edition* **2000**, *39*, 634–636.

[9] Wakita, K.; Tokitoh, N.; Okazaki, R.; Takagi, N.; Nagase, S. *Journal of the American Chemical Society* **2000**, *122*, 5648–5649.

[10] Tokitoh, N.; Wakita, K.; Matsumoto, T.; Sasamori, T.; Okazaki, R.; Takagi, N.; Kimurac, M.; Nagasec, S. *Journal of the Chinese Chemical Society* **2008**, *55*, 487–507.

[11] Tokitoh, N.; Wakita, K.; Okazaki, R.; Nagase, S.; von Ragué Schleyer, P.; Jiao, H. *Journal of the American Chemical Society* **1997**, *119*, 6951–6952.

[12] Wakita, K.; Tokitoh, N.; Okazaki, R.; Nagase, S.; Schleyer, P. v. R.; Jiao, H. *Journal of the American Chemical Society* **1999**, *121*, 11336–11344.

[13] Takeda, N.; Shinohara, A.; Tokitoh, N. *Organometallics* **2002**, *21*, 256–258.

[14] Takeda, N.; Shinohara, A.; Tokitoh, N. *Organometallics* **2002**, *21*, 4024–4026.

[15] Tokitoh, N.; Shinohara, A.; Matsumoto, T.; Sasamori, T.; Takeda, N.; Furukawa, Y. *Organometallics* **2007**, *26*, 4048–4053.

[16] Rich, J. D.; West, R. *Journal of the American Chemical Society* **1982**, *104*, 6884–6886.

[17] Kabe, Y.; Ohkubo, K.; Ishikawa, H.; Ando, W. *Journal of the American Chemical Society* **2000**, *122*, 3775–3776.

[18] Kinjo, R.; Ichinohe, M.; Sekiguchi, A.; Takagi, N.; Sumimoto, M.; Nagase, S. *Journal of the American Chemical Society* **2007**, *129*, 7766–7767, PMID: 17542592.

[19] Sen, S. S.; Khan, S.; Nagendran, S.; Roesky, H. W. *Accounts of Chemical Research* **2012**, *45*, 578–587.

[20] Bjarnason, A.; Arnason, I. *Angewandte Chemie International Edition in English* **1992**, *31*, 1633–1634.

[21] King, R. A.; Vacek, G.; Schaefer III, H. F. *Journal of Molecular Structure: THEOCHEM* **1995**, *358*, 1–14.

[22] Baldridge, K. K.; Uzan, O.; Martin, J. M. L. *Organometallics* **2000**, *19*, 1477–1487.

[23] Lide, D. R., Haynes, W. M., Eds. *CRC Handbook of Chemistry and Physics, Internet Version*, 90th ed.; CRC Press, 2010.

[24] Ref. 3, p. 20.

[25] Jónsdóttir, N. R. Conformational behaviour of selected silicon- and germanium-containing ring systems. M.Sc. thesis, University of Iceland, 2013.

[26] Lambert, J. B.; Stern, C. L.; Zhao, Y.; Tse, W. C.; Shawl, C. E.; Lentz, K. T.; Kania, L. *Journal of Organometallic Chemistry* **1998**, *568*, 21–31.

[27] Lambert, J. B.; Lin, L. *The Journal of Organic Chemistry* **2001**, *66*, 8537–8539.

[28] Tilstam, U.; Weinmann, H. *Organic Process Research & Development* **2002**, *6*, 384–393.

[29] Varaprath, S.; Stutts, D. H. *Journal of Organometallic Chemistry* **2007**, *692*, 1892–1897.

[30] Hohenberger, K. Si-übergangsmetallsubstituierte 1,3,5-trisilacyclohexane. Ph.D. thesis, Universität Karlsruhe, 1979.

[31] Panda, T. K.; Gamer, M. T.; Roesky, P. W. *Organometallics* **2003**, *22*, 877–878.

[32] Ellis, J. E.; Flom, E. A. *Journal of Organometallic Chemistry* **1975**, *99*, 263–268.

[33] Kleinberg, J., Ed. *Inorganic Syntheses*; McGraw-Hill, 1963; Vol. VII.

[34] Ref. 33, p. 105.

[35] Ref. 30, p. 113.

[36] Theys, R. D.; Dudley, M. E.; Hossain, M. M. *Coordination Chemistry Reviews* **2009**, *253*, 180–234.

[37] Snæbjörnsson, Þ. 1-Halogen-1-silacyclohexan: Smíði, hreinsun og auðkenning. University of Iceland, 2012.

[38] Ref. 23, **15**-3 - **15**-4.

[39] Fulmer, G. R.; Miller, A. J. M.; Sherden, N. H.; Gottlieb, H. E.; Nudelman, A.; Stoltz, B. M.; Bercaw, J. E.; Goldberg, K. I. *Organometallics* **2010**, *29*, 2176–2179.

[40] Ref. 30, p. 113.

# Appendices

# Appendix A

$^{1}$H NMR spectrum of **1**

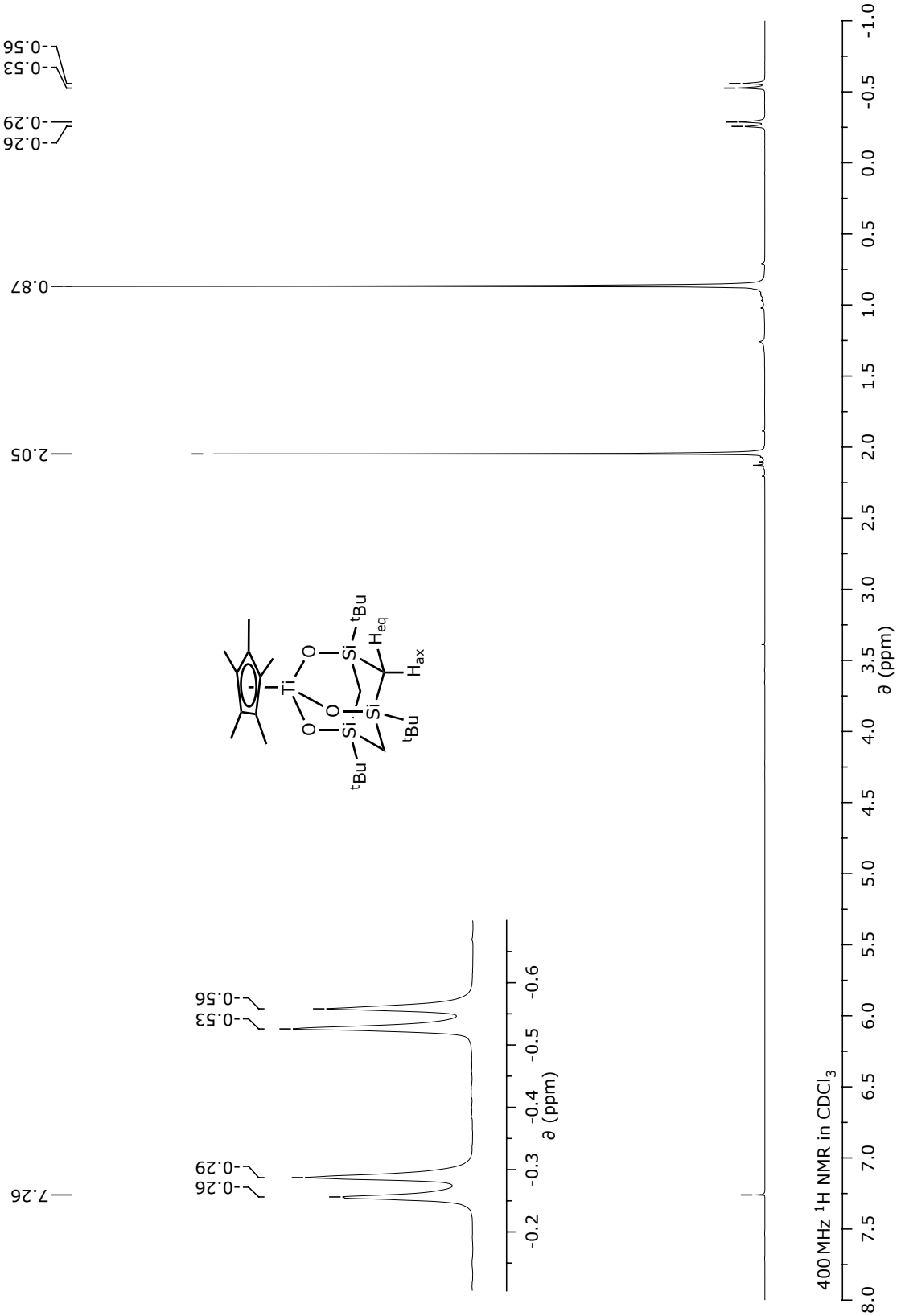

# Appendix B

NMR spectra of **4**

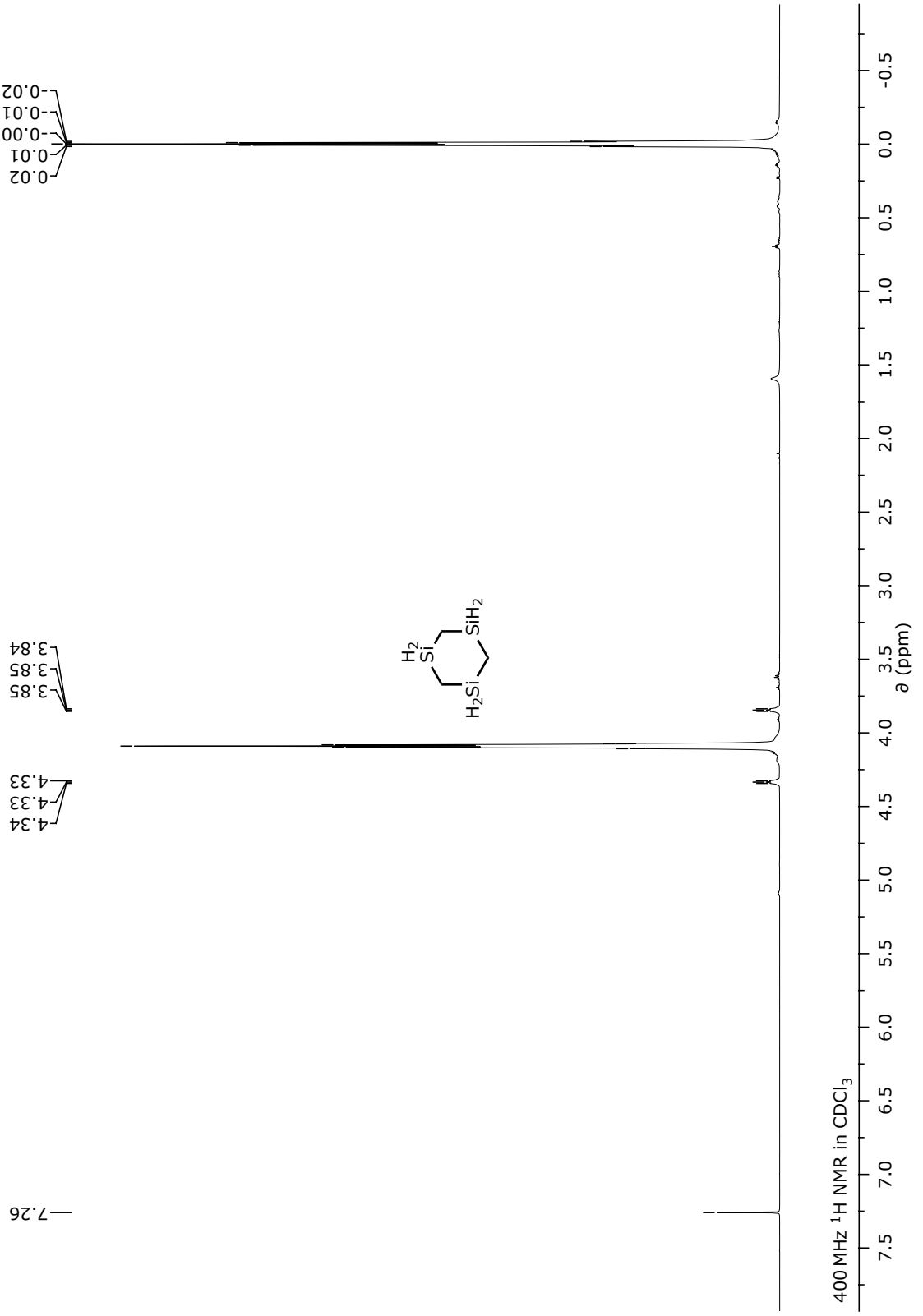

101 MHz $^{13}C\{^1H\}$ NMR in $CDCl_3$
85 80 75 70 65 60 55 50 45 40 35 30 25 20 15 10 5 0 -5 -10 -15 -20
∂ (ppm)
77.48
77.16
76.84
-10.02
-10.23
-10.44
$H_2Si$
$SiH_2$
$H_2$
Si

# Appendix C

$^{1}$H NMR spectrum of **5**

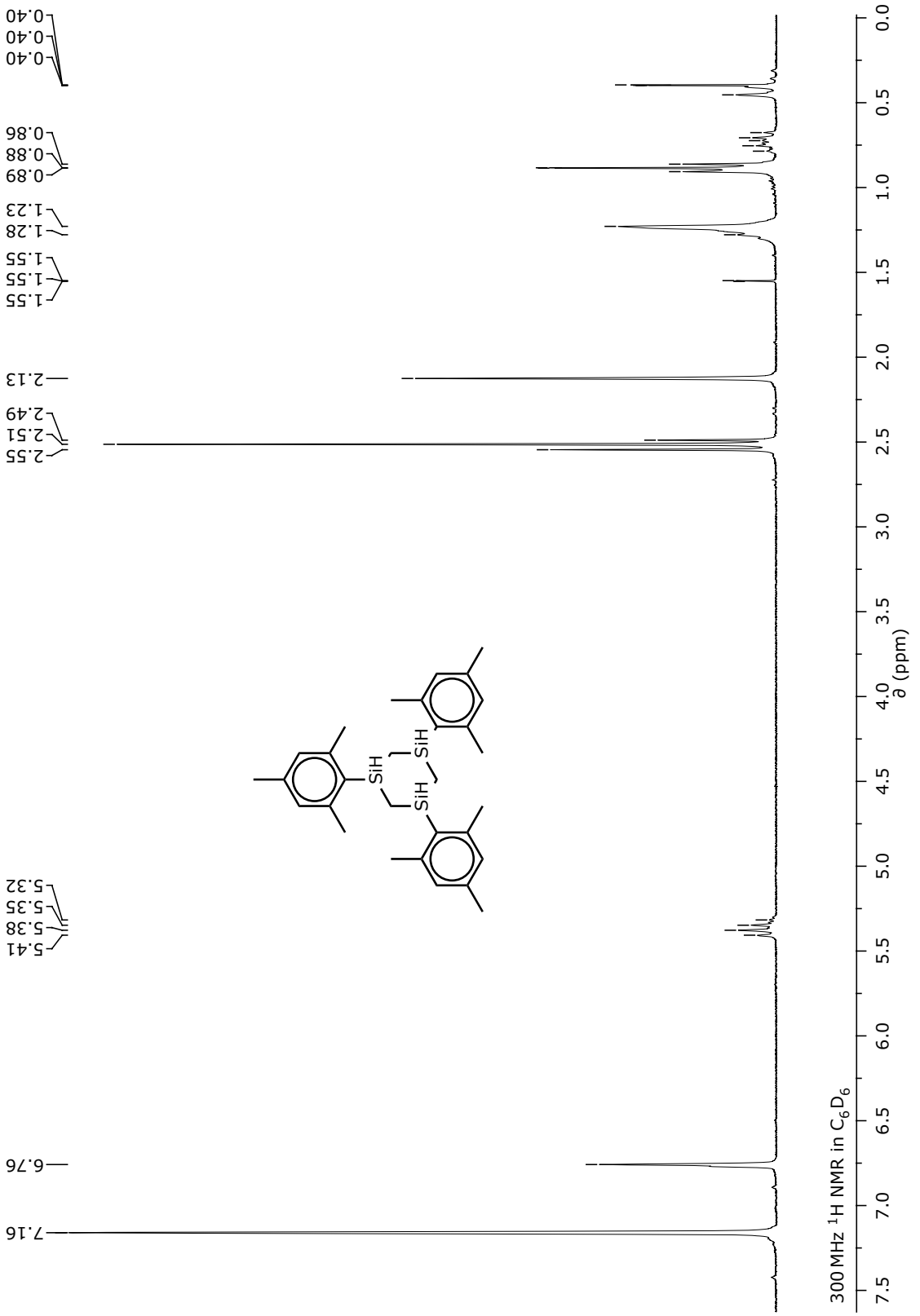

# Appendix D

NMR spectra of **6**

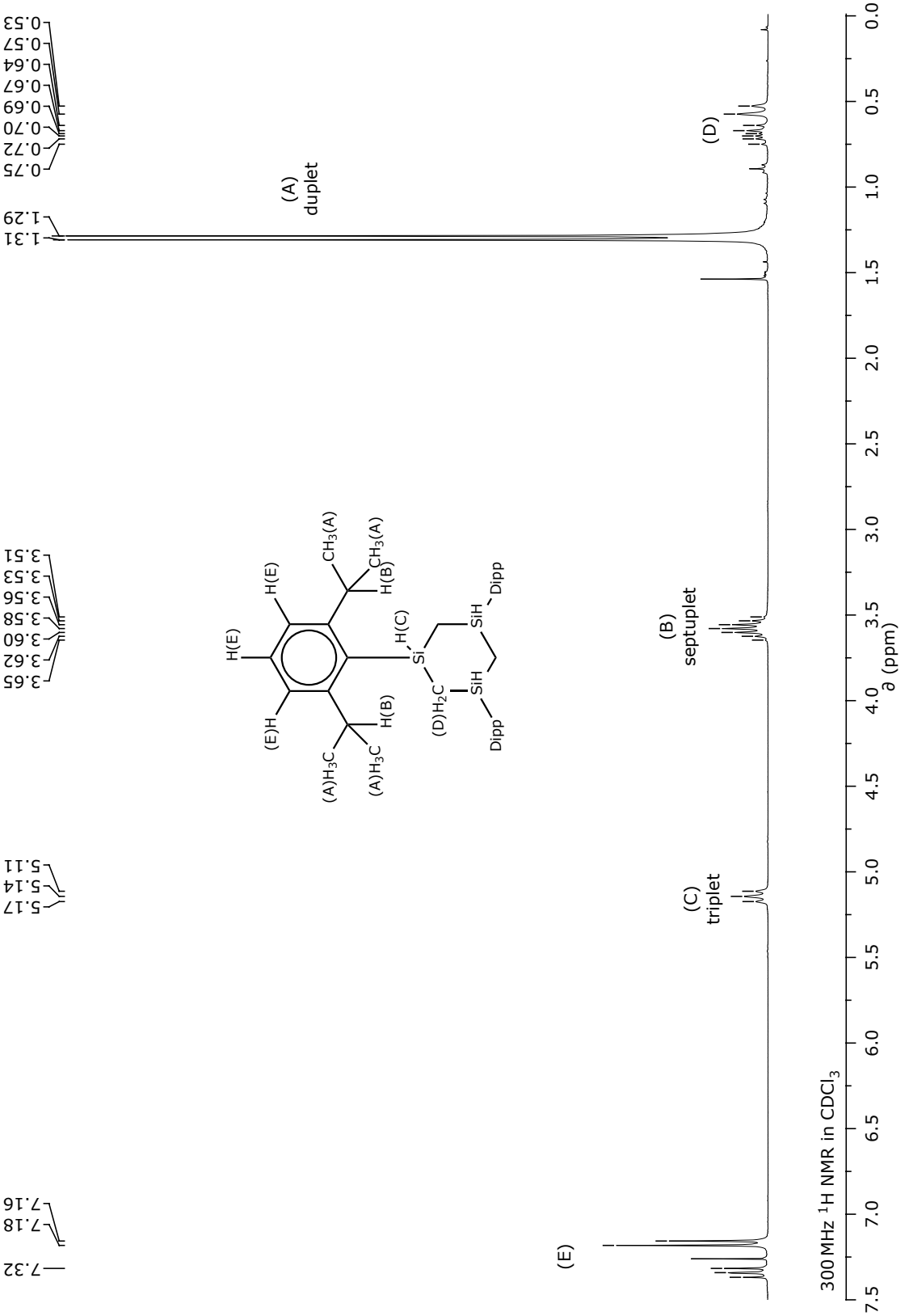

76 MHz $^{13}C\{^1H\}$ NMR in $CDCl_3$
160
150
140
130
120
110
100
90
80
70
60
50
40
30
20
10
0
-10
∂ (ppm)
155.33
133.51
130.12
123.00
77.59
77.16
76.73
33.50
24.99
1.79
Si
H
SiH
SiH

# Appendix E

$^{1}$H NMR spectrum of **7**

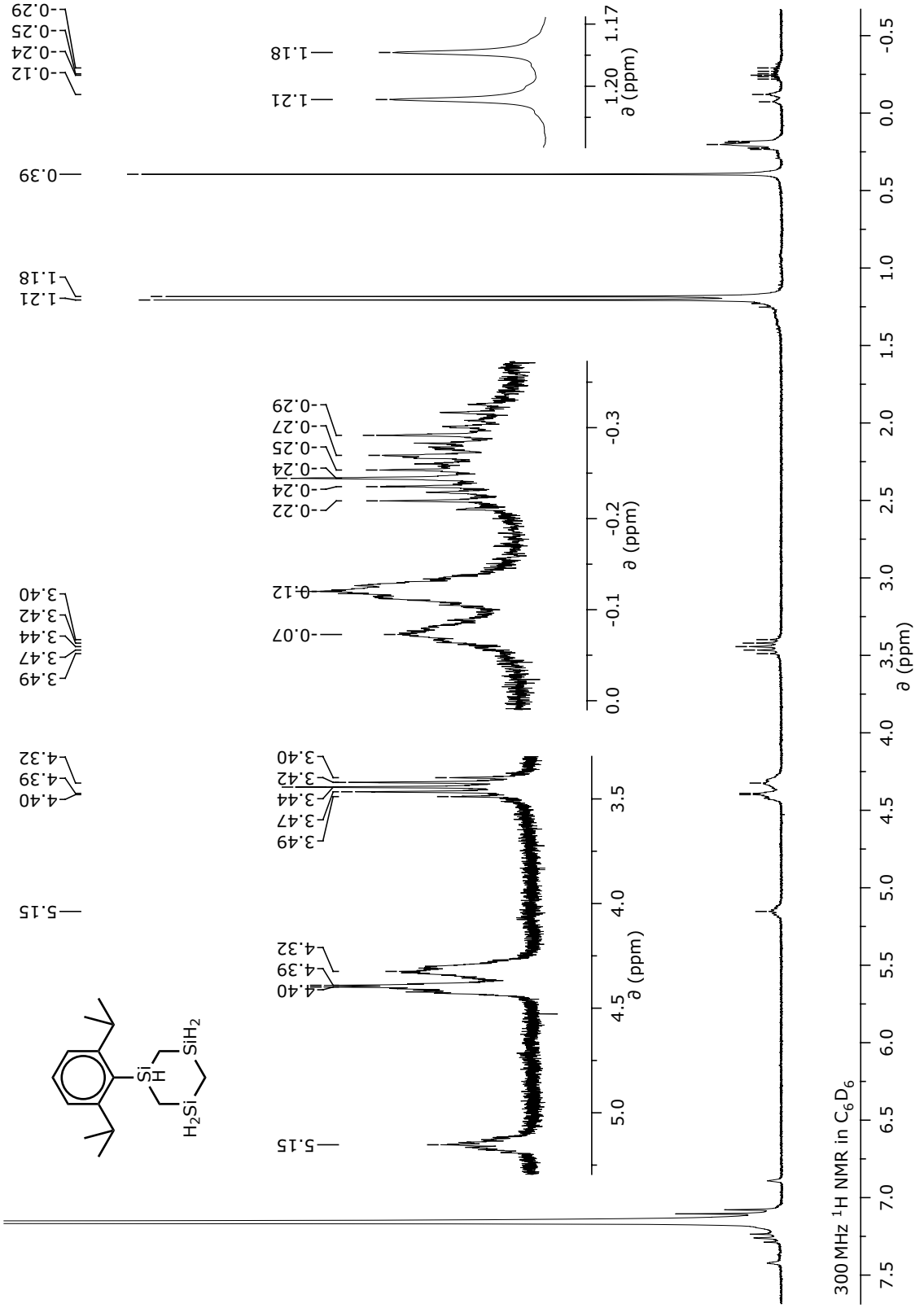

# Appendix F

DEPT-135 spectrum from bromination attempt of **5**

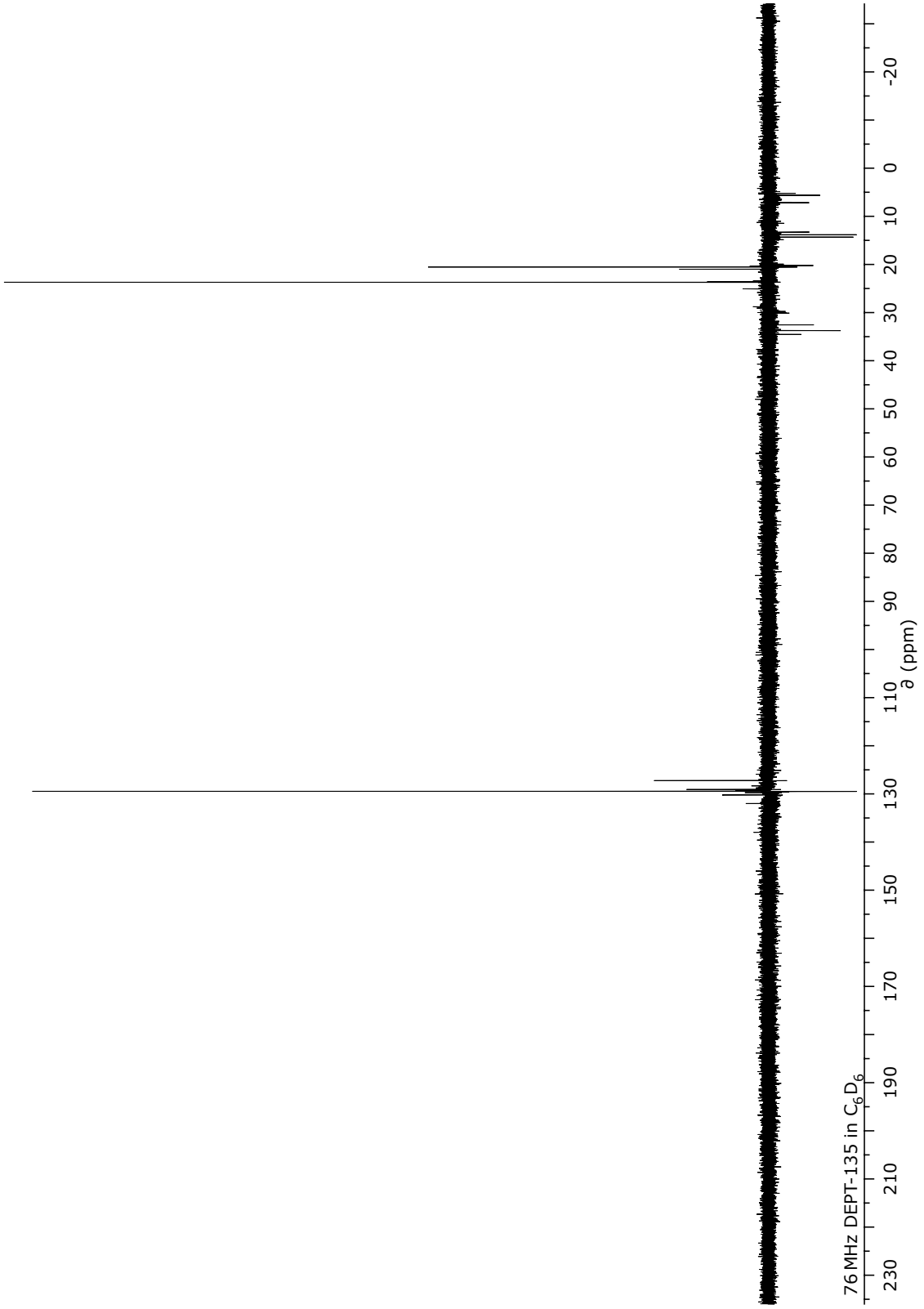

# Appendix G

$^1$H NMR spectrum of **8**

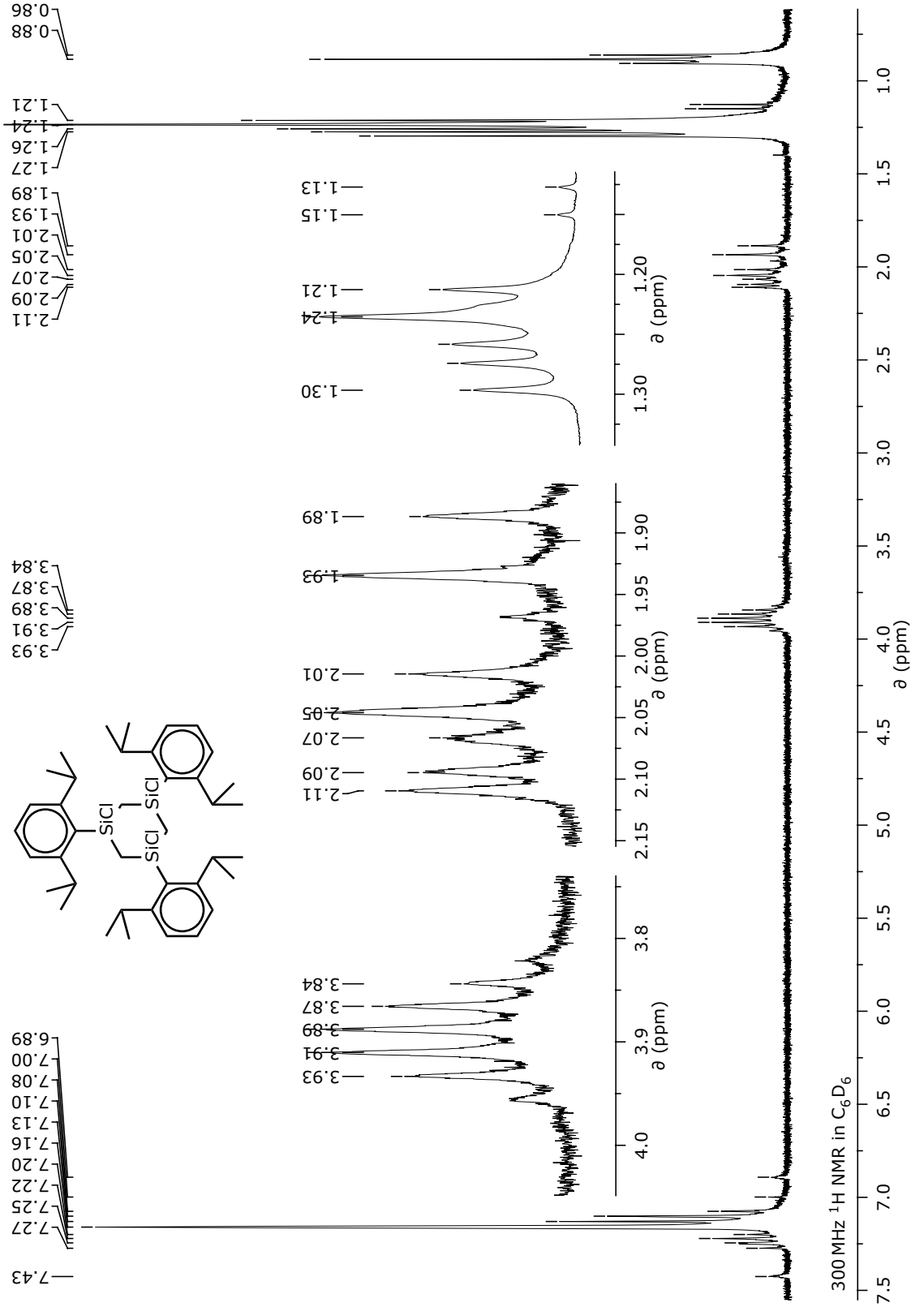

# Appendix H

X-ray data for **5**

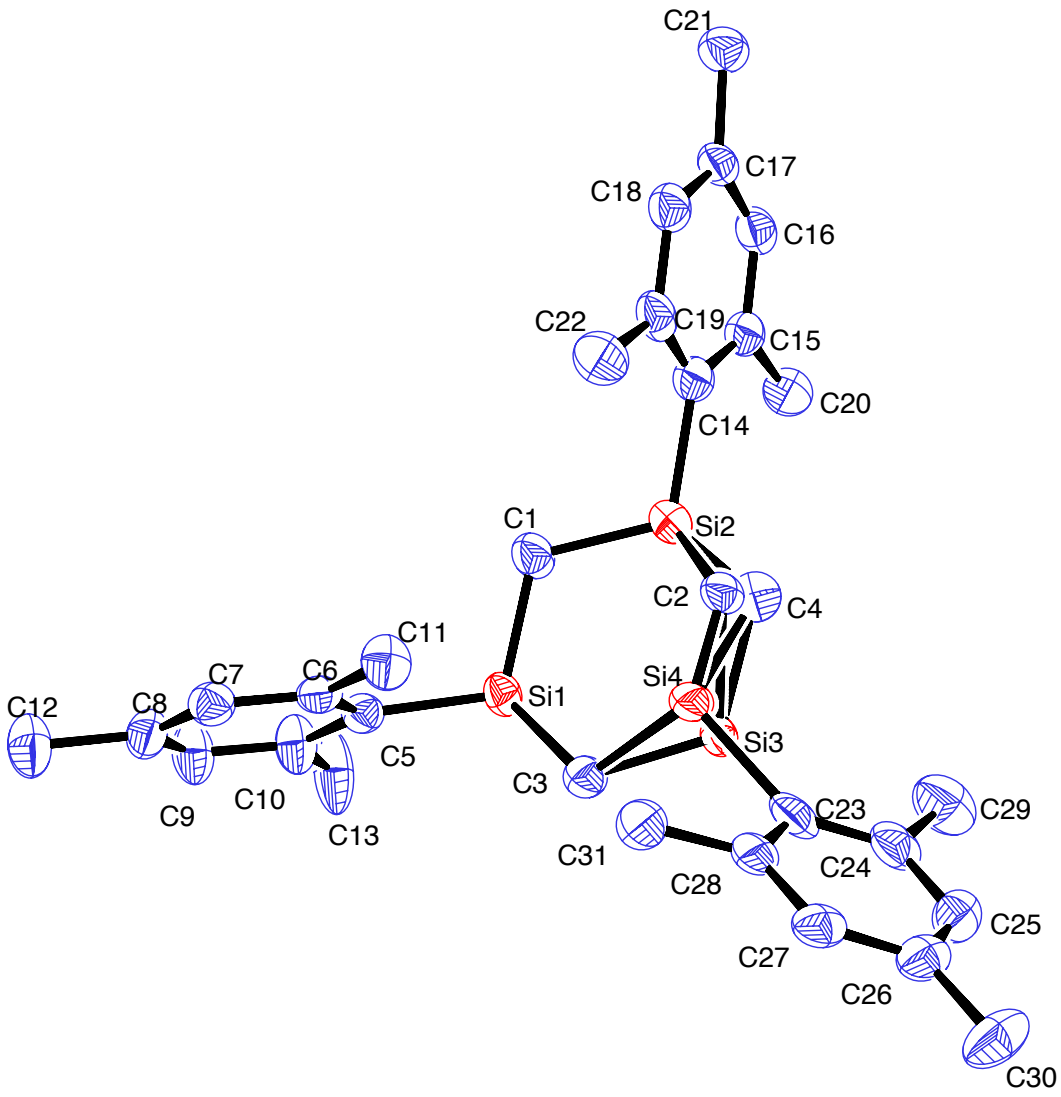


*Figure H.1: Numbering scheme for all non-H atoms in **5**.*

*Table H.1: X-ray crystallographic data for **5**.*

| | | |
|---|---|---|
| Empirical formula | $C_{30}H_{42}Si_3$ | |
| Formula weight | 486.91 | |
| Temperature | 103(2) K | |
| Wavelength | 0.71075 Å | |
| Crystal system | trigonal | |
| Space group | $P3_1$ (#144) | |
| Unit cell dimensions | $a$ = 13.5058(5) Å | $\alpha$ = 90.00° |
| | $b$ = 13.506 Å | $\beta$ = 90.00° |
| | $c$ = 13.5848(6) Å | $\gamma$ = 120.00° |
| Volume | 2145.97(12) Å$^3$ | |
| Z | 3 | |
| Density (calculated) | 1.130 $^{Mg}/_{m^3}$ | |
| Absorption coefficient | 0.182 mm$^{-1}$ | |
| F(000) | 792 | |
| Crystal size | 0.25 x 0.20 x 0.05 mm$^3$ | |
| Theta range for data collection | 2.30 to 24.99° | |
| Index ranges | $-15 \leq h \leq 16$ | |
| | $-15 \leq k \leq 16$ | |
| | $-15 \leq l \leq 16$ | |
| Reflections collected | 17809 | |
| Independent reflections | 5014 [R(int) = 0.0744] | |
| Completeness to theta | 99.9% (24.99°) | |
| Max. and min. transmission | 0.9910 and 0.9559 | |
| Refinement method | Full-matrix least-squares on F$^2$ | |
| Data / restraints / parameters | 5014 / 1 / 342 | |
| Goodness of fit on F$^2$ | 1.033 | |
| Final R indices [$I > 2\sigma(I)$] | R1 = 0.0456, wR2 = 0.1061 | |
| Final R indices (all data) | R1 = 0.0579, wR2 = 0.1121 | |
| Largest diff. peak and hole | 0.556 and −0.305 e.Å$^{-3}$ | |

*Table H.2: Bond lengths from crystallographic analysis of **5**.*

| **Bond lengths** [Å] | | **Bond lengths** [Å] | | **Bond lengths** [Å] | |
|---|---|---|---|---|---|
| Si1–C1 | 1.872(3) | C6–C7 | 1.385(4) | C20–H20 | 0.98 |
| Si1–C3 | 1.878(3) | C6–C11 | 1.509(4) | C20–H20A | 0.98 |
| Si1–C5 | 1.885(3) | C7–C8 | 1.383(5) | C20–H20B | 0.98 |
| Si1–H4D | 1.43(3) | C7–H7 | 0.95 | C21–H21 | 0.98 |
| Si2–C1 | 1.868(3) | C8–C9 | 1.380(5) | C21–H21A | 0.98 |
| Si2–C2 | 1.930(5) | C8–C12 | 1.521(5) | C21–H21B | 0.98 |
| Si2–C4 | 1.710(18) | C9–C10 | 1.387(5) | C22–H22 | 0.98 |
| Si2–C14 | 1.901(3) | C9–H9 | 0.95 | C22–H22A | 0.98 |
| Si2–H2 | 1.30(4) | C10–C13 | 1.532(5) | C22–H22B | 0.98 |
| Si3–C2 | 1.872(6) | C11–H11 | 0.98 | C23–C24 | 1.391(5) |
| Si3–C3 | 1.828(3) | C11–H11A | 0.98 | C23–C28 | 1.413(6) |
| Si3–C23 | 1.895(4) | C11–H11B | 0.98 | C24–C25 | 1.389(5) |
| Si3–H4B | 1.28(7) | C12–H12 | 0.98 | C24–C29 | 1.531(6) |
| Si4–C3 | 1.960(5) | C12–H12A | 0.98 | C25–C26 | 1.372(5) |
| Si4–C4 | 1.90(2) | C12–H12B | 0.98 | C25–H25 | 0.95 |
| Si4–C23 | 2.008(5) | C13–H13 | 0.98 | C26–C27 | 1.394(5) |
| Si4–H4C | 1.54(16) | C13–H13A | 0.98 | C26–C30 | 1.504(5) |
| C1–H1 | 0.99 | C13–H13B | 0.98 | C27–C28 | 1.403(5) |
| C1–H1A | 0.99 | C14–C15 | 1.393(5) | C27–H27 | 0.95 |
| C2–H2A | 0.99 | C14–C19 | 1.410(5) | C28–C31 | 1.510(5) |
| C2–H2B | 0.99 | C15–C16 | 1.384(5) | C29–H29 | 0.98 |
| C3–H3 | 0.99 | C15–C20 | 1.526(5) | C29–H29A | 0.98 |
| C3–H3A | 0.99 | C16–C17 | 1.385(5) | C29–H29B | 0.98 |
| C3–H3B | 0.99 | C16–H16 | 0.95 | C30–H30 | 0.98 |
| C3–H3C | 0.99 | C17–C18 | 1.383(5) | C30–H30A | 0.98 |
| C4–H4 | 0.99 | C17–C21 | 1.509(5) | C30–H30B | 0.98 |
| C4–H4A | 0.99 | C18–C19 | 1.403(5) | C31–H31 | 0.98 |
| C5–C6 | 1.418(4) | C18–H18 | 0.95 | C31–H31A | 0.98 |
| C5–C10 | 1.406(4) | C19–C22 | 1.512(5) | C31–H31B | 0.98 |

*Table H.3: Bond to bond angles from crystallographic analysis of **5**.*

| Angles [°] | | Angles [°] | | Angles [°] | |
|---|---|---|---|---|---|
| Si1–C1–Si2 | 116.22(18) | C4–Si4–C23 | 112.5(6) | C24–C25–H25 | 118.6 |
| Si1–C1–H1 | 108.2 | C4–Si4–H4C | 91(6) | C24–C29–H29 | 109.5 |
| Si1–C1–H1A | 108.2 | C5–Si1–H4D | 111.1(14) | C24–C29–H29A | 109.5 |
| Si1–C3–Si3 | 118.48(17) | C5–C6–C11 | 122.4(3) | C24–C29–H29B | 109.5 |
| Si1–C3–Si4 | 115.10(18) | C5–C10–C13 | 122.0(3) | C25–C24–C23 | 119.8(4) |
| Si1–C3–H3 | 107.7 | C6–C7–H7 | 118.9 | C25–C24–C29 | 117.4(4) |
| Si1–C3–H3A | 107.7 | C6–C11–H11 | 109.5 | C25–C26–C27 | 118.1(3) |
| Si1–C3–H3B | 108.5 | C6–C11–H11A | 109.5 | C25–C26–C30 | 121.3(3) |
| Si1–C3–H3C | 108.5 | C6–C11–H11B | 109.5 | C26–C25–C24 | 122.8(3) |
| Si1–C5–C6 | 120.0(2) | C7–C6–C5 | 120.4(3) | C26–C25–H25 | 118.6 |
| Si1–C5–C10 | 123.0(2) | C7–C6–C11 | 117.2(3) | C26–C27–C28 | 120.5(3) |
| Si2–C1–H1 | 108.2 | C7–C8–C12 | 121.3(3) | C26–C27–H27 | 119.7 |
| Si2–C1–H1A | 108.2 | C8–C7–C6 | 122.3(3) | C26–C30–H30 | 109.5 |
| Si2–C2–Si3 | 108.4(3) | C8–C7–H7 | 118.9 | C26–C30–H30A | 109.5 |
| Si2–C2–H2A | 110 | C8–C9–C10 | 122.6(3) | C26–C30–H30B | 109.5 |
| Si2–C2–H2B | 110 | C8–C9–H9 | 118.7 | C27–C26–C30 | 120.7(3) |
| Si2–C4–Si4 | 113.8(10) | C8–C12–H12 | 109.5 | C27–C28–C23 | 120.4(3) |
| Si2–C4–H4 | 108.8 | C8–C12–H12A | 109.5 | C27–C28–C31 | 116.9(4) |
| Si2–C4–H4A | 108.8 | C8–C12–H12B | 109.5 | C28–C27–H27 | 119.7 |
| Si2–C14–C15 | 121.5(3) | C9–C8–C7 | 117.2(3) | C28–C31–H31 | 109.5 |
| Si2–C14–C19 | 119.8(3) | C9–C8–C12 | 121.4(3) | C28–C31–H31A | 109.5 |
| Si3–C2–H2A | 110 | C9–C10–C5 | 120.4(3) | C28–C31–H31B | 109.5 |
| Si3–C2–H2B | 110 | C9–C10–C13 | 117.6(3) | H1–C1–H1A | 107.4 |
| Si3–C3–Si4 | 28.27(15) | C10–C5–C6 | 117.1(3) | H11–C11–H11A | 109.5 |
| Si3–C3–H3 | 107.7 | C10–C9–H9 | 118.7 | H11–C11–H11B | 109.5 |
| Si3–C3–H3A | 107.7 | C10–C13–H13 | 109.5 | H11A–C11–H11B | 109.5 |
| Si3–C3–H3B | 81.5 | C10–C13–H13A | 109.5 | H12–C12–H12A | 109.5 |
| Si3–C3–H3C | 126.4 | C10–C13–H13B | 109.5 | H12–C12–H12B | 109.5 |
| Si3–C23–Si4 | 27.49(16) | C14–Si2–C2 | 113.5(2) | H12A–C12–H12B | 109.5 |
| Si3–C23–C24 | 115.2(3) | C14–Si2–H2 | 108.5(16) | H13–C13–H13A | 109.5 |
| Si3–C23–C28 | 126.4(3) | C14–C15–C20 | 123.3(3) | H13–C13–H13B | 109.5 |
| Si4–C3–H3 | 83.4 | C14–C19–C22 | 123.5(3) | H13A–C13–H13B | 109.5 |
| Si4–C3–H3A | 130.2 | C15–C14–C19 | 118.7(3) | H20–C20–H20A | 109.5 |
| Si4–C3–H3B | 108.5 | C15–C16–C17 | 123.2(3) | H20–C20–H20B | 109.5 |
| Si4–C3–H3C | 108.5 | C15–C16–H16 | 118.4 | H20A–C20–H20B | 109.5 |
| Si4–C4–H4 | 108.8 | C15–C20–H20 | 109.5 | H21–C21–H21A | 109.5 |
| Si4–C4–H4A | 108.8 | C15–C20–H20A | 109.5 | H21–C21–H21B | 109.5 |
| Si4–C23–C24 | 136.1(3) | C15–C20–H20B | 109.5 | H21A–C21–H21B | 109.5 |
| Si4–C23–C28 | 103.8(3) | C16–C15–C14 | 119.7(3) | H22–C22–H22A | 109.5 |
| C1–Si1–C3 | 113.79(15) | C16–C15–C20 | 117.0(3) | H22–C22–H22B | 109.5 |
| C1–Si1–C5 | 109.19(15) | C16–C17–C21 | 121.0(3) | H22A–C22–H22B | 109.5 |
| C1–Si1–H4D | 101.2(14) | C17–C16–H16 | 118.4 | H29–C29–H29A | 109.5 |
| C1–Si2–C2 | 105.6(2) | C17–C18–C19 | 122.1(3) | H29–C29–H29B | 109.5 |
| C1–Si2–C14 | 112.96(15) | C17–C18–H18 | 118.9 | H29A–C29–H29B | 109.5 |
| C1–Si2–H2 | 110.4(16) | C17–C21–H21 | 109.5 | H2A–C2–H2B | 108.4 |
| C2–Si2–H2 | 105.6(16) | C17–C21–H21A | 109.5 | H3–C3–H3A | 107.1 |
| C2–Si3–C23 | 110.5(2) | C17–C21–H21B | 109.5 | H3–C3–H3B | 131.7 |
| C2–Si3–H4B | 110(3) | C18–C17–C16 | 116.8(3) | H3–C3–H3C | 29.3 |
| C3–Si1–C5 | 111.53(15) | C18–C17–C21 | 122.1(3) | H30–C30–H30A | 109.5 |
| C3–Si1–H4D | 109.6(14) | C18–C19–C14 | 119.4(3) | H30–C30–H30B | 109.5 |
| C3–Si3–C2 | 109.6(3) | C18–C19–C22 | 117.2(3) | H30A–C30–H30B | 109.5 |
| C3–Si3–C23 | 114.37(15) | C19–C18–H18 | 118.9 | H31–C31–H31A | 109.5 |
| C3–Si3–H4B | 107(3) | C19–C22–H22 | 109.5 | H31–C31–H31B | 109.5 |
| C3–Si4–C23 | 104.1(2) | C19–C22–H22A | 109.5 | H31A–C31–H31B | 109.5 |
| C3–Si4–H4C | 122(6) | C19–C22–H22B | 109.5 | H3A–C3–H3B | 30.6 |
| C4–Si2–C1 | 121.2(6) | C23–Si3–H4B | 105(3) | H3A–C3–H3C | 79.3 |
| C4–Si2–C2 | 25.4(7) | C23–Si4–H4C | 115(6) | H3B–C3–H3C | 107.5 |
| C4–Si2–C14 | 117.0(6) | C23–C24–C29 | 122.8(3) | H4–C4–H4A | 107.7 |
| C4–Si2–H2 | 81.0(18) | C23–C28–C31 | 122.7(3) | | |
| C4–Si4–C3 | 112.2(8) | C24–C23–C28 | 118.3(3) | | |

*Table H.4: Torsion angles from crystallographic analysis of **5**.*

| **Torsion angles [°]** | | **Torsion angles [°]** | |
|---|---|---|---|
| Si1–C1–Si2–C2 | −54.5(3) | C2–Si2–C14–C15 | 124.0(3) |
| Si1–C1–Si2–C4 | −32.6(10) | C2–Si2–C14–C19 | −56.2(4) |
| Si1–C1–Si2–C14 | −179.13(19) | C2–Si3–C23–C24 | −100.9(4) |
| Si1–C3–Si3–C2 | −45.3(3) | C2–Si3–C23–C28 | 83.2(4) |
| Si1–C3–Si3–C23 | −170.0(2) | C3–Si1–C5–C6 | 58.5(3) |
| Si1–C3–Si4–C4 | −42.6(8) | C3–Si1–C5–C10 | −122.2(3) |
| Si1–C3–Si4–C23 | −164.5(2) | C3–Si3–C23–C24 | 134.8(3) |
| Si1–C5–C6–C7 | 177.0(2) | C3–Si3–C23–C28 | −41.0(4) |
| Si1–C5–C6–C11 | −3.1(4) | C3–Si4–C23–C24 | 107.5(4) |
| Si1–C5–C10–C9 | −177.2(3) | C3–Si4–C23–C28 | −89.1(4) |
| Si1–C5–C10–C13 | 5.1(5) | C4–Si2–C14–C15 | 96.1(10) |
| Si2–C1–Si1–C3 | −36.7(3) | C4–Si2–C14–C19 | −84.1(10) |
| Si2–C1–Si1–C5 | −162.06(19) | C4–Si4–C23–C24 | −14.2(11) |
| Si2–C2–Si3–C3 | −63.5(4) | C4–Si4–C23–C28 | 149.2(9) |
| Si2–C2–Si3–C23 | 169.6(2) | C5–C6–C7–C8 | 1.5(5) |
| Si2–C4–Si4–C3 | 48.8(15) | C6–C5–C10–C9 | 2.1(5) |
| Si2–C4–Si4–C23 | 165.8(9) | C6–C5–C10–C13 | −175.6(4) |
| Si2–C14–C15–C16 | 177.3(2) | C6–C7–C8–C9 | 0.3(5) |
| Si2–C14–C15–C20 | −2.3(5) | C6–C7–C8–C12 | 179.0(3) |
| Si2–C14–C19–C18 | −176.9(2) | C7–C8–C9–C10 | 0.0(6) |
| Si2–C14–C19–C22 | 3.5(4) | C8–C9–C10–C5 | −1.0(6) |
| Si3–C2–Si2–C1 | −67.6(4) | C8–C9–C10–C13 | 176.8(4) |
| Si3–C2–Si2–C4 | 64.3(16) | C10–C5–C6–C7 | −2.4(4) |
| Si3–C2–Si2–C14 | 168.1(3) | C10–C5–C6–C11 | 177.6(3) |
| Si3–C3–Si1–C1 | 31.2(3) | C11–C6–C7–C8 | −178.4(3) |
| Si3–C3–Si1–C5 | 155.2(2) | C12–C8–C9–C10 | −179.2(4) |
| Si3–C3–Si4–C4 | 61.3(8) | C14–C15–C16–C17 | 0.7(5) |
| Si3–C3–Si4–C23 | −60.6(3) | C15–C14–C19–C18 | 2.9(5) |
| Si3–C23–Si4–C3 | −59.6(3) | C15–C14–C19–C22 | −176.7(3) |
| Si3–C23–Si4–C4 | 62.1(9) | C15–C16–C17–C18 | 3.4(5) |
| Si3–C23–C24–C25 | −173.4(3) | C15–C16–C17–C21 | −173.7(3) |
| Si3–C23–C24–C29 | 8.0(5) | C16–C17–C18–C19 | −2.9(5) |
| Si3–C23–C28–C27 | 173.9(3) | C17–C18–C19–C14 | 0.1(5) |
| Si3–C23–C28–C31 | −4.8(5) | C17–C18–C19–C22 | 179.4(3) |
| Si4–C3–Si1–C1 | 0.4(3) | C19–C14–C15–C16 | −2.5(5) |
| Si4–C3–Si1–C5 | 123.7(3) | C19–C14–C15–C20 | 177.9(3) |
| Si4–C3–Si3–C2 | 45.3(3) | C20–C15–C16–C17 | 178.9(3) |
| Si4–C3–Si3–C23 | −79.4(3) | C21–C17–C18–C19 | 174.2(3) |
| Si4–C4–Si2–C1 | 12.0(18) | C23–C24–C25–C26 | −2.5(5) |
| Si4–C4–Si2–C2 | −44.9(12) | C24–C23–C28–C27 | −1.8(5) |
| Si4–C4–Si2–C14 | −133.2(9) | C24–C23–C28–C31 | 179.5(3) |
| Si4–C23–Si3–C2 | −44.4(4) | C24–C25–C26–C27 | 1.1(5) |
| Si4–C23–Si3–C3 | 79.9(3) | C24–C25–C26–C30 | −179.7(3) |
| Si4–C23–C24–C25 | 164.4(4) | C25–C26–C27–C28 | 0.0(5) |
| Si4–C23–C24–C29 | −14.3(6) | C26–C27–C28–C23 | 0.4(5) |
| Si4–C23–C28–C27 | −168.8(3) | C26–C27–C28–C31 | 179.2(3) |
| Si4–C23–C28–C31 | 12.5(4) | C28–C23–C24–C25 | 2.8(5) |
| C1–Si1–C5–C6 | −68.2(3) | C28–C23–C24–C29 | −175.8(3) |
| C1–Si1–C5–C10 | 111.2(3) | C29–C24–C25–C26 | 176.2(3) |
| C1–Si2–C14–C15 | −115.8(3) | C30–C26–C27–C28 | −179.3(3) |
| C1–Si2–C14–C19 | 64.0(3) | | |

# Appendix I

X-ray data for **6** - mixed crystal (**6a**,**6b**)

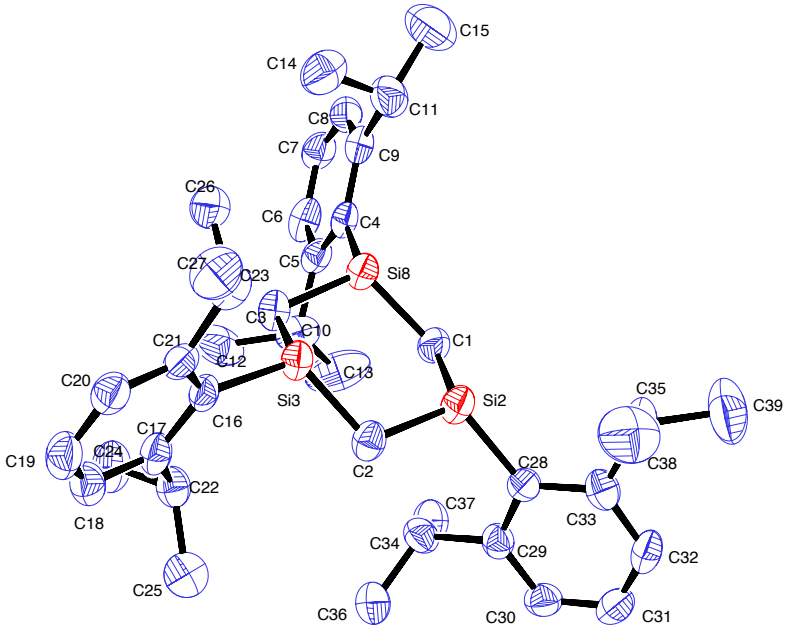


*Figure I.1: Numbering scheme for all non-H atoms in the disorder free molecule of the crystal.*

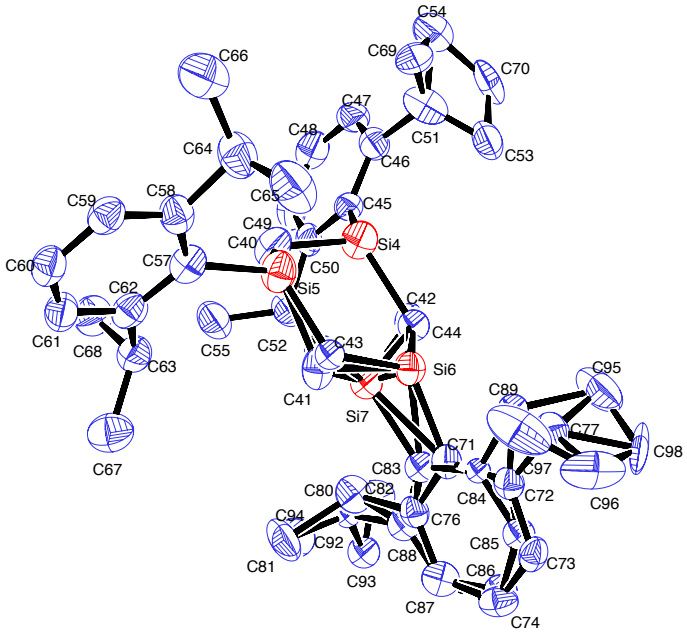


*Figure I.2: Numbering scheme for all non-H atoms in the disordered molecule of the crystal.*

*Table I.1: X-ray crystallographic data for **6** (mixed crystal). This analysis is not fully refined. The compound crystallizes as two independent molecules and one of them has disorders between chair and boat (7:3) which spread to a whole Dipp group making them very difficult to divide.*

| | | |
|---|---|---|
| Empirical formula | $C_{39}H_{60}Si_3$ | |
| Formula weight | 613.14 | |
| Temperature | 103(2) K | |
| Wavelength | 0.71075 Å | |
| Crystal system | triclinic | |
| Space group | $P\bar{1}$ (#2) | |
| Unit cell dimensions | $a$ = 13.6926(6) Å | $\alpha$ = 89.352(8)° |
| | $b$ = 15.7867(12) Å | $\beta$ = 85.839(7)° |
| | $c$ = 18.4851(18) Å | $\gamma$ = 71.961(2)° |
| Volume | 3789.1(5) Å$^3$ | |
| Z | 4 | |
| Density (calculated) | 1.075 $^{Mg}/_{m^3}$ | |
| Absorption coefficient | 0.149 mm$^{-1}$ | |
| F(000) | 1344 | |
| Crystal size | 0.20 x 0.20 x 0.05 mm$^3$ | |
| Theta range for data collection | 1.36 to 25.00° | |
| Index ranges | $-16 \leq h \leq 16$ | |
| | $-18 \leq k \leq 18$ | |
| | $-21 \leq l \leq 21$ | |
| Reflections collected | 29707 | |
| Independent reflections | 12728 [R(int) = 0.0730] | |
| Completeness to theta | 95.4% (25.00°) | |
| Max. and min. transmission | 0.9926 and 0.9707 | |
| Refinement method | Full-matrix least-squares on F$^2$ | |
| Data / restraints / parameters | 12728 / 0 / 875 | |
| Goodness of fit on F$^2$ | 0.998 | |
| Final R indices [$I > 2\sigma(I)$] | R1 = 0.0672, wR2 = 0.1640 | |
| Final R indices (all data) | R1 = 0.1525, wR2 = 0.2122 | |
| Largest diff. peak and hole | 0.583 and −0.325 e.Å$^{-3}$ | |

*Table I.2: Bond lengths from crystallographic analysis of **6** (mixed crystal).*

| **Bond lengths** [Å] | | **Bond lengths** [Å] | | **Bond lengths** [Å] | |
|---|---|---|---|---|---|
| Si2–C1 | 1.864(5) | C17–C22 | 1.512(6) | C58–C64 | 1.529(6) |
| Si2–C2 | 1.871(4) | C18–C19 | 1.367(6) | C59–C60 | 1.371(6) |
| Si2–C28 | 1.888(4) | C19–C20 | 1.364(6) | C60–C61 | 1.372(6) |
| Si3–C2 | 1.863(4) | C20–C21 | 1.374(6) | C61–C62 | 1.405(6) |
| Si3–C3 | 1.881(4) | C21–C23 | 1.543(6) | C62–C63 | 1.519(6) |
| Si3–C16 | 1.886(4) | C22–C24 | 1.536(6) | C63–C67 | 1.530(6) |
| Si4–C40 | 1.849(5) | C22–C25 | 1.534(7) | C63–C68 | 1.533(6) |
| Si4–C42 | 1.84(3) | C23–C26 | 1.537(6) | C64–C65 | 1.489(7) |
| Si4–C44 | 1.98(6) | C23–C27 | 1.543(6) | C64–C66 | 1.565(8) |
| Si4–C45 | 1.887(4) | C28–C29 | 1.403(6) | C71–C72 | 1.430(10) |
| Si5–C40 | 1.882(5) | C28–C33 | 1.431(6) | C71–C76 | 1.415(13) |
| Si5–C41 | 1.918(11) | C29–C30 | 1.378(6) | C72–C73 | 1.389(13) |
| Si5–C43 | 1.82(3) | C29–C34 | 1.547(6) | C72–C77 | 1.528(9) |
| Si5–C57 | 1.898(5) | C30–C31 | 1.356(6) | C73–C74 | 1.384(12) |
| Si6–C41 | 1.878(10) | C31–C32 | 1.373(6) | C74–C75 | 1.359(9) |
| Si6–C42 | 1.89(3) | C32–C33 | 1.382(6) | C75–C76 | 1.374(12) |
| Si6–C71 | 1.883(7) | C33–C35 | 1.520(7) | C76–C80 | 1.499(12) |
| Si7–C43 | 1.83(3) | C34–C36 | 1.522(6) | C77–C95 | 1.393(10) |
| Si7–C44 | 1.79(6) | C34–C37 | 1.530(6) | C77–C96 | 1.541(15) |
| Si7–C83 | 1.891(16) | C35–C38 | 1.512(7) | C77–C97 | 1.436(11) |
| Si8–C1 | 1.861(5) | C35–C39 | 1.553(7) | C77–C98 | 1.60(2) |
| Si8–C3 | 1.886(4) | C45–C46 | 1.431(6) | C80–C81 | 1.64(2) |
| Si8–C4 | 1.887(5) | C45–C50 | 1.400(6) | C80–C82 | 1.527(10) |
| C4–C5 | 1.414(6) | C46–C47 | 1.393(7) | C83–C84 | 1.3900 |
| C4–C9 | 1.420(6) | C46–C51 | 1.513(7) | C83–C88 | 1.3900 |
| C5–C6 | 1.405(6) | C47–C48 | 1.352(7) | C84–C85 | 1.3900 |
| C5–C10 | 1.516(7) | C48–C49 | 1.365(7) | C84–C89 | 1.57(2) |
| C6–C7 | 1.371(7) | C49–C50 | 1.375(6) | C85–C86 | 1.3900 |
| C7–C8 | 1.354(7) | C50–C52 | 1.527(6) | C86–C87 | 1.3900 |
| C8–C9 | 1.388(7) | C51–C53 | 1.418(9) | C87–C88 | 1.3900 |
| C9–C11 | 1.534(7) | C51–C54 | 1.564(10) | C88–C92 | 1.51(3) |
| C10–C12 | 1.523(7) | C51–C69 | 1.348(15) | C89–C95 | 1.699(19) |
| C10–C13 | 1.531(7) | C51–C70 | 1.755(17) | C89–C97 | 1.62(2) |
| C11–C14 | 1.546(7) | C52–C55 | 1.517(6) | C92–C93 | 1.52(3) |
| C11–C15 | 1.552(7) | C52–C56 | 1.532(7) | C92–C94 | 1.24(5) |
| C16–C17 | 1.416(6) | C57–C58 | 1.423(6) | C95–C98 | 1.44(3) |
| C16–C21 | 1.421(6) | C57–C62 | 1.405(6) | C96–C98 | 1.60(4) |
| C17–C18 | 1.393(6) | C58–C59 | 1.389(6) | C97–C96 | 1.48(2) |

*Table I.3: Bond to bond angles from crystallographic analysis of **6** (mixed crystal).*

| Angles [°] | | Angles [°] | | Angles [°] | | Angles [°] | |
|---|---|---|---|---|---|---|---|
| Si2–C1–Si8 | 115.0(2) | C18–C17–C22 | 117.6(4) | C47–C46–C51 | 118.7(5) | C75–C74–C73 | 119.0(11) |
| Si2–C2–Si3 | 112.3(2) | C19–C18–C17 | 121.3(5) | C47–C48–C49 | 121.7(5) | C75–C76–C71 | 119.8(8) |
| Si2–C28–C29 | 120.2(3) | C19–C20–C21 | 121.3(5) | C48–C47–C46 | 120.1(5) | C75–C76–C80 | 117.9(11) |
| Si2–C28–C33 | 122.4(3) | C20–C19–C18 | 120.0(5) | C48–C49–C50 | 120.4(5) | C76–C71–Si6 | 120.8(7) |
| Si3–C3–Si8 | 110.3(2) | C20–C21–C16 | 120.2(4) | C49–C50–C45 | 120.2(4) | C76–C71–C72 | 118.4(6) |
| Si3–C16–C17 | 119.7(3) | C20–C21–C23 | 119.0(4) | C49–C50–C52 | 118.1(4) | C76–C80–C81 | 113.7(10) |
| Si3–C16–C21 | 122.4(3) | C21–C23–C27 | 114.3(4) | C50–C45–C46 | 118.1(4) | C76–C80–C82 | 111.2(7) |
| Si4–C40–Si5 | 111.6(3) | C25–C22–C24 | 110.4(4) | C50–C52–C56 | 109.6(4) | C77–C95–C89 | 29.7(6) |
| Si4–C42–Si6 | 116.2(12) | C26–C23–C21 | 109.9(4) | C53–C51–C46 | 113.4(6) | C77–C95–C98 | 68.9(13) |
| Si4–C44–Si7 | 107(3) | C26–C23–C27 | 109.8(4) | C53–C51–C54 | 114.0(6) | C77–C96–C98 | 61.3(11) |
| Si4–C45–C46 | 120.9(3) | C28–C29–C34 | 121.3(4) | C53–C51–C70 | 63.6(7) | C77–C97–C89 | 31.5(6) |
| Si4–C45–C50 | 120.5(3) | C28–C33–C35 | 120.6(4) | C54–C51–C70 | 57.7(7) | C77–C97–C96 | 63.9(9) |
| Si5–C41–Si6 | 112.0(5) | C29–C28–C33 | 117.4(4) | C55–C52–C50 | 114.1(4) | C82–C80–C81 | 110.6(11) |
| Si5–C43–Si7 | 108.2(16) | C30–C29–C28 | 120.5(4) | C55–C52–C56 | 110.4(4) | C83–C84–C85 | 120.0 |
| C1–Si2–C2 | 112.9(2) | C30–C29–C34 | 118.1(4) | C57–Si5–C41 | 113.1(3) | C83–C84–C89 | 129.6(17) |
| C1–Si2–C28 | 112.0(2) | C30–C31–C32 | 120.5(5) | C57–C58–C64 | 122.2(4) | C83–C88–C92 | 118(2) |
| C1–Si8–C3 | 111.0(2) | C31–C30–C29 | 121.1(5) | C57–C62–C63 | 121.7(4) | C84–C83–Si7 | 116.1(15) |
| C1–Si8–C4 | 112.9(2) | C31–C32–C33 | 120.6(4) | C58–C57–Si5 | 122.5(4) | C84–C83–C88 | 120.0 |
| C2–Si2–C28 | 112.0(2) | C32–C33–C28 | 119.7(4) | C58–C64–C66 | 114.3(4) | C84–C89–C95 | 111.8(12) |
| C2–Si3–C3 | 111.1(2) | C32–C33–C35 | 119.7(4) | C59–C58–C57 | 119.6(4) | C84–C89–C97 | 113.3(13) |
| C2–Si3–C16 | 113.50(19) | C33–C35–C39 | 113.1(4) | C59–C58–C64 | 118.1(5) | C85–C84–C89 | 110.3(17) |
| C3–Si3–C16 | 113.31(19) | C36–C34–C29 | 112.7(4) | C59–C60–C61 | 119.4(5) | C86–C85–C84 | 120.0 |
| C3–Si8–C4 | 114.06(19) | C36–C34–C37 | 111.5(4) | C60–C59–C58 | 121.7(5) | C86–C87–C88 | 120.0 |
| C4–C5–C10 | 122.3(4) | C37–C34–C29 | 110.6(4) | C60–C61–C62 | 121.3(5) | C87–C86–C85 | 120.0 |
| C4–C9–C11 | 121.5(4) | C38–C35–C33 | 110.5(5) | C61–C62–C57 | 119.7(4) | C87–C88–C83 | 120.0 |
| C5–C4–Si8 | 120.0(4) | C38–C35–C39 | 112.7(5) | C61–C62–C63 | 118.4(4) | C87–C88–C92 | 122.0(19) |
| C5–C4–C9 | 118.0(4) | C40–Si4–C44 | 110.9(17) | C62–C57–Si5 | 119.1(4) | C88–C83–Si7 | 123.8(15) |
| C5–C10–C12 | 112.2(4) | C40–Si4–C45 | 109.4(2) | C62–C57–C58 | 118.2(4) | C88–C92–C93 | 111.4(17) |
| C5–C10–C13 | 110.9(5) | C40–Si5–C41 | 104.4(4) | C62–C63–C67 | 114.1(4) | C94–C92–C88 | 103(4) |
| C6–C5–C4 | 119.8(5) | C40–Si5–C57 | 115.5(2) | C62–C63–C68 | 109.7(4) | C94–C92–C93 | 113(4) |
| C6–C5–C10 | 117.8(4) | C41–Si6–C42 | 112.0(9) | C65–C64–C58 | 111.1(4) | C95–C77–C72 | 109.9(6) |
| C7–C6–C5 | 121.1(5) | C41–Si6–C71 | 110.5(4) | C65–C64–C66 | 107.3(5) | C95–C77–C96 | 112.8(11) |
| C7–C8–C9 | 122.9(5) | C42–Si4–C40 | 111.6(9) | C67–C63–C68 | 111.1(4) | C95–C77–C97 | 139.5(7) |
| C8–C7–C6 | 119.2(5) | C42–Si4–C44 | 3(2) | C69–C51–C46 | 127.0(9) | C95–C77–C98 | 57.0(15) |
| C8–C9–C4 | 119.0(5) | C42–Si4–C45 | 115.8(7) | C69–C51–C53 | 113.9(9) | C95–C98–C77 | 54.2(9) |
| C8–C9–C11 | 119.5(5) | C43–Si5–C40 | 114.7(9) | C69–C51–C54 | 68.1(8) | C95–C98–C96 | 106.7(15) |
| C9–C4–Si8 | 122.1(4) | C43–Si5–C41 | 14.3(10) | C69–C51–C70 | 112.7(10) | C96–C77–C98 | 61.3(15) |
| C9–C11–C14 | 109.5(4) | C43–Si5–C57 | 113.9(10) | C71–Si6–C42 | 115.5(8) | C96–C97–C89 | 95.4(12) |
| C9–C11–C15 | 113.9(5) | C43–Si7–C83 | 115.0(12) | C71–C72–C77 | 123.1(7) | C96–C98–C77 | 57.4(10) |
| C12–C10–C13 | 111.7(5) | C44–Si7–C43 | 122.4(18) | C71–C76–C80 | 122.3(8) | C97–C77–C72 | 109.1(6) |
| C14–C11–C15 | 109.9(5) | C44–Si7–C83 | 104.5(19) | C72–C71–Si6 | 120.7(7) | C97–C77–C96 | 59.3(10) |
| C16–C17–C22 | 123.0(4) | C45–Si4–C44 | 118.8(15) | C72–C77–C96 | 113.6(8) | C97–C77–C98 | 117.8(15) |
| C16–C21–C23 | 120.7(4) | C45–C46–C51 | 122.2(5) | C72–C77–C98 | 109.8(10) | C97–C89–C95 | 106.4(12) |
| C17–C16–C21 | 117.8(4) | C45–C50–C52 | 121.7(4) | C73–C72–C71 | 118.4(6) | C97–C96–C77 | 56.8(7) |
| C17–C22–C24 | 112.3(4) | C46–C51–C54 | 111.5(6) | C73–C72–C77 | 118.5(7) | C97–C96–C98 | 115.4(13) |
| C17–C22–C25 | 111.8(4) | C46–C51–C70 | 108.7(7) | C74–C73–C72 | 122.1(9) | C98–C95–C89 | 98.5(14) |
| C18–C17–C16 | 119.3(4) | C47–C46–C45 | 119.2(4) | C74–C75–C76 | 122.3(11) | | |

*Table I.4: Torsion angles from crystallographic analysis of **6** (mixed crystal).*

| Torsion angle [°] | | Torsion angle [°] | | Torsion angle [°] | |
|---|---|---|---|---|---|
| Si2–C1–Si8–C3 | −50.4(3) | C9–C4–Si8–C3 | 115.8(4) | C59–C60–C61–C62 | 2.0(7) |
| Si2–C1–Si8–C4 | −179.8(2) | C9–C4–C5–C6 | 0.2(6) | C60–C61–C62–C57 | 0.4(7) |
| Si2–C2–Si3–C3 | −55.5(3) | C9–C4–C5–C10 | −178.9(4) | C60–C61–C62–C63 | −174.1(4) |
| Si2–C2–Si3–C16 | 175.4(2) | C10–C5–C6–C7 | 178.6(4) | C61–C62–C63–C67 | −51.3(6) |
| Si2–C28–C29–C30 | −176.3(3) | C16–C17–C18–C19 | 0.3(7) | C61–C62–C63–C68 | 74.1(5) |
| Si2–C28–C29–C34 | 7.1(5) | C16–C17–C22–C24 | −114.1(5) | C62–C57–C58–C59 | 1.8(6) |
| Si2–C28–C33–C32 | 176.3(3) | C16–C17–C22–C25 | 121.2(5) | C62–C57–C58–C64 | −176.1(4) |
| Si2–C28–C33–C35 | −6.1(6) | C16–C21–C23–C26 | 73.3(5) | C64–C58–C59–C60 | 178.6(4) |
| Si3–C2–Si2–C1 | 48.8(3) | C16–C21–C23–C27 | −162.7(4) | C71–C72–C73–C74 | 0.7(9) |
| Si3–C2–Si2–C28 | 176.3(2) | C17–C16–C21–C20 | 0.7(6) | C71–C72–C77–C95 | −82.8(9) |
| Si3–C3–Si8–C1 | 55.5(3) | C17–C16–C21–C23 | −177.0(4) | C71–C72–C77–C96 | 149.8(13) |
| Si3–C3–Si8–C4 | −175.7(2) | C17–C18–C19–C20 | 0.7(7) | C71–C72–C77–C97 | 85.8(9) |
| Si3–C16–C17–C18 | 175.2(3) | C18–C17–C22–C24 | 65.6(5) | C71–C72–C77–C98 | −143.7(17) |
| Si3–C16–C17–C22 | −5.1(6) | C18–C17–C22–C25 | −59.1(5) | C71–C76–C80–C81 | −118.0(12) |
| Si3–C16–C21–C20 | −174.9(3) | C18–C19–C20–C21 | 0.5(7) | C71–C76–C80–C82 | 116.4(8) |
| Si3–C16–C21–C23 | 7.4(6) | C19–C20–C21–C16 | 0.3(7) | C72–C71–C76–C75 | 0.8(9) |
| Si4–C40–Si5–C41 | −65.9(4) | C19–C20–C21–C23 | 177.5(4) | C72–C71–C76–C80 | −179.2(7) |
| Si4–C40–Si5–C43 | −55.4(11) | C20–C21–C23–C26 | −104.5(5) | C72–C73–C74–C75 | 0.4(11) |
| Si4–C40–Si5–C57 | 169.1(2) | C20–C21–C23–C27 | 19.5(6) | C72–C77–C95–C89 | 72.9(14) |
| Si4–C42–Si6–C41 | −41.0(17) | C21–C16–C17–C18 | 0.5(6) | C72–C77–C95–C98 | −101.3(13) |
| Si4–C42–Si6–C71 | −168.7(10) | C21–C16–C17–C22 | 179.2(4) | C72–C77–C96–C97 | −98.9(8) |
| Si4–C44–Si7–C43 | 50(3) | C22–C17–C18–C19 | −179.9(4) | C72–C77–C96–C98 | 100.5(12) |
| Si4–C44–Si7–C83 | −177.0(18) | C28–C29–C30–C31 | −1.1(7) | C72–C77–C97–C89 | −69.5(14) |
| Si4–C45–C46–C47 | −165.4(4) | C28–C29–C34–C36 | −124.0(5) | C72–C77–C97–C96 | 106.7(9) |
| Si4–C45–C46–C51 | 15.1(6) | C28–C29–C34–C37 | 110.4(5) | C72–C77–C98–C95 | 101.3(9) |
| Si4–C45–C50–C49 | 166.1(3) | C28–C33–C35–C38 | 87.3(6) | C72–C77–C98–C96 | −106.8(10) |
| Si4–C45–C50–C52 | −16.8(6) | C28–C33–C35–C39 | −145.3(5) | C73–C72–C77–C95 | 97.6(8) |
| Si5–C40–Si4–C42 | −58.2(8) | C29–C28–C33–C32 | −3.5(6) | C73–C72–C77–C96 | −29.8(14) |
| Si5–C40–Si4–C44 | −54.6(16) | C29–C28–C33–C35 | 174.1(4) | C73–C72–C77–C97 | −93.8(9) |
| Si5–C40–Si4–C45 | 172.4(2) | C29–C30–C31–C32 | −1.4(7) | C73–C72–C77–C98 | 36.7(18) |
| Si5–C41–Si6–C42 | −50.7(10) | C30–C29–C34–C36 | 59.4(6) | C73–C74–C75–C76 | 0.3(12) |
| Si5–C41–Si6–C71 | 178.9(5) | C30–C29–C34–C37 | −66.2(5) | C74–C75–C76–C71 | 0.5(12) |
| Si5–C43–Si7–C44 | 52(3) | C30–C31–C32–C33 | 1.3(7) | C74–C75–C76–C80 | 179.5(9) |
| Si5–C43–Si7–C83 | −179.8(12) | C31–C32–C33–C28 | 1.2(7) | C75–C76–C80–C81 | 62.0(13) |
| Si5–C57–C58–C59 | −174.2(3) | C31–C32–C33–C35 | −176.4(4) | C75–C76–C80–C82 | −63.6(10) |
| Si5–C57–C58–C64 | 7.9(6) | C32–C33–C35–C38 | −95.1(6) | C76–C71–C72–C73 | 0.9(8) |
| Si5–C57–C62–C61 | 173.8(3) | C32–C33–C35–C39 | 32.4(7) | C76–C71–C72–C77 | 179.5(6) |
| Si5–C57–C62–C63 | −11.9(6) | C33–C28–C29–C30 | 3.5(6) | C77–C72–C73–C74 | −179.7(8) |
| Si6–C41–Si5–C40 | −62.2(6) | C33–C28–C29–C34 | −173.1(4) | C77–C95–C98–C96 | −24.5(11) |
| Si6–C41–Si5–C43 | 75(5) | C34–C29–C30–C31 | 175.5(4) | C77–C96–C98–C95 | 23.5(11) |
| Si6–C41–Si5–C57 | 171.4(4) | C40–Si4–C45–C46 | 114.3(4) | C77–C97–C96–C98 | 18.9(12) |
| Si6–C42–Si4–C40 | 44.2(16) | C40–Si4–C45–C50 | −57.3(4) | C83–C84–C85–C86 | 0.0 |
| Si6–C42–Si4–C44 | −35(42) | C40–Si5–C57–C58 | −119.2(4) | C83–C84–C89–C95 | −115.4(17) |
| Si6–C42–Si4–C45 | 170.1(9) | C40–Si5–C57–C62 | 64.9(4) | C83–C84–C89–C97 | 124.4(17) |
| Si6–C71–C72–C73 | 178.1(5) | C41–Si5–C57–C58 | 120.5(5) | C83–C88–C92–C93 | 143.7(18) |
| Si6–C71–C72–C77 | −1.4(8) | C41–Si5–C57–C62 | −55.4(5) | C83–C88–C92–C94 | −95(4) |

*Continued on next page*

*Table I.4 – Continued from previous page*

| Torsion angle [°] | | Torsion angle [°] | | Torsion angle [°] | |
|---|---|---|---|---|---|
| Si6–C71–C76–C75 | −178.3(8) | C41–Si6–C71–C72 | −111.1(6) | C84–C83–C88–C87 | 0.0 |
| Si6–C71–C76–C80 | 1.7(9) | C41–Si6–C71–C76 | 67.9(7) | C84–C83–C88–C92 | −177(2) |
| Si7–C43–Si5–C40 | −4.7(19) | C42–Si4–C45–C46 | −118.6(10) | C84–C85–C86–C87 | 0.0 |
| Si7–C43–Si5–C41 | −51(4) | C42–Si4–C45–C50 | 69.8(10) | C84–C89–C95–C77 | −87.1(19) |
| Si7–C43–Si5–C57 | −140.9(12) | C42–Si6–C71–C72 | 120.4(10) | C84–C89–C95–C98 | −81.6(17) |
| Si7–C44–Si4–C40 | 6(3) | C42–Si6–C71–C76 | −60.6(11) | C84–C89–C97–C77 | 89.6(18) |
| Si7–C44–Si4–C42 | 108(44) | C43–Si5–C57–C58 | 104.9(10) | C84–C89–C97–C96 | 86.1(15) |
| Si7–C44–Si4–C45 | 134.3(17) | C43–Si5–C57–C62 | −71.0(10) | C85–C84–C89–C95 | 60.1(17) |
| Si7–C83–C84–C85 | 175.4(16) | C43–Si7–C83–C84 | −53.2(18) | C85–C84–C89–C97 | −60.1(17) |
| Si7–C83–C84–C89 | −9(2) | C43–Si7–C83–C88 | 122.0(17) | C85–C86–C87–C88 | 0.0 |
| Si7–C83–C88–C87 | −175.0(17) | C44–Si4–C45–C46 | −116.9(19) | C86–C87–C88–C83 | 0.0 |
| Si7–C83–C88–C92 | 8(2) | C44–Si4–C45–C50 | 71.5(19) | C86–C87–C88–C92 | 177(2) |
| Si8–C1–Si2–C2 | 47.0(3) | C44–Si7–C83–C84 | 84(2) | C87–C88–C92–C93 | −33(2) |
| Si8–C1–Si2–C28 | 174.4(2) | C44–Si7–C83–C88 | −101(2) | C87–C88–C92–C94 | 89(4) |
| Si8–C3–Si3–C2 | 58.8(3) | C45–C46–C47–C48 | −2.5(7) | C88–C83–C84–C85 | 0.0 |
| Si8–C3–Si3–C16 | −172.0(2) | C45–C46–C51–C53 | 62.2(7) | C88–C83–C84–C89 | 175(2) |
| Si8–C4–C5–C6 | 180.0(3) | C45–C46–C51–C54 | −167.4(6) | C89–C84–C85–C86 | −176.0(17) |
| Si8–C4–C5–C10 | 1.3(6) | C45–C46–C51–C69 | −89.3(11) | C89–C95–C98–C77 | −2.9(9) |
| Si8–C4–C9–C8 | 179.3(3) | C45–C46–C51–C70 | 130.9(8) | C89–C95–C98–C96 | −27.4(16) |
| Si8–C4–C9–C11 | −2.6(6) | C45–C50–C52–C55 | 126.9(5) | C89–C97–C96–C77 | 2.0(8) |
| C1–Si2–C28–C29 | −67.5(4) | C45–C50–C52–C56 | −108.8(5) | C89–C97–C96–C98 | 20.9(15) |
| C1–Si2–C28–C33 | 112.7(4) | C46–C45–C50–C49 | −5.7(6) | C95–C77–C96–C97 | 135.2(9) |
| C2–Si2–C28–C29 | 60.4(4) | C46–C45–C50–C52 | 171.3(4) | C95–C77–C96–C98 | −25.4(13) |
| C2–Si2–C28–C33 | −119.4(4) | C46–C47–C48–C49 | −2.3(8) | C95–C77–C97–C89 | 93.9(19) |
| C2–Si3–C16–C17 | −59.9(4) | C47–C46–C51–C53 | −117.3(6) | C95–C77–C97–C96 | −89.9(14) |
| C2–Si3–C16–C21 | 115.6(4) | C47–C46–C51–C54 | 13.1(8) | C95–C77–C98–C96 | 151.9(13) |
| C3–Si3–C16–C17 | 68.1(4) | C47–C46–C51–C69 | 91.2(11) | C95–C89–C97–C77 | −33.6(9) |
| C3–Si3–C16–C21 | −116.4(4) | C47–C46–C51–C70 | −48.6(9) | C95–C89–C97–C96 | −37.1(12) |
| C4–C5–C6–C7 | 0.1(7) | C47–C48–C49–C50 | 3.1(7) | C96–C77–C95–C89 | −159.2(19) |
| C4–C5–C10–C12 | 112.0(5) | C48–C49–C50–C45 | 1.1(7) | C96–C77–C95–C98 | 26.6(14) |
| C4–C5–C10–C13 | −122.4(5) | C48–C49–C50–C52 | −176.1(4) | C96–C77–C97–C89 | −176.2(16) |
| C4–C9–C11–C14 | −79.7(6) | C49–C50–C52–C55 | −56.0(6) | C96–C77–C98–C95 | −151.9(13) |
| C4–C9–C11–C15 | 156.8(5) | C49–C50–C52–C56 | 68.4(5) | C97–C77–C95–C89 | −90(2) |
| C5–C4–Si8–C1 | 63.4(4) | C50–C45–C46–C47 | 6.4(6) | C97–C77–C95–C98 | 95.4(17) |
| C5–C4–Si8–C3 | −64.4(4) | C50–C45–C46–C51 | −173.1(5) | C97–C77–C96–C98 | −160.5(13) |
| C5–C4–C9–C8 | 0.5(6) | C51–C46–C47–C48 | 177.0(5) | C97–C77–C98–C95 | −133.0(11) |
| C5–C4–C9–C11 | 177.6(4) | C57–C58–C59–C60 | 0.6(7) | C97–C77–C98–C96 | 18.9(13) |
| C5–C6–C7–C8 | 1.2(7) | C57–C58–C64–C65 | −91.4(6) | C97–C89–C95–C77 | 37.0(10) |
| C6–C5–C10–C12 | −66.7(6) | C57–C58–C64–C66 | 147.0(5) | C97–C89–C95–C98 | 42.5(15) |
| C6–C5–C10–C13 | 58.9(6) | C57–C62–C63–C67 | 134.4(5) | C97–C96–C98–C77 | −18.0(11) |
| C6–C7–C8–C9 | −2.0(8) | C57–C62–C63–C68 | −100.3(5) | C97–C96–C98–C95 | 6(2) |
| C7–C8–C9–C4 | 1.6(7) | C58–C57–C62–C61 | −2.3(6) | C98–C77–C95–C89 | 174.2(18) |
| C7–C8–C9–C11 | −176.5(5) | C58–C57–C62–C63 | 172.1(4) | C98–C77–C96–C97 | 160.5(13) |
| C8–C9–C11–C14 | 98.4(5) | C58–C59–C60–C61 | −2.5(7) | C98–C77–C97–C89 | 165(2) |
| C8–C9–C11–C15 | −25.1(7) | C59–C58–C64–C65 | 90.7(6) | C98–C77–C97–C96 | −19.3(14) |
| C9–C4–Si8–C1 | −116.4(4) | C59–C58–C64–C66 | −31.0(7) | | |

# Appendix J

X-ray data for **6a**

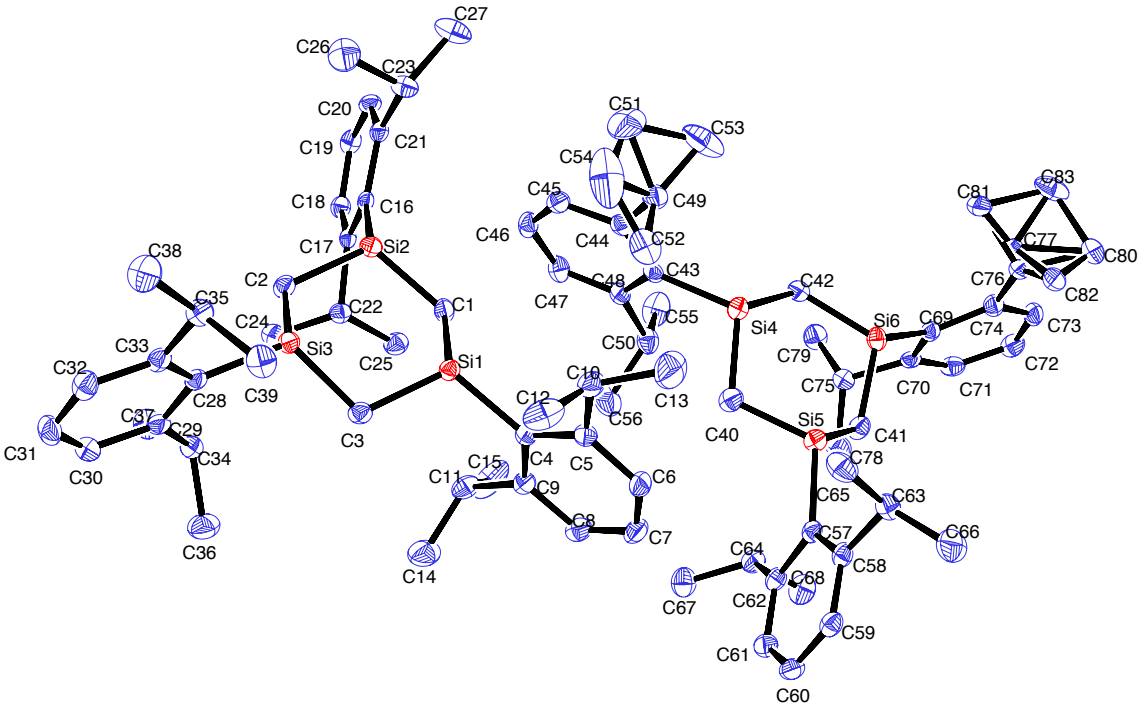


*Figure J.1: Numbering scheme for all non-H atoms in **6a**. Mole 1 is disorder free (left) but some disorders are present in the $^{i}$Pr groups of Mole 2 (right).*

*Table J.1: X-ray crystallographic data for **6a**.*

| | | |
|---|---|---|
| Empirical formula | $C_{39}H_{60}Si_3$ | |
| Formula weight | 613.14 | |
| Temperature | 103(2) K | |
| Wavelength | 0.71075 Å | |
| Crystal system | triclinic | |
| Space group | $P\bar{1}$ (#2) | |
| Unit cell dimensions | $a$ = 13.6987(2) Å | $\alpha$ = 89.8511(13)° |
| | $b$ = 15.7706(3) Å | $\beta$ = 93.8214(9)° |
| | $c$ = 18.5544(4) Å | $\gamma$ = 108.3342(8)° |
| Volume | 3795.78(12) Å$^3$ | |
| Z | 4 | |
| Density (calculated) | 1.073 $^{Mg}/_{m^3}$ | |
| Absorption coefficient | 0.149 mm$^{-1}$ | |
| F(000) | 1344 | |
| Crystal size | 0.20 x 0.20 x 0.10 mm$^3$ | |
| Theta range for data collection | 1.98 to 25.00° | |
| Index ranges | $-16 \leq h \leq 16$ | |
| | $-18 \leq k \leq 18$ | |
| | $-22 \leq l \leq 22$ | |
| Reflections collected | 31815 | |
| Independent reflections | 13305 [R(int) = 0.0331] | |
| Completeness to theta | 99.4% (25.00°) | |
| Max. and min. transmission | 0.9852 and 0.9708 | |
| Refinement method | Full-matrix least-squares on F$^2$ | |
| Data / restraints / parameters | 13305 / 6 / 842 | |
| Goodness of fit on F$^2$ | 1.062 | |
| Final R indices [$I > 2\sigma(I)$] | R1 = 0.0377, wR2 = 0.0903 | |
| Final R indices (all data) | R1 = 0.0563, wR2 = 0.0959 | |
| Largest diff. peak and hole | 0.377 and −0.296 e.Å$^{-3}$ | |

*Table J.2: Bond lengths from crystallographic analysis of **6a**.*

| **Bond lengths** [Å] | | **Bond lengths** [Å] | | **Bond lengths** [Å] | |
|---|---|---|---|---|---|
| Si1–C1 | 1.8691(17) | C17–C18 | 1.391(2) | C49–C53 | 1.490(6) |
| Si1–C3 | 1.8788(17) | C17–C22 | 1.527(2) | C49–C54 | 1.516(7) |
| Si1–C4 | 1.8979(17) | C18–C19 | 1.380(2) | C50–C55 | 1.527(3) |
| Si2–C1 | 1.8783(17) | C19–C20 | 1.377(2) | C50–C56 | 1.534(3) |
| Si2–C2 | 1.8776(17) | C20–C21 | 1.395(2) | C57–C58 | 1.425(2) |
| Si2–C16 | 1.8951(17) | C21–C23 | 1.523(2) | C57–C62 | 1.415(2) |
| Si3–C2 | 1.8769(17) | C22–C24 | 1.531(2) | C58–C59 | 1.396(2) |
| Si3–C3 | 1.8811(17) | C22–C25 | 1.533(2) | C58–C63 | 1.526(2) |
| Si3–C28 | 1.8975(17) | C23–C26 | 1.522(3) | C59–C60 | 1.377(2) |
| Si4–C40 | 1.8752(18) | C23–C27 | 1.535(3) | C60–C61 | 1.381(3) |
| Si4–C42 | 1.8898(18) | C28–C29 | 1.411(2) | C61–C62 | 1.394(2) |
| Si4–C43 | 1.8951(18) | C28–C33 | 1.430(2) | C62–C64 | 1.525(2) |
| Si5–C40 | 1.8719(18) | C29–C30 | 1.395(2) | C63–C65 | 1.524(3) |
| Si5–C41 | 1.8732(18) | C29–C34 | 1.524(2) | C63–C66 | 1.532(3) |
| Si5–C57 | 1.8978(18) | C30–C31 | 1.381(3) | C64–C67 | 1.525(3) |
| Si6–C41 | 1.8774(18) | C31–C32 | 1.378(3) | C64–C68 | 1.533(2) |
| Si6–C42 | 1.8799(18) | C32–C33 | 1.390(2) | C69–C70 | 1.410(2) |
| Si6–C69 | 1.8963(18) | C33–C35 | 1.527(2) | C69–C74 | 1.426(2) |
| C4–C5 | 1.420(2) | C34–C36 | 1.532(3) | C70–C71 | 1.394(2) |
| C4–C9 | 1.412(2) | C34–C37 | 1.535(2) | C70–C75 | 1.526(2) |
| C5–C6 | 1.397(2) | C35–C38 | 1.537(2) | C71–C72 | 1.374(3) |
| C5–C10 | 1.530(3) | C35–C39 | 1.541(2) | C72–C73 | 1.383(3) |
| C6–C7 | 1.380(3) | C43–C44 | 1.423(2) | C73–C74 | 1.392(3) |
| C7–C8 | 1.373(3) | C43–C48 | 1.421(2) | C74–C76 | 1.497(5) |
| C8–C9 | 1.397(2) | C44–C45 | 1.394(2) | C74–C77 | 1.74(2) |
| C9–C11 | 1.524(2) | C44–C49 | 1.525(2) | C75–C78 | 1.530(2) |
| C10–C12 | 1.532(3) | C45–C46 | 1.378(3) | C75–C79 | 1.530(2) |
| C10–C13 | 1.530(3) | C46–C47 | 1.374(3) | C76–C80 | 1.530(5) |
| C11–C14 | 1.528(3) | C47–C48 | 1.399(2) | C76–C81 | 1.543(3) |
| C11–C15 | 1.532(3) | C48–C50 | 1.521(2) | C77–C82 | 1.52(2) |
| C16–C17 | 1.414(2) | C49–C51 | 1.557(4) | C77–C83 | 1.56(2) |
| C16–C21 | 1.425(2) | C49–C52 | 1.513(4) | | |

*Table J.3: Bond to bond angles from crystallographic analysis of **6a**.*

| **Angles [°]** | | **Angles [°]** | | **Angles [°]** | |
|---|---|---|---|---|---|
| Si1–C1–Si2 | 114.73(9) | C18–C17–C22 | 117.54(15) | C52–C49–C51 | 109.1(3) |
| Si1–C3–Si3 | 110.20(9) | C19–C18–C17 | 120.96(16) | C52–C49–C54 | 59.3(4) |
| Si1–C4–C5 | 121.78(13) | C19–C20–C21 | 121.12(16) | C53–C49–C44 | 110.1(3) |
| Si1–C4–C9 | 119.64(13) | C20–C19–C18 | 119.94(16) | C53–C49–C51 | 67.9(3) |
| Si2–C2–Si3 | 111.66(9) | C20–C21–C16 | 119.55(16) | C53–C49–C52 | 136.8(3) |
| Si2–C16–C17 | 118.88(12) | C20–C21–C23 | 119.39(15) | C53–C49–C54 | 113.6(5) |
| Si2–C16–C21 | 122.89(12) | C21–C23–C27 | 113.04(15) | C54–C49–C44 | 116.5(3) |
| Si3–C28–C29 | 119.78(13) | C24–C22–C25 | 110.82(14) | C54–C49–C51 | 51.9(4) |
| Si3–C28–C33 | 121.61(13) | C26–C23–C21 | 111.23(15) | C55–C50–C56 | 110.97(17) |
| Si4–C40–Si5 | 112.21(9) | C26–C23–C27 | 110.83(16) | C57–C58–C63 | 122.45(15) |
| Si4–C42–Si6 | 114.41(9) | C28–C29–C34 | 122.98(15) | C57–C62–C64 | 121.37(16) |
| Si4–C43–C44 | 122.02(13) | C28–C33–C35 | 121.43(15) | C58–C63–C66 | 113.58(15) |
| Si4–C43–C48 | 119.44(13) | C29–C28–C33 | 118.54(15) | C59–C58–C57 | 119.41(16) |
| Si5–C41–Si6 | 110.21(9) | C29–C34–C36 | 111.17(15) | C59–C58–C63 | 118.14(15) |
| Si5–C57–C58 | 122.68(13) | C29–C34–C37 | 112.06(15) | C59–C60–C61 | 119.47(17) |
| Si5–C57–C62 | 119.19(13) | C30–C29–C28 | 120.04(16) | C60–C59–C58 | 121.67(17) |
| Si6–C69–C70 | 119.30(13) | C30–C29–C34 | 116.98(16) | C60–C61–C62 | 120.99(17) |
| Si6–C69–C74 | 121.71(13) | C31–C30–C29 | 120.95(18) | C61–C62–C57 | 120.32(16) |
| C1–Si1–C3 | 110.34(8) | C31–C32–C33 | 121.80(17) | C61–C62–C64 | 118.13(16) |
| C1–Si1–C4 | 112.33(8) | C32–C31–C30 | 119.61(17) | C62–C57–C58 | 118.02(16) |
| C1–Si2–C16 | 111.50(7) | C32–C33–C28 | 119.02(16) | C62–C64–C67 | 114.52(15) |
| C2–Si2–C1 | 112.86(8) | C32–C33–C35 | 119.52(16) | C62–C64–C68 | 108.78(15) |
| C2–Si2–C16 | 111.38(7) | C33–C35–C38 | 114.41(15) | C65–C63–C58 | 110.78(15) |
| C2–Si3–C3 | 110.38(8) | C33–C35–C39 | 110.51(15) | C65–C63–C66 | 110.05(16) |
| C2–Si3–C28 | 113.04(8) | C36–C34–C37 | 110.72(16) | C67–C64–C68 | 111.61(15) |
| C3–Si1–C4 | 114.19(8) | C38–C35–C39 | 109.22(15) | C69–C70–C75 | 122.66(15) |
| C3–Si3–C28 | 113.80(8) | C40–Si4–C42 | 113.66(8) | C69–C74–C76 | 121.7(2) |
| C4–C5–C10 | 122.08(16) | C40–Si4–C43 | 110.41(8) | C69–C74–C77 | 118.8(9) |
| C4–C9–C11 | 122.89(15) | C40–Si5–C41 | 106.56(8) | C70–C69–C74 | 118.40(15) |
| C5–C10–C12 | 110.10(15) | C40–Si5–C57 | 114.05(8) | C70–C75–C78 | 113.60(15) |
| C6–C5–C4 | 119.21(17) | C41–Si5–C57 | 115.84(8) | C70–C75–C79 | 110.05(14) |
| C6–C5–C10 | 118.65(16) | C41–Si6–C42 | 110.27(8) | C71–C70–C69 | 120.19(16) |
| C7–C6–C5 | 121.50(17) | C41–Si6–C69 | 109.42(8) | C71–C70–C75 | 117.06(16) |
| C7–C8–C9 | 121.13(18) | C42–Si4–C43 | 113.12(8) | C71–C72–C73 | 119.86(17) |
| C8–C7–C6 | 119.64(17) | C42–Si6–C69 | 116.58(8) | C72–C71–C70 | 120.79(17) |
| C8–C9–C4 | 119.94(16) | C43–C44–C49 | 122.21(16) | C72–C73–C74 | 121.38(17) |
| C8–C9–C11 | 117.16(16) | C43–C48–C50 | 123.54(16) | C73–C74–C69 | 119.12(17) |
| C9–C4–C5 | 118.58(16) | C44–C49–C51 | 112.9(2) | C73–C74–C76 | 119.2(2) |
| C9–C11–C14 | 111.30(15) | C45–C44–C43 | 119.29(16) | C73–C74–C77 | 120.3(9) |
| C9–C11–C15 | 111.86(16) | C45–C44–C49 | 118.50(16) | C74–C76–C80 | 115.3(3) |
| C13–C10–C5 | 114.53(17) | C46–C45–C44 | 121.50(17) | C74–C76–C81 | 110.1(3) |
| C13–C10–C12 | 109.66(18) | C46–C47–C48 | 120.95(17) | C76–C74–C77 | 14.7(7) |
| C14–C11–C15 | 111.20(17) | C47–C46–C45 | 120.01(17) | C78–C75–C79 | 110.47(15) |
| C16–C17–C22 | 122.28(15) | C47–C48–C43 | 119.73(16) | C80–C76–C81 | 108.2(3) |
| C16–C21–C23 | 121.06(15) | C47–C48–C50 | 116.72(16) | C82–C77–C74 | 107.9(11) |
| C17–C16–C21 | 118.23(15) | C48–C43–C44 | 118.51(16) | C82–C77–C83 | 109.6(16) |
| C17–C22–C24 | 112.98(14) | C48–C50–C55 | 110.91(16) | C83–C77–C74 | 113.3(15) |
| C17–C22–C25 | 110.11(14) | C48–C50–C56 | 112.28(15) | | |
| C18–C17–C16 | 120.08(15) | C52–C49–C44 | 110.24(18) | | |

*Table J.4: Torsion angles from crystallographic analysis of **6a**.*

| Torsion angle [°] | | Torsion angle [°] | | Torsion angle [°] | |
|---|---|---|---|---|---|
| Si2–C1–Si8–C3 | −50.4(3) | C9–C4–Si8–C3 | 115.8(4) | C59–C60–C61–C62 | 2.0(7) |
| Si2–C1–Si8–C4 | −179.8(2) | C9–C4–C5–C6 | 0.2(6) | C60–C61–C62–C57 | 0.4(7) |
| Si2–C2–Si3–C3 | −55.5(3) | C9–C4–C5–C10 | −178.9(4) | C60–C61–C62–C63 | −174.1(4) |
| Si2–C2–Si3–C16 | 175.4(2) | C10–C5–C6–C7 | 178.6(4) | C61–C62–C63–C67 | −51.3(6) |
| Si2–C28–C29–C30 | −176.3(3) | C16–C17–C18–C19 | 0.3(7) | C61–C62–C63–C68 | 74.1(5) |
| Si2–C28–C29–C34 | 7.1(5) | C16–C17–C22–C24 | −114.1(5) | C62–C57–C58–C59 | 1.8(6) |
| Si2–C28–C33–C32 | 176.3(3) | C16–C17–C22–C25 | 121.2(5) | C62–C57–C58–C64 | −176.1(4) |
| Si2–C28–C33–C35 | −6.1(6) | C16–C21–C23–C26 | 73.3(5) | C64–C58–C59–C60 | 178.6(4) |
| Si3–C2–Si2–C1 | 48.8(3) | C16–C21–C23–C27 | −162.7(4) | C71–C72–C73–C74 | 0.7(9) |
| Si3–C2–Si2–C28 | 176.3(2) | C17–C16–C21–C20 | 0.7(6) | C71–C72–C77–C95 | −82.8(9) |
| Si3–C3–Si8–C1 | 55.5(3) | C17–C16–C21–C23 | −177.0(4) | C71–C72–C77–C96 | 149.8(13) |
| Si3–C3–Si8–C4 | −175.7(2) | C17–C18–C19–C20 | 0.7(7) | C71–C72–C77–C97 | 85.8(9) |
| Si3–C16–C17–C18 | 175.2(3) | C18–C17–C22–C24 | 65.6(5) | C71–C72–C77–C98 | −143.7(17) |
| Si3–C16–C17–C22 | −5.1(6) | C18–C17–C22–C25 | −59.1(5) | C71–C76–C80–C81 | −118.0(12) |
| Si3–C16–C21–C20 | −174.9(3) | C18–C19–C20–C21 | 0.5(7) | C71–C76–C80–C82 | 116.4(8) |
| Si3–C16–C21–C23 | 7.4(6) | C19–C20–C21–C16 | 0.3(7) | C72–C71–C76–C75 | 0.8(9) |
| Si4–C40–Si5–C41 | −65.9(4) | C19–C20–C21–C23 | 177.5(4) | C72–C71–C76–C80 | −179.2(7) |
| Si4–C40–Si5–C43 | −55.4(11) | C20–C21–C23–C26 | −104.5(5) | C72–C73–C74–C75 | 0.4(11) |
| Si4–C40–Si5–C57 | 169.1(2) | C20–C21–C23–C27 | 19.5(6) | C72–C77–C95–C89 | 72.9(14) |
| Si4–C42–Si6–C41 | −41.0(17) | C21–C16–C17–C18 | 0.5(6) | C72–C77–C95–C98 | −101.3(13) |
| Si4–C42–Si6–C71 | −168.7(10) | C21–C16–C17–C22 | 179.2(4) | C72–C77–C96–C97 | −98.9(8) |
| Si4–C44–Si7–C43 | 50(3) | C22–C17–C18–C19 | −179.9(4) | C72–C77–C96–C98 | 100.5(12) |
| Si4–C44–Si7–C83 | −177.0(18) | C28–C29–C30–C31 | −1.1(7) | C72–C77–C97–C89 | −69.5(14) |
| Si4–C45–C46–C47 | −165.4(4) | C28–C29–C34–C36 | −124.0(5) | C72–C77–C97–C96 | 106.7(9) |
| Si4–C45–C46–C51 | 15.1(6) | C28–C29–C34–C37 | 110.4(5) | C72–C77–C98–C95 | 101.3(9) |
| Si4–C45–C50–C49 | 166.1(3) | C28–C33–C35–C38 | 87.3(6) | C72–C77–C98–C96 | −106.8(10) |
| Si4–C45–C50–C52 | −16.8(6) | C28–C33–C35–C39 | −145.3(5) | C73–C72–C77–C95 | 97.6(8) |
| Si5–C40–Si4–C42 | −58.2(8) | C29–C28–C33–C32 | −3.5(6) | C73–C72–C77–C96 | −29.8(14) |
| Si5–C40–Si4–C44 | −54.6(16) | C29–C28–C33–C35 | 174.1(4) | C73–C72–C77–C97 | −93.8(9) |
| Si5–C40–Si4–C45 | 172.4(2) | C29–C30–C31–C32 | −1.4(7) | C73–C72–C77–C98 | 36.7(18) |
| Si5–C41–Si6–C42 | −50.7(10) | C30–C29–C34–C36 | 59.4(6) | C73–C74–C75–C76 | 0.3(12) |
| Si5–C41–Si6–C71 | 178.9(5) | C30–C29–C34–C37 | −66.2(5) | C74–C75–C76–C71 | 0.5(12) |
| Si5–C43–Si7–C44 | 52(3) | C30–C31–C32–C33 | 1.3(7) | C74–C75–C76–C80 | 179.5(9) |
| Si5–C43–Si7–C83 | −179.8(12) | C31–C32–C33–C28 | 1.2(7) | C75–C76–C80–C81 | 62.0(13) |
| Si5–C57–C58–C59 | −174.2(3) | C31–C32–C33–C35 | −176.4(4) | C75–C76–C80–C82 | −63.6(10) |
| Si5–C57–C58–C64 | 7.9(6) | C32–C33–C35–C38 | −95.1(6) | C76–C71–C72–C73 | 0.9(8) |
| Si5–C57–C62–C61 | 173.8(3) | C32–C33–C35–C39 | 32.4(7) | C76–C71–C72–C77 | 179.5(6) |
| Si5–C57–C62–C63 | −11.9(6) | C33–C28–C29–C30 | 3.5(6) | C77–C72–C73–C74 | −179.7(8) |
| Si6–C41–Si5–C40 | −62.2(6) | C33–C28–C29–C34 | −173.1(4) | C77–C95–C98–C96 | −24.5(11) |
| Si6–C41–Si5–C43 | 75(5) | C34–C29–C30–C31 | 175.5(4) | C77–C96–C98–C95 | 23.5(11) |
| Si6–C41–Si5–C57 | 171.4(4) | C40–Si4–C45–C46 | 114.3(4) | C77–C97–C96–C98 | 18.9(12) |
| Si6–C42–Si4–C40 | 44.2(16) | C40–Si4–C45–C50 | −57.3(4) | C83–C84–C85–C86 | 0.0 |
| Si6–C42–Si4–C44 | −35(42) | C40–Si5–C57–C58 | −119.2(4) | C83–C84–C89–C95 | −115.4(17) |
| Si6–C42–Si4–C45 | 170.1(9) | C40–Si5–C57–C62 | 64.9(4) | C83–C84–C89–C97 | 124.4(17) |
| Si6–C71–C72–C73 | 178.1(5) | C41–Si5–C57–C58 | 120.5(5) | C83–C88–C92–C93 | 143.7(18) |
| Si6–C71–C72–C77 | −1.4(8) | C41–Si5–C57–C62 | −55.4(5) | C83–C88–C92–C94 | −95(4) |

*Continued on next page*

*Table J.4 – Continued from previous page*

| Torsion angle [°] | | Torsion angle [°] | | Torsion angle [°] | |
|---|---|---|---|---|---|
| Si6–C71–C76–C75 | −178.3(8) | C41–Si6–C71–C72 | −111.1(6) | C84–C83–C88–C87 | 0.0 |
| Si6–C71–C76–C80 | 1.7(9) | C41–Si6–C71–C76 | 67.9(7) | C84–C83–C88–C92 | −177(2) |
| Si7–C43–Si5–C40 | −4.7(19) | C42–Si4–C45–C46 | −118.6(10) | C84–C85–C86–C87 | 0.0 |
| Si7–C43–Si5–C41 | −51(4) | C42–Si4–C45–C50 | 69.8(10) | C84–C89–C95–C77 | −87.1(19) |
| Si7–C43–Si5–C57 | −140.9(12) | C42–Si6–C71–C72 | 120.4(10) | C84–C89–C95–C98 | −81.6(17) |
| Si7–C44–Si4–C40 | 6(3) | C42–Si6–C71–C76 | −60.6(11) | C84–C89–C97–C77 | 89.6(18) |
| Si7–C44–Si4–C42 | 108(44) | C43–Si5–C57–C58 | 104.9(10) | C84–C89–C97–C96 | 86.1(15) |
| Si7–C44–Si4–C45 | 134.3(17) | C43–Si5–C57–C62 | −71.0(10) | C85–C84–C89–C95 | 60.1(17) |
| Si7–C83–C84–C85 | 175.4(16) | C43–Si7–C83–C84 | −53.2(18) | C85–C84–C89–C97 | −60.1(17) |
| Si7–C83–C84–C89 | −9(2) | C43–Si7–C83–C88 | 122.0(17) | C85–C86–C87–C88 | 0.0 |
| Si7–C83–C88–C87 | −175.0(17) | C44–Si4–C45–C46 | −116.9(19) | C86–C87–C88–C83 | 0.0 |
| Si7–C83–C88–C92 | 8(2) | C44–Si4–C45–C50 | 71.5(19) | C86–C87–C88–C92 | 177(2) |
| Si8–C1–Si2–C2 | 47.0(3) | C44–Si7–C83–C84 | 84(2) | C87–C88–C92–C93 | −33(2) |
| Si8–C1–Si2–C28 | 174.4(2) | C44–Si7–C83–C88 | −101(2) | C87–C88–C92–C94 | 89(4) |
| Si8–C3–Si3–C2 | 58.8(3) | C45–C46–C47–C48 | −2.5(7) | C88–C83–C84–C85 | 0.0 |
| Si8–C3–Si3–C16 | −172.0(2) | C45–C46–C51–C53 | 62.2(7) | C88–C83–C84–C89 | 175(2) |
| Si8–C4–C5–C6 | 180.0(3) | C45–C46–C51–C54 | −167.4(6) | C89–C84–C85–C86 | −176.0(17) |
| Si8–C4–C5–C10 | 1.3(6) | C45–C46–C51–C69 | −89.3(11) | C89–C95–C98–C77 | −2.9(9) |
| Si8–C4–C9–C8 | 179.3(3) | C45–C46–C51–C70 | 130.9(8) | C89–C95–C98–C96 | −27.4(16) |
| Si8–C4–C9–C11 | −2.6(6) | C45–C50–C52–C55 | 126.9(5) | C89–C97–C96–C77 | 2.0(8) |
| C1–Si2–C28–C29 | −67.5(4) | C45–C50–C52–C56 | −108.8(5) | C89–C97–C96–C98 | 20.9(15) |
| C1–Si2–C28–C33 | 112.7(4) | C46–C45–C50–C49 | −5.7(6) | C95–C77–C96–C97 | 135.2(9) |
| C2–Si2–C28–C29 | 60.4(4) | C46–C45–C50–C52 | 171.3(4) | C95–C77–C96–C98 | −25.4(13) |
| C2–Si2–C28–C33 | −119.4(4) | C46–C47–C48–C49 | −2.3(8) | C95–C77–C97–C89 | 93.9(19) |
| C2–Si3–C16–C17 | −59.9(4) | C47–C46–C51–C53 | −117.3(6) | C95–C77–C97–C96 | −89.9(14) |
| C2–Si3–C16–C21 | 115.6(4) | C47–C46–C51–C54 | 13.1(8) | C95–C77–C98–C96 | 151.9(13) |
| C3–Si3–C16–C17 | 68.1(4) | C47–C46–C51–C69 | 91.2(11) | C95–C89–C97–C77 | −33.6(9) |
| C3–Si3–C16–C21 | −116.4(4) | C47–C46–C51–C70 | −48.6(9) | C95–C89–C97–C96 | −37.1(12) |
| C4–C5–C6–C7 | 0.1(7) | C47–C48–C49–C50 | 3.1(7) | C96–C77–C95–C89 | −159.2(19) |
| C4–C5–C10–C12 | 112.0(5) | C48–C49–C50–C45 | 1.1(7) | C96–C77–C95–C98 | 26.6(14) |
| C4–C5–C10–C13 | −122.4(5) | C48–C49–C50–C52 | −176.1(4) | C96–C77–C97–C89 | −176.2(16) |
| C4–C9–C11–C14 | −79.7(6) | C49–C50–C52–C55 | −56.0(6) | C96–C77–C98–C95 | −151.9(13) |
| C4–C9–C11–C15 | 156.8(5) | C49–C50–C52–C56 | 68.4(5) | C97–C77–C95–C89 | −90(2) |
| C5–C4–Si8–C1 | 63.4(4) | C50–C45–C46–C47 | 6.4(6) | C97–C77–C95–C98 | 95.4(17) |
| C5–C4–Si8–C3 | −64.4(4) | C50–C45–C46–C51 | −173.1(5) | C97–C77–C96–C98 | −160.5(13) |
| C5–C4–C9–C8 | 0.5(6) | C51–C46–C47–C48 | 177.0(5) | C97–C77–C98–C95 | −133.0(11) |
| C5–C4–C9–C11 | 177.6(4) | C57–C58–C59–C60 | 0.6(7) | C97–C77–C98–C96 | 18.9(13) |
| C5–C6–C7–C8 | 1.2(7) | C57–C58–C64–C65 | −91.4(6) | C97–C89–C95–C77 | 37.0(10) |
| C6–C5–C10–C12 | −66.7(6) | C57–C58–C64–C66 | 147.0(5) | C97–C89–C95–C98 | 42.5(15) |
| C6–C5–C10–C13 | 58.9(6) | C57–C62–C63–C67 | 134.4(5) | C97–C96–C98–C77 | −18.0(11) |
| C6–C7–C8–C9 | −2.0(8) | C57–C62–C63–C68 | −100.3(5) | C97–C96–C98–C95 | 6(2) |
| C7–C8–C9–C4 | 1.6(7) | C58–C57–C62–C61 | −2.3(6) | C98–C77–C95–C89 | 174.2(18) |
| C7–C8–C9–C11 | −176.5(5) | C58–C57–C62–C63 | 172.1(4) | C98–C77–C96–C97 | 160.5(13) |
| C8–C9–C11–C14 | 98.4(5) | C58–C59–C60–C61 | −2.5(7) | C98–C77–C97–C89 | 165(2) |
| C8–C9–C11–C15 | −25.1(7) | C59–C58–C64–C65 | 90.7(6) | C98–C77–C97–C96 | −19.3(14) |
| C9–C4–Si8–C1 | −116.4(4) | C59–C58–C64–C66 | −31.0(7) | | |

# Appendix K

X-ray data for **7**

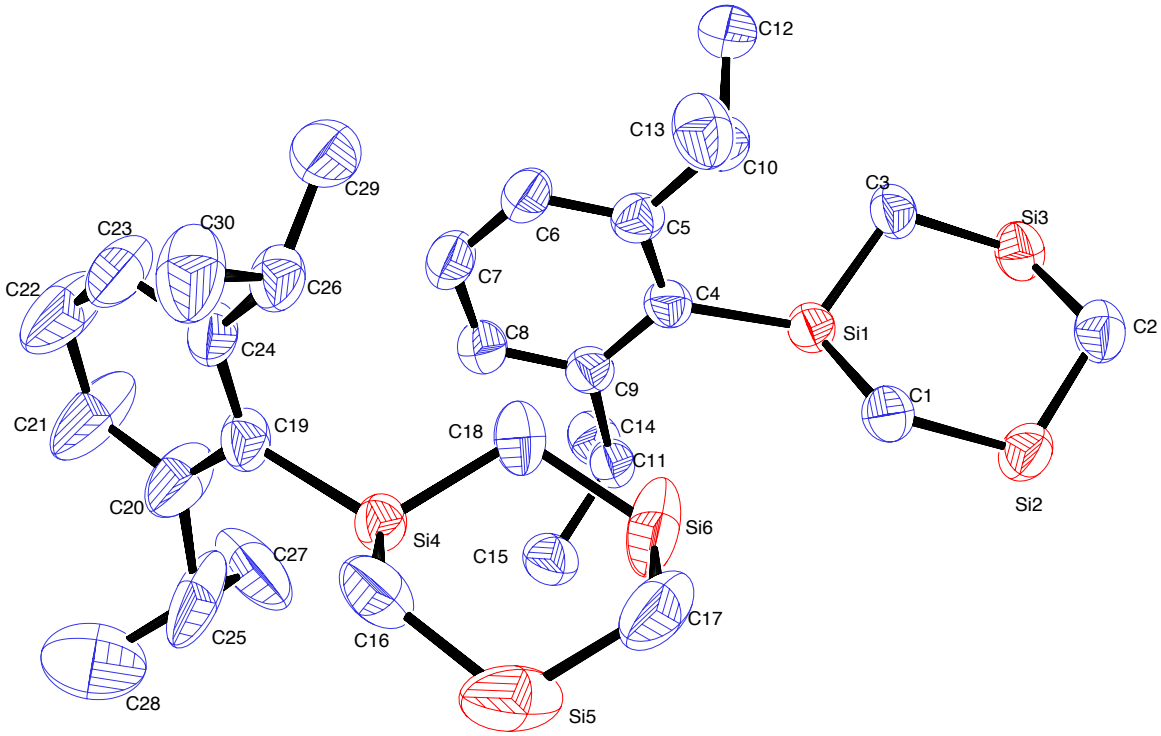


*Figure K.1: Numbering scheme for all non-H atoms in **7**. Mole 1 is on the right and Mole 2 on the left.*

*Table K.1: X-ray crystallographic data for* **7**.

| | | |
|---|---|---|
| Empirical formula | $C_{15}H_{28}Si_3$ | |
| Formula weight | 292.64 | |
| Temperature | 103(2) K | |
| Wavelength | 0.71075 Å | |
| Crystal system | monoclinic | |
| Space group | $P2_1/n$ (#14) | |
| Unit cell dimensions | $a$ = 15.1267(13) Å | $\alpha$ = 90.00° |
| | $b$ = 10.7858(14) Å | $\beta$ = 108.568(10)° |
| | $c$ = 22.741(3) Å | $\gamma$ = 90.00° |
| Volume | 3517.1(7) Å$^3$ | |
| Z | 8 | |
| Density (calculated) | 1.105 $^{Mg}/_{m^3}$ | |
| Absorption coefficient | 0.255 mm$^{-1}$ | |
| F(000) | 1280 | |
| Crystal size | 0.60 x 0.30 x 0.10 mm$^3$ | |
| Theta range for data collection | 2.11 to 25.00° | |
| Index ranges | $-16 \leq h \leq 17$ | |
| | $-12 \leq k \leq 12$ | |
| | $-26 \leq l \leq 27$ | |
| Reflections collected | 26026 | |
| Independent reflections | 6104 [R(int) = 0.1127] | |
| Completeness to theta | 98.7% (25.00°) | |
| Max. and min. transmission | 0.9750 and 0.8622 | |
| Refinement method | Full-matrix least-squares on F$^2$ | |
| Data / restraints / parameters | 6104 / 0 / 366 | |
| Goodness of fit on F$^2$ | 1.001 | |
| Final R indices [$I > 2\sigma(I)$] | R1 = 0.0697, wR2 = 0.1670 | |
| Final R indices (all data) | R1 = 0.1440, wR2 = 0.2025 | |
| Largest diff. peak and hole | 0.485 and −0.478 e.Å$^{-3}$ | |

*Table K.2: Bond lengths from crystallographic analysis of **7**.*

| **Bond lengths** [Å] | | **Bond lengths** [Å] | | **Bond lengths** [Å] | |
|---|---|---|---|---|---|
| Si1–C1 | 1.847(5) | Si6–C18 | 1.837(5) | C19–C20 | 1.399(6) |
| Si1–C3 | 1.861(5) | C4–C5 | 1.404(6) | C19–C24 | 1.391(6) |
| Si1–C4 | 1.904(5) | C4–C9 | 1.402(6) | C20–C21 | 1.381(8) |
| Si2–C1 | 1.865(5) | C5–C6 | 1.398(6) | C20–C25 | 1.585(8) |
| Si2–C2 | 1.859(5) | C5–C10 | 1.522(6) | C21–C22 | 1.377(8) |
| Si3–C2 | 1.840(5) | C6–C7 | 1.356(6) | C22–C23 | 1.371(8) |
| Si3–C3 | 1.870(5) | C7–C8 | 1.375(6) | C23–C24 | 1.383(7) |
| Si4–C16 | 1.846(5) | C8–C9 | 1.415(6) | C24–C26 | 1.504(6) |
| Si4–C18 | 1.861(5) | C9–C11 | 1.502(6) | C25–C27 | 1.501(10) |
| Si4–C19 | 1.891(5) | C10–C12 | 1.514(7) | C25–C28 | 1.474(9) |
| Si5–C16 | 1.844(6) | C10–C13 | 1.528(6) | C26–C29 | 1.506(7) |
| Si5–C17 | 1.841(7) | C11–C14 | 1.519(6) | C26–C30 | 1.537(7) |
| Si6–C17 | 1.834(7) | C11–C15 | 1.529(6) | | |

*Table K.3: Bond to bond angles from crystallographic analysis of **7**.*

| **Angles** [°] | | **Angles** [°] | | **Angles** [°] | |
|---|---|---|---|---|---|
| Si1–C1–Si2 | 114.8(3) | C5–C10–C13 | 111.4(4) | C19–C20–C25 | 122.6(5) |
| Si1–C3–Si3 | 111.7(2) | C6–C5–C4 | 120.0(4) | C19–C24–C26 | 122.8(4) |
| Si1–C4–C5 | 121.9(3) | C6–C5–C10 | 118.0(4) | C21–C20–C19 | 120.0(5) |
| Si1–C4–C9 | 119.5(3) | C6–C7–C8 | 119.8(5) | C21–C20–C25 | 117.3(5) |
| Si2–C2–Si3 | 113.3(2) | C7–C6–C5 | 121.2(5) | C22–C21–C20 | 121.3(5) |
| Si4–C16–Si5 | 111.9(3) | C7–C8–C9 | 120.9(4) | C22–C23–C24 | 121.1(5) |
| Si4–C18–Si6 | 113.4(3) | C8–C9–C11 | 116.9(4) | C23–C22–C21 | 118.7(6) |
| Si4–C19–C20 | 121.7(4) | C9–C4–C5 | 118.6(4) | C23–C24–C19 | 120.5(4) |
| Si4–C19–C24 | 120.1(3) | C9–C11–C14 | 110.5(4) | C23–C24–C26 | 116.7(4) |
| Si5–C17–Si6 | 114.7(3) | C9–C11–C15 | 113.0(4) | C24–C19–C20 | 118.2(4) |
| C1–Si1–C3 | 108.2(2) | C12–C10–C5 | 111.7(4) | C24–C26–C29 | 112.9(5) |
| C1–Si1–C4 | 111.9(2) | C12–C10–C13 | 111.1(4) | C24–C26–C30 | 110.6(4) |
| C2–Si2–C1 | 110.5(2) | C14–C11–C15 | 110.3(4) | C27–C25–C20 | 102.4(6) |
| C2–Si3–C3 | 109.0(2) | C16–Si4–C18 | 107.9(2) | C28–C25–C20 | 115.4(5) |
| C3–Si1–C4 | 117.9(2) | C16–Si4–C19 | 115.6(2) | C28–C25–C27 | 110.2(5) |
| C4–C5–C10 | 122.0(4) | C17–Si5–C16 | 109.7(3) | C29–C26–C30 | 110.4(5) |
| C4–C9–C8 | 119.1(4) | C17–Si6–C18 | 110.8(3) | | |
| C4–C9–C11 | 124.0(4) | C18–Si4–C19 | 114.4(2) | | |

*Table K.4: Torsion angles from crystallographic analysis of **7**.*

| **Torsion angles [°]** | | **Torsion angles [°]** | |
|---|---|---|---|
| Si1–C1–Si2–C2 | 50.9(3) | C5–C4–C9–C11 | −173.9(4) |
| Si1–C3–Si3–C2 | 60.1(3) | C5–C6–C7–C8 | 1.1(8) |
| Si1–C4–C5–C6 | 173.4(4) | C6–C5–C10–C12 | −72.4(6) |
| Si1–C4–C5–C10 | −7.1(6) | C6–C5–C10–C13 | 52.6(6) |
| Si1–C4–C9–C8 | −174.8(3) | C6–C7–C8–C9 | −2.5(8) |
| Si1–C4–C9–C11 | 6.6(6) | C7–C8–C9–C4 | 0.4(7) |
| Si2–C1–Si1–C3 | 54.3(3) | C7–C8–C9–C11 | 178.3(4) |
| Si2–C1–Si1–C4 | −174.1(2) | C8–C9–C11–C14 | 77.7(5) |
| Si2–C2–Si3–C3 | 56.1(3) | C8–C9–C11–C15 | −46.5(6) |
| Si3–C2–Si2–C1 | 51.3(3) | C9–C4–C5–C6 | −6.2(7) |
| Si3–C3–Si1–C1 | −58.5(3) | C9–C4–C5–C10 | 173.4(4) |
| Si3–C3–Si1–C4 | 173.4(2) | C10–C5–C6–C7 | −176.2(5) |
| Si4–C16–Si5–C17 | 57.5(4) | C16–Si4–C19–C20 | −113.7(5) |
| Si4–C18–Si6–C17 | 52.2(4) | C16–Si4–C19–C24 | 66.1(5) |
| Si4–C19–C20–C21 | −174.6(6) | C18–Si4–C19–C20 | 120.0(5) |
| Si4–C19–C20–C25 | 9.2(9) | C18–Si4–C19–C24 | −60.2(5) |
| Si4–C19–C24–C23 | 176.4(5) | C19–C20–C21–C22 | −3.3(13) |
| Si4–C19–C24–C26 | −3.5(7) | C19–C20–C25–C27 | −105.6(7) |
| Si5–C16–Si4–C18 | 59.6(3) | C19–C20–C25–C28 | 134.7(7) |
| Si5–C16–Si4–C19 | −170.9(2) | C19–C24–C26–C29 | 122.8(5) |
| Si5–C17–Si6–C18 | −49.7(4) | C19–C24–C26–C30 | −113.0(6) |
| Si6–C17–Si5–C16 | 52.2(4) | C20–C19–C24–C23 | −3.8(8) |
| Si6–C18–Si4–C16 | −57.1(3) | C20–C19–C24–C26 | 176.3(5) |
| Si6–C18–Si4–C19 | 172.7(2) | C20–C21–C22–C23 | −1.1(14) |
| C1–Si1–C4–C5 | 86.4(4) | C21–C20–C25–C27 | 78.0(8) |
| C1–Si1–C4–C9 | −94.1(4) | C21–C20–C25–C28 | −41.7(10) |
| C3–Si1–C4–C5 | −40.1(5) | C21–C22–C23–C24 | 3.0(12) |
| C3–Si1–C4–C9 | 139.5(4) | C22–C23–C24–C19 | 0.5(10) |
| C4–C5–C6–C7 | 3.3(7) | C22–C23–C24–C26 | 179.4(6) |
| C4–C5–C10–C12 | 108.1(5) | C23–C24–C26–C29 | −57.1(7) |
| C4–C5–C10–C13 | −127.0(5) | C23–C24–C26–C30 | 67.1(7) |
| C4–C9–C11–C14 | −103.7(5) | C24–C19–C20–C21 | 5.6(10) |
| C4–C9–C11–C15 | 132.2(5) | C24–C19–C20–C25 | −170.6(6) |
| C5–C4–C9–C8 | 4.7(7) | C25–C20–C21–C22 | 173.1(8) |

# Appendix L

## Functions and other data pertaining to the calibration of NMR probe head

### data.txt

Note: The columns are in the order $T_{NMR}$ [K], $T_{ref}$ [°C], $V_{thc}$ [mV].

```
289.8   18.6   -0.07
272.5   19.0   -0.89
259.5   19.0   -1.48
249.6   18.6   -1.90
240.5   18.2   -2.27
229.1   18.2   -2.75
220.4   18.0   -3.08
209.8   18.1   -3.48
200.3   18.2   -3.80
189.4   18.2   -4.17
181.0   18.0   -4.41
170.7   17.5   -4.65
161.0   17.8   -4.91
151.0   18.0   -5.16
140.5   18.0   -5.40
130.0   18.0   -5.63
123.0   17.8   -5.78
122.9   17.8   -5.78
```

### mv2degC.m

```
function T=mV2degC(Eread,Tref)
if sign(Eread) == -1
   c0=0;
   c1=3.9450128025e-2;
   c2=2.3622373598e-5;
   c3=-3.2858906784e-7;
   c4=-4.9904828777e-9;
   c5=-6.7509059173e-11;
   c6=-5.7410327428e-13;
   c7=-3.1088872894e-15;
   c8=-1.0451609365e-17;
```

```
  c9=-1.9889266878e-20;
  c10=-1.6322697486e-23;
  Eref=c0+c1*Tref+c2*Tref^2+c3*Tref^3+c4*Tref^4+c5*Tref^5+c6*Tref^6 ...
    +c7*Tref^7+c8*Tref^8+c9*Tref^9+c10*Tref^10;
else
  c0=-1.7600413686e-2;
  c1=3.8921204975e-2;
  c2=1.8558770032e-5;
  c3=-9.9457592874e-8;
  c4=3.1840945719e-10;
  c5=-5.6072844889e-13;
  c6=5.6075059059e-16;
  c7=-3.2020720003e-19;
  c8=9.7151147152e-23;
  c9=-1.2104721275e-26;
  ce0=1.185976e-1;
  ce1=-1.183432e-4;
  Eref=c0+c1*Tref+c2*Tref^2+c3*Tref^3+c4*Tref^4+c5*Tref^5+c6*Tref^6 ...
    +c7*Tref^7+c8*Tref^8+c9*Tref^9+ce0*exp(ce1*(Tref-126.9686)^2);
end
E=Eread+Eref;
if sign(E) == -1
  c0=0;
  c1=3.9450128025e-2;
  c2=2.3622373598e-5;
  c3=-3.2858906784e-7;
  c4=-4.9904828777e-9;
  c5=-6.7509059173e-11;
  c6=-5.7410327428e-13;
  c7=-3.1088872894e-15;
  c8=-1.0451609365e-17;
  c9=-1.9889266878e-20;
  c10=-1.6322697486e-23;
  eq=horzcat(num2str(E,5),'=',num2str(c0),'+',num2str(c1,11),'*T','+', ...
    num2str(c2,11),'*T^2','+',num2str(c3,11),'*T^3','+',num2str(c4,11), ...
    '*T^4','+',num2str(c5,11),'*T^5','+',num2str(c6,11),'*T^6','+', ...
    num2str(c7,11),'*T^7','+',num2str(c8,11),'*T^8','+',num2str(c9,11), ...
    '*T^9','+',num2str(c10,11),'*T^10');
```

```
   T=solve(eq);
   T=subs(T);
   T=T(1);
else
   c0=-1.7600413686e-2;
   c1=3.8921204975e-2;
   c2=1.8558770032e-5;
   c3=-9.9457592874e-8;
   c4=3.1840945719e-10;
   c5=-5.6072844889e-13;
   c6=5.6075059059e-16;
   c7=-3.2020720003e-19;
   c8=9.7151147152e-23;
   c9=-1.2104721275e-26;
   ce0=1.185976e-1;
   ce1=-1.183432e-4;
   eq=horzcat(num2str(E,5),'=',num2str(c0),'+',num2str(c1,11),'*T','+', ...
      num2str(c2,11),'*T^2','+',num2str(c3,11),'*T^3','+',num2str(c4,11), ...
      '*T^4','+',num2str(c5,11),'*T^5','+',num2str(c6,11),'*T^6','+', ...
      num2str(c7,11),'*T^7','+',num2str(c8,11),'*T^8','+',num2str(c9,11), ...
      '*T^9','+',num2str(ce0,11),'*exp(',num2str(ce1,11),'*(T-126.9686)^2)');
   T=solve(eq);
   T=subs(T);
   T=T(1);
end
```

## calculations.m

```
clear all
close all
load data.txt
Tabs=273.15;
n=length(data);
TNMRK=data(:,1);
TrefC=data(:,2);
Eread=data(:,3);
TNMRC=TNMRK-Tabs;
TcorrC=zeros(size(TNMRC));
for i=1:n
```

```
  TcorrC(i)=mV2degC(Eread(i),TrefC(i));
end
TcorrK=TcorrC+Tabs;

%x-data centered and scaled
mu = 196.72;
sigma = 52.967;
z = (TNMRK-mu)/sigma;

%5th degree fit
p1 = 0.39864;
p2 = -1.2534;
p3 = -0.63813;
p4 = 6.2902;
p5 = 54.024;
p6 = 184.31;
TcalcK=p1*z.^5+p2*z.^4+p3*z.^3+p4*z.^2+p5*z+p6;
TcalcC=TcalcK-Tabs;

TNMR_fit=[TNMRK(length(TNMRK)):0.01:TNMRK(1)];
z = (TNMR_fit-mu)/sigma;
Tcalc_fit=p1*z.^5+p2*z.^4+p3*z.^3+p4*z.^2+p5*z+p6;

nidurstodur=[TNMRK TNMRC Eread TrefC TcorrK TcorrC TcalcK TcalcC]

plot(TNMRK,TcorrK,'ko',TNMR_fit,Tcalc_fit,'b')
grid
xlabel('T_NMR [K]')
ylabel('T_corr [K]')
legend('T_corr vs.  T_NMR','5th degree fit','Location','NorthWest')
print -depsc Tcorr_vs_TNMR.eps
```